Aspects of monitoring wild and captive Nile crocodile (*Crocodylus niloticus*) populations in southern Africa

Hendrik Albert Myburgh

Submitted in fulfilment of the academic requirements for the degree of

Doctor of Philosophy

in the Discipline of Ecology

School of Life Sciences

College of Agriculture, Science and Engineering

University of KwaZulu-Natal

Pietermaritzburg Campus

2021

ABSTRACT

As biodiversity across the globe declines because of anthropogenic activities, the need for conservation efforts increases. For conservation efforts to be successful, it is imperative that detailed information about species and their populations; size and status within and outside of protected areas be collected. In freshwater systems, crocodile population demographics can provide an integrated view of ecosystem state, but the habitat and cryptic nature of crocodilians confound the derivation of population demographics for the taxa. Crocodile populations were historically monitored by fixed-wing aircraft, helicopter or limited spotlight surveys in those areas that are navigable by boat. These techniques are costly and labour-intensive; require specialised personnel and equipment, and are subject to observer bias and low accuracy in size class estimations. Furthermore, they produce population demographic data that is not verifiable as they rely on decisions and opinions of observers in the moment of surveying, often from fast-moving platforms. Lately, unmanned aerial vehicle (UAV) techniques have been shown to accurately and effectively count crocodiles, but they still require costly software and hardware packages. In this study, low-cost, open-source UAV techniques were developed as an alternative method to monitor and survey crocodilians, particularly Nile crocodiles (*Crocodylus niloticus*), both in captivity and in the wild. In South Africa, Nile crocodiles occur in open bedrock systems with relatively little riparian vegetation, an ideal scenario for the application of UAVs. The possibility of improved population demographic data for wild Nile crocodile populations by converting size data derived from UAVs to age data was explored by radiocarbon dating Nile crocodile claws. Morphometric correction factors applicable to UAV census are derived, and a fixed-wing survey is compared with a commercial-grade UAV survey of wild Nile crocodile populations in the Kruger National Park. The limitations and applicability of these approaches for crocodilian and other ecological studies were assessed. Their future applications in ecology and management are proposed.

PREFACE

The data described in this thesis were collected at various locations throughout the Gauteng, Mpumalanga and Limpopo Provinces (including the Kruger National Park), Republic of South Africa, from February 2019 to June 2021. Experimental work was carried out while registered at the School of Life Sciences, University of KwaZulu-Natal, Pietermaritzburg campus, under the supervision of Prof Colleen T. Downs and Prof. Stephan Woodborne.

This thesis, submitted for the degree of Doctor of Philosophy in the College of Agriculture, Science and Engineering, University of KwaZulu-Natal, Pietermaritzburg campus, represents original work by the author and has not otherwise been submitted in any form for any degree or diploma to any University. Where use has been made of the work of others, it is duly acknowledged in the text.

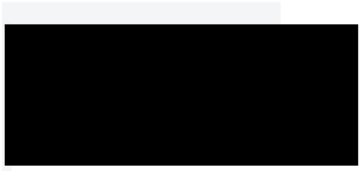

Hendrik Albert Myburgh

November 2021

I certify that the above statement is correct, and as the candidate's main supervisor I have approved this thesis for submission.

Professor Colleen T. Downs

Supervisor

November 2021

COLLEGE OF AGRICULTURE, SCIENCE AND ENGINEERING

DECLARATION 1 – PLAGIARISM

I, Hendrik Albert Myburgh, declare that

1. The research reported in this thesis, except where otherwise indicated, is my original research.
2. This thesis has not been submitted for any degree or examination at any other university.
3. This thesis does not contain other persons' data, pictures, graphs or other information, unless specifically acknowledged as being sourced from other persons.
4. This thesis does not contain other persons' writing, unless specifically acknowledged as being sourced from other researchers. Where other written sources have been quoted, then:
    a. Their words have been re-written but the general information attributed to them has been referenced
    b. Where their exact words have been used, then their writing has been placed in italics and inside quotation marks, and referenced.
5. This thesis does not contain text, graphics or tables copied and pasted from the Internet, unless specifically acknowledged, and the source being detailed in the thesis and in the References sections.

Signed: 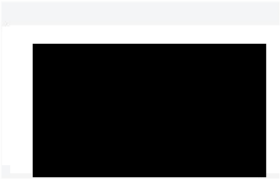

Hendrik Albert Myburgh

November 2021

COLLEGE OF AGRICULTURE, SCIENCE AND ENGINEERING

DECLARATION 2 – PUBLICATIONS

Details of contributions to draft or completed publications that form part and/or include research presented in this thesis.

Publication 1- published in African Journal of Wildlife Research, December 2021

Myburgh, A., Botha, H., Downs, C.T., Woodborne, S. The application and limitations of a low-cost UAV platform and open source-software combination for ecological mapping and monitoring

Author contributions:

AM conceived the paper. HB and SW assisted in the collection of data. AM processed and analysed all data and wrote the manuscript. SW and CTD contributed valuable comments to the manuscript.

Publication 2- submitted to Animal Welfare (provisionally accepted).

Myburgh, A., Veldsman, D.M., Myburgh, J.G., Downs, C.T., Webb, E.C., Woodborne, S. Quantifying crocodile numbers and welfare parameters in open pens on commercial crocodile farms in South Africa using a UAV and open-source software.

Author contributions:

AM, SW and JGM conceived the paper. AM collected and processed all data. AM wrote the manuscript with assistance from JGM, ECW and DMV. SW and CTD contributed valuable comments to the manuscript.

Publication 3- incorporated into additional datasets of the Exotic leather Research Centre, University of Pretoria and in prep.

Myburgh, A., Downs, C.T., Woodborne, S. Morphometric relationships between crocodilian measurements and their use in UAV based crocodile population monitoring

Author contributions:

AM conceived the paper, collected the data and wrote the manuscript. SW and CTD contributed valuable comments to the manuscript.

Publication 4- in prep.

Myburgh, A., Myburgh J.G., Steyl, J., Downs, C.T., Botha, H., and Woodborne. S. Calibrating growth rates of Nile crocodile (*Crocodylus niloticus*) claws

Author contributions:

AM and SW conceived the paper. AM, JGM and SW collected the samples. AM prepared radiocarbon samples and JGS prepared histological samples. AM wrote the manuscript with guidance from all co-authors. SW and CTD contributed valuable comments to the manuscript

Publication 5- in prep

Myburgh, A., Woodborne, S., Pienaar, D., Ferreira, S., Downs, C.T., Davies., A.

Evaluating the population demographics of the Kruger National Park Olifants River Gorge Nile crocodile population: a case study using a large multirotor UAV

Author contributions:

AM, SF, DP, CTD, SW and AD conceived the paper. AM and AD collected the data. AD and AM processed the data. AM wrote the manuscript. CTD and SW provided valuable comments to the manuscript.

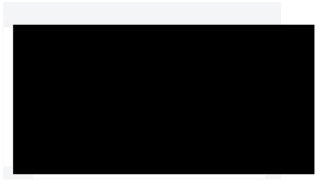

Hendrik Albert Myburgh

November 2021

ACKNOWLEDGEMENTS

Compiling this collection of chapters in the midst of a pandemic would not have been possible without the support of a network of individuals and organisations. First and foremost, I would like to thank my supervisors for their guidance and support. Prof Colleen T. Downs, thank you for the academic guidance, financial assistance and administerial support that you have given me throughout the last three years. Thank you for assisting me with the submission and review processes of the respective papers that come out of this work and many thanks for helping to submit these chapters as a PhD thesis. Prof Stephan Woodborne, thank you for guiding me through the last six years of undergraduate research, from catching crocodiles to extracting groundwater for analyses, and so much more in between; you have opened up a world that I would otherwise not have been exposed to, I will be forever grateful.

To the staff of the Mpumalanga Tourism and Parks Agency (MTPA) at the Loskop and Nelspruit offices, thank you for allowing me to conduct surveys and for revealing to me the problems and challenges that you face in the management and policy space around wild Nile crocodile populations. I would like to specifically thank Dr Hannes Botha from the Loskop offices of the MTPA for teaching me the tricks of the trade when it comes to crocodile catching and wild population management. From the Onderstepoort Veterinary Faculty, I would like to thank Prof Jan Myburgh for guiding me through some of the questions and challenges of the various chapters, for arranging meetings with crocodile farm owners and for providing me with guidance and materials that allowed the successful completion of the work in this thesis. I would also like to thank Prof Johan Steyl, for his assistance with the histological examination of crocodile claws. To the owners and managers at the various crocodile farms, thank you, none of this work would have been possible without your inviting welcome and enthusiasm on every visit.

Mr Danie Pienaar, Dr Sam Ferreira, Mr Robin Petersen, Dr Eddie Riddell, Dr Danny Govender, Mr Jacques Venter and Mr Pauli Viljoen from SANParks; thank you for allowing me to be a part of the crocodile and aquatic research in the Kruger National Park over the last 6 years, your guidance in the field and conversations around camp fires, in boardrooms and at conferences is invaluable. A large portion of the motivation for this research stems from shortcomings and suggestions derived during these events, and I hope that this piece of research, together with the various other aquatic projects that we have in and outside of the Park, aids in the conservation of the unique habitats and species that make the Kruger National Park and the rivers that feed into it truly unique (Figures a,b,c,d and e).

To the team from the Davies Lab at Harvard, Prof Andrew Davies, Dr Peter Brehm Boucher, Mr Evan Hockridge and Mr Tom Lautenbach, thank you for assisting me in the surveys and the processing of data for Chapter 6 of this thesis; you have given me valuable insight into the world of remote sensing. Mr Piero Toffanin, the head developer of Open Drone Map, thank you for your efforts in producing this piece of software, for your swift replies in forums on various queries, and for providing me with a copy of your book at no cost. This work would not have been possible without your efforts.

Prof Wynand Steyn and Mr Andre Broekman from Engineering 4.0 at the University of Pretoria, thank you for the assistance and guidance around UAV flights and mapping, and for allowing me to conduct test flights and processing with the use of your GPS system.

For those who provided me with the financial assistance; a special thank you to the NRF for providing the funds that supported this research and to the IUCN Crocodile Specialist Group for granting the funds that allowed me to complete my Remote Pilots Licence.

Lastly, I would like to thank my family for their love and support, you have provided the foundations which have enabled me to strive and achieve so many goals.

To my wife, Mrs Dedrè Myburgh (CA(SA)), without your unwavering support, understanding, patience, assistance and love, I would not be where I am today.

Figures a-e: a and b depict a portion of the Letaba river during the wet (a) and dry (b) season and figure c shows the Letaba-Olifants confluence as seen from the Letaba river just before the confluence. Figures d and e show large individual Nile crocodiles as seen from the perspective of a UAV during the dry season at low flow.

TABLE OF CONTENTS

FIGURES

TABLES

CHAPTER 1

INTRODUCTION

1.1 Background

Apex predator ecology provides an integrated view of ecosystem state, and the monitoring of their population dynamics is becoming increasingly important (Biggs et al. 2009; Schmidt et al. 2018; Gangoso et al. 2020). In the coming decades, ecosystems will experience regime shifts (disruptive, degradative state changes) at greater frequencies than before, and population monitoring of large vertebrates may lack the resolution required to detect the resulting perturbations (Perretti and Munch 2012; Xu et al. 2020; Su et al. 2021; Tanaka et al. 2021). Crocodilians persist in freshwater and marine systems (Pooley and Gans 1976; Martin 2007), and anthropogenic expansion is driving habitat destruction, resource utilisation and pollution, all of which are negatively affecting aquatic systems and crocodilian populations globally (Grant and Lewis 2010; Nair et al. 2012; Shaney et al. 2019; González-Desales et al. 2021). The Nile crocodile *Crocodylus niloticus* is one of the largest crocodilians, the largest species in Africa and the only crocodilian that occurs naturally in South Africa (Cott and Pooley 1971; IUCN 2021).

Of South Africa's major water drainage regions (N = 24), five have naturally occurring Nile crocodile populations (IUCN 2021) (Fig. 1.1). The majority of Nile crocodiles occur in the north-eastern regions of South Africa, with a satellite population in the Boesmans River catchment in the Eastern Cape Province on the southern coast (IUCN 2021). The largest Nile crocodile populations are located in protected and conservation areas in the KwaZulu-Natal, Mpumalanga and Limpopo Provinces, with high numbers in the Kruger National Park and the iSimangaliso Wetland Park (Combrink 2014). Unlike other large vertebrate predators (e.g., lions (*Panthera leo*)), Nile crocodiles occur both within and outside of protected areas which

confounds their population management, and surveys are often conducted on subpopulations where funds are available (Ferreira and Pienaar 2011).

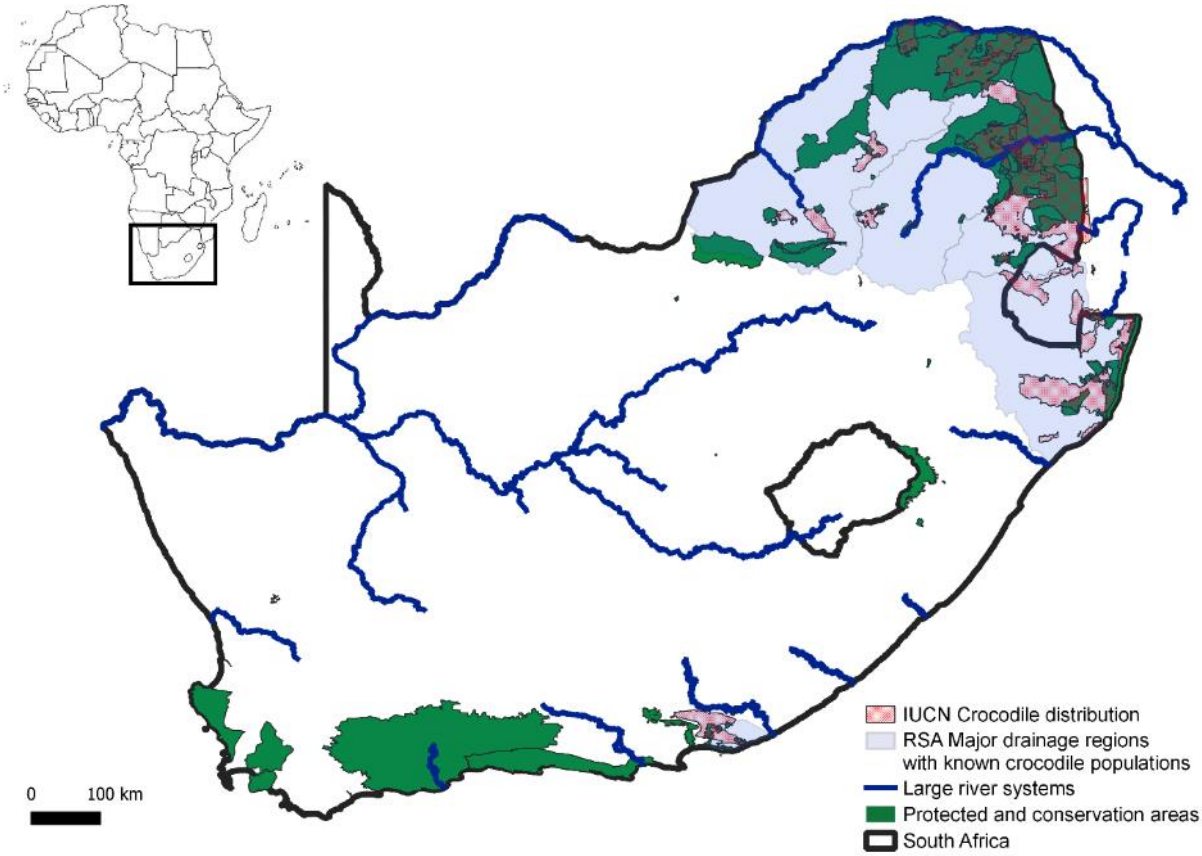

Figure 1.1: The IUCN crocodile distribution (IUCN 2021) and water drainage regions and major river systems (DWS 2021) with naturally occurring Nile crocodile populations in South Africa. Notice the distribution of crocodiles both within and outside of protected areas in South Africa.

Crocodiles are large vertebrate predators that have important top-down effects on ecosystems (Morris and Letnic 2017; Rees et al. 2017), and they form an integral part of terrestrial, aquatic interfaces (Evans et al. 2017). The degradation of freshwater systems can lead to trophic cascades that negatively affect crocodile populations (Swanepoel 1999; Ashton

2010; Woodborne et al. 2012). Habitat destruction, pollution and unlawful hunting have caused declines in Nile crocodile numbers throughout South Africa despite protective legislation (Pooley 1982; Jacobsen 1984; Swanepoel, 2001; Botha 2011; Combrink et al. 2011; Ferreira and Pienaar 2011; Calverley and Downs 2017; Cavalier et al. 2021). Nile Crocodiles are presently listed as *Vulnerable* in the South African Atlas and Red List of Reptiles (Marais 2014). Their management requires accurate demographic data, but generally, this is difficult to obtain as they are cryptic, have high ontogenetic size dimorphism (range in size from <50 cm to over 500 cm during their lifespan) and exhibit traits of fast and slow-growing species, produce many young and typically have a long life span if they reach adulthood (Dendi and Luisell 2017; Briggs Gonzalez et al. 2017).

In KwaZulu-Natal Province, South Africa, Nile crocodile populations are relatively well surveyed as they mostly occur in estuaries and large lake ecosystems, which are easily navigable by boat and spotlight surveys are easily conducted. Several authors have investigated the population dynamics and sustainability of these populations (Combrink et al. 2011; Calverley and Downs, 2014; Warner et al. 2016; Champion and Downs 2017). In contrast, the Nile crocodile populations in the North-eastern regions of South Africa, especially those of the Kruger National Park, are constrained to long river reaches in >3rd order streams with little information on their populations due to a lack of research that results from the costs associated with the monitoring of these animals and the limited availability of navigable waterways in this region, which make spotlight surveys unfeasible (Ferreira and Pienaar 2011). In the Limpopo, Letaba, Olifants and Inkomati-Usuthu catchments, the river systems are shallow and often moribund with phragmites and are mostly unnavigable by boat. Of the crocodile populations in these river systems, the Olifants River gorge population has received much attention in the last 13 years (Ashton 2010; Ferreira and Pienaar 2011; Woodborne et al. 2012; Lane et al. 2013; Woodborne et al. (in prep)). Here, the largest and most dominant animals maintain

breeding territories (Swanepoel et al. 2000; Ferreira and Pienaar 2011), but this population reached a tipping point in 2008-2009 when more than 180 large Nile crocodiles succumbed to pansteatitis, a dietary disease linked to chronic pollution and river dynamics in the catchment (Ashton 2010; Ferreira and Pienaar 2011; Woodborne et al. 2012; see https://youtu.be/7XiXPt6Ujgk?t=5584).

Previous surveys of the Nile crocodile populations of the Kruger National Park (from 1989 to 2008) relied on helicopter-based platforms where crocodiles were counted at the same time as common hippopotamus *Hippopotamus amphibius* censuses (Ferreira and Pienaar, 2011). Dedicated crocodile monitoring (2008-present) was initiated in response to the pansteatitis epidemic. Fixed-wing aircraft, helicopters and motorboats were routinely used for monitoring, which allowed some attempts to mathematically account for several factors that influence bias during population census data from these techniques (Ferreira and Pienaar, 2011).

Traditional Nile crocodile population census techniques include fixed-wing or helicopter-based surveys or counts from boats where waterways are accessible (Combrink 2014; Ferreira and Pienaar 2011, Wallace et al. 2013). These techniques are costly, require expensive equipment and, at best, group crocodiles into very broad size classes based on the perspective of the observers (Woodward and Moore 1993). Survey platforms driven by internal combustion engines are also relatively large, noisy and are known to cause disturbance to crocodiles (Elsey and Trosclair 2016). Spotlight surveys often detect a greater quantity of smaller individuals when compared with aerial platforms, but many more are often recorded as "eyes only" with no information on the size of the animal (Wallace et al. 2013). It may be feasible to survey crocodiles from small, agile platforms that are not limited by shallow waterways and phragmites, such as small motorboats or paddleboats, but such platforms are perilous in African systems, especially in protected areas where rivers are full of hippopotamus,

are patrolled by leopard and lion and where elephants may be startled at night (pers. obs. Kruger National Park, Olifants and Letaba river systems).

Table 1.1: Summary of 18 of the 24 extant crocodilians and recent population survey methods.

Species	Common name	Survey method	Reference
Alligator mississippiensis	American alligator	Spotlight survey	Strickland et al. 2018
Alligator sinensis	Chinese alligator	DNA analysis	Pan et al. 2019
Melanosuchus niger	Black caiman	Spotlight survey	Naveda-Rodríguez et al. 2020
Caiman latirostris	Broad-snouted Caiman	DNA analysis	Zucoloto et al. 2021
Caiman crocodilus	Spectacled caiman	Spotlight survey and mark recapture	Ortiz et al. 2020
Paleosuchus trigonatus	Cuvier's dwarf caiman	DNA analysis	Muniz et al. 2019
Mecistops cataphractus	West African slender-snouted crocodile	Spotlight survey	Ahizi et al. 2020
Crocodylus acutus	American crocodile	Spotlight survey	Ortega-León et al. 2020
Crocodylus johnstoni	Australian freshwater crocodile	DNA analysis	Cao et al. 2020
Crocodylus moreletii	Morelet's crocodile	Spotlight survey	Flores-Escalona et al. 2021
Crocodylus palustris	Mugger crocodile	Spotlight survey	Prasad et al. 2018
Crocodylus novaeguineae	New Guinea freshwater crocodile	Spotlight survey	Suharno et al. 2021
Crocodylus niloticus	Nile crocodile	Spotlight survey and UAV survey	Jordaan 2021
Crocodylus suchus	West African crocodile	Spotlight	Ahizi et al. 2021
Crocodylus intermedius	Orinoco crocodile	DNA analysis	Saldarriaga Gómez 2021
Crocodylus porosus	Saltwater crocodile	Spotlight survey and camera traps	Than et al. 2020
Crocodylus siamensis	Siamese crocodile	Spotlight survey and daytime ground searches	Cox and Phothitay 2021
Gavialis gangeticus	Gharial	UAV survey	Thapa et al. 2018

Estimating crocodile population demographics using traditional survey techniques (aerial and spotlight counts) is also subject to bias and variability with data that cannot be externally verified, and the observer's ability can influence size class categorisation and count data (Caughly 1974; Da Silveira et al. 2008; pers. obs). Furthermore, they typically lack the temporal and spatial scale required to detect subtle changes indicative of impending ecosystem change (Perretti and Munch 2012). Most recent crocodilian population surveys use spotlight counts, but unmanned aerial vehicles (UAVs) are being incorporated as a tool for crocodilian population monitoring (Jordaan 2021) (Table 1.1).

1.2 New technologies for monitoring

Ecological data such as habitat classification and wildlife counts are obtainable through emerging technologies. For example, high-resolution satellites, or UAVs, generally decrease the cost and increase the efficiency of remote sensing in ecology (Christie et al. 2016; Wang et al. 2019). UAVs can monitor, map and track wildlife populations, vegetation dynamics and resource quantities at a fraction of the cost and with much higher resolution and reliability than previous methods (Guo et al. 2018; Ventura et al. 2018; Ren et al. 2019; Tmušić et al. 2020).

Many authors have compared the benefits of UAVs over more traditional survey techniques (Ezat et al. 2018; Nowak et al. 2018; Thapa et al. 2018), and one of the greatest advantages is the elimination of bias in size class categorisation during wildlife surveys. This is because rectified aerial imagery can be used to measure animals, and crocodiles in particular, very accurately (Ezat et al. 2018). Additionally, survey frequencies can be increased, allowing for annual or intra-annual surveys with costs that are orders of magnitude less than traditional techniques (Ezat et al. 2018; Jordaan 2021). UAVs allow the acquisition of population demographic data that is forfeit of observer bias and accurate enough that size classes can be more precisely and easily defined.

Accurate size estimation from aerial imagery is attainable through photogrammetry software (Hodgson et al. 2016; Crutsinger et al. 2016; Hodgson et al. 2018; Ezat et al. 2018; Groos et al. 2019; Scarpa and Pina 2019). Overlapping images are used to identify key scene features, and combined with global positioning system (GPS) tags, allow for the virtual rendering of geometrically correct three-dimensional models of large areas (Fuller et al. 2008; Gatziolis et al. 2015). The ground sampling distance (GSD: the distance on the ground represented by each pixel in an aerial photograph), heterogeneity of the area being photographed, and amount of overlap between images determine the accuracy of models (Gatziolis et al. 2015; Toffanin, 2019). Relatively costly UAVs and proprietary photogrammetry software packages have limited the widespread adoption of UAVs for ecological monitoring (Anderson and Gaston 2013; Buters et al. 2019; Groos et al. 2019), but hobbyist UAVs are now widely available and are already incorporated into many conservation agencies (e.g., Mpumalanga Tourism and Parks Agency). Well-funded entities can afford to implement commercially available UAV platforms and service providers, but many ecological studies, wildlife managers and field rangers would benefit from low-cost UAV mapping and monitoring, especially in the developing world. This is true for the case of Nile crocodile population demographics in South Africa, where relatively little to no information on its present population dynamics exists because of a lack of funding for population surveys.

Population censuses of Nile crocodiles are conducted under the mandates of National parks, but Nile crocodiles occur throughout the upstream catchments outside of protected areas in South Africa. Little is known about the demographics and population sizes of the apex predators in these buffer zones. Intermittent and often a complete lack of data in the upstream catchment regions of the Limpopo, Letaba, Olifants and Inkomati- Usuthu catchments result in unknown ecosystem resilience, upon which areas like the Kruger National Park rely. There

is a need for inexpensive methods to monitor Nile crocodile populations to make informed management decisions to prevent impending ecological change.

1.3 Aims and structure of the thesis

This multidisciplinary study explored emerging open-source technologies and low-cost UAVs as methods for Nile crocodile population monitoring. All data chapters were formatted for submission to international peer-reviewed journals. Therefore, some repetition in the framing of the different studies was unavoidable. The hypotheses or predictions, and outcomes are presented in the respective chapters.

Chapter 2 is a method development that evaluated a combination of a popular consumer-grade UAV camera with open-source photogrammetry software as a low-budget mapping solution for ecology. It outlined the aspects and limitations of the approach and evaluated its applicability for ecological monitoring. The flight settings and processing requirements for centimeter-level accuracy were derived, and various applications in ecology were explored.

Chapter 3 tests the abilities and applicability of the methods described in Chapter 2 on Nile crocodiles in particular. Under controlled circumstances, the methods were applied at a crocodile farm, and several welfare parameters for crocodiles were described. This is a first of its kind approach to welfare parametrisation for farmed Nile crocodiles and showed that low-cost UAVs and open-source software could be applied to derive remote estimations of crocodile and holding facility metrics.

Chapter 4 addresses the need for morphometric relationships from UAV imagery. Low-resolution aerial imagery makes the identification of the tail and circumcircle scute layer associated with the vent of a crocodile difficult. Snout to neck and snout to hind limb lengths were explored, and the relationship between these and the total lengths of Nile crocodiles was

derived. The method used easily recognisable features, the front and hind limbs, to estimate crocodile lengths. Correction equations make it possible to determine the size of crocodiles from UAV imagery. This may prove vital in future applications where artificial intelligence may automatically detect and measure crocodilians in real-time.

Chapter 5 is an attempt at deriving size-age relationships from the radiocarbon dating of crocodile claw keratin. During this work, Nile crocodilian claw growth rates were derived from the sampling of cornified tissues informed by histological investigations of growth patterns of crocodilian claws. A size-age model necessitates the development of a method that can produce more accurate remote size estimations of crocodiles and was the motivation for Chapters 2 and 6. Success with this objective would allow measurements of crocodile sizes in an age- rather than size-based assessment of population dynamics. Claws could not be used for the age-estimation of individuals because wear removes the older part of the claws, but sufficient integrity in the remaining claw means that they can be used to reconstruct the diet of Nile crocodiles. This information provided time scales that could be linked to dietary trends in previous studies of crocodilian claws.

Chapter 6 is the first-ever UAV survey of the Nile crocodile population of the Olifants River Gorge, Kruger National Park, South Africa. It was conducted over two days, and the technique resulted in a population estimate four times greater than a fixed-wing aircraft manned count a few weeks prior. Additionally, size classes of Nile crocodiles were determined with centimeter level accuracy, and population demographic data were derived without observer bias. The demographics were compared with matrix models, and the implications of UAV based monitoring of this population are discussed as a case study. It is presented as a case study that highlights the resolution, accuracy and amount of data that can be derived from large scale UAV based crocodile surveys.

Chapter 7 provides concluding remarks on the future of crocodilian monitoring in light of emerging technologies and suggests future applications for the use of open-source software and low-cost UAV platforms for crocodilian monitoring.

1.4 References

Anderson, K., and Gaston, K.J., 2013. Lightweight unmanned aerial vehicles will revolutionize spatial ecology. *Frontiers in Ecology and the Environment*, *11*, 138-146.

Ahizi, M.N., Kouman, C.Y., Ouattara, A., Kouamé, N.P., Dede, A., Fairet, E. and Shirley, M.H., 2021. Detectability and impact of repetitive surveys on threatened West African crocodylians. *Ecology and Evolution*, 00, 1–15. https://doi.org/10.1002/ece3.8188

Ashton, P.J., 2010. Demise of the Nile crocodile (*Crocodylus niloticus*) as a keystone species for aquatic ecosystem conservation in South Africa: the case of the Olifants River. *Aquatic Conservation: Marine and Freshwater Ecosystems*, *20*, 489-493.

Biggs, R., Carpenter, S.R. and Brock, W.A., 2009. Turning back from the brink: detecting an impending regime shift in time to avert it. *Proceedings of the National Academy of Sciences*, *106*, 826-831.

Briggs-Gonzalez, V., Bonenfant, C., Basille, M., Cherkiss, M., Beauchamp, J. and Mazzotti, F., 2017. Life histories and conservation of long-lived reptiles, an illustration with the American crocodile (*Crocodylus acutus*). *Journal of Animal Ecology*, *86*, 1102-1113.

Botha, H., Van Hoven, W. and Guillette Jr, L.J., 2011. The decline of the Nile crocodile population in Loskop dam, Olifants River, South Africa. *Water SA*, 37.

Buters, T.M., Bateman, P.W., Robinson, T., Belton, D., Dixon, K.W. and Cross, A.T., 2019. Methodological ambiguity and inconsistency constrain unmanned aerial vehicles as a silver bullet for monitoring ecological restoration. *Remote Sensing*, *11*, 1180.

Calverley, P.M. and Downs, C.T., 2014. Population status of Nile crocodiles in Ndumo Game Reserve, KwaZulu-Natal, South Africa (1971–2012). *Herpetologica*, *70*, 417-425.

Calverley, P.M. and Downs, C.T., 2017. The past and present nesting ecology of Nile crocodiles in Ndumo Game Reserve, South Africa: Reason for concern? *Journal of Herpetology*, *51*, 19-26.

Cao, R., Somaweera, R., Brittain, K., FitzSimmons, N.N., Georges, A. and Gongora, J., 2020. Genetic structure and diversity of Australian freshwater crocodiles (*Crocodylus johnstoni*) from the Kimberley, Western Australia. *Conservation Genetics*, *21*, 421-429.

Caughley, G., 1974. Bias in aerial survey. *Journal of Wildlife Management*, *38*, 921-933.

Cavalier, R., Pratt, E.N., Serenari, C. and Rubino, E.C., 2021. Human dimensions of crocodilians: a review of the drivers of coexistence. *Human Dimensions of Wildlife*, *26*, 1-17

Champion, G. and Downs, C.T., 2017. Status of the Nile crocodile population in Pongolapoort Dam after river impoundment. *African Zoology*, *52*, 55-63.

Christie, K.S., Gilbert, S.L., Brown, C.L., Hatfield, M. and Hanson, L., 2016. Unmanned aircraft systems in wildlife research: current and future applications of a transformative technology. *Frontiers in Ecology and the Environment*, *14*, 241-251.

Cott, H.B. and Pooley, A.C., 1971. The status of crocodiles in Africa. *Proceedings of the first working group of the Crocodile Specialist Group*, *2*, 98.

Combrink, X., Korrûbel, J.L., Taylor, R., Kyle, R. and Ross, P., 2011. Evidence of a declining Nile crocodile (*Crocodylus niloticus*) population at Lake Sibaya, South Africa. *South African Journal of Wildlife Research*, *41*, 145-157.

Combrink, A.S., 2014. Spatial and reproductive ecology and population status of the Nile Crocodile (*Crocodylus niloticus*) in the Lake St Lucia estuarine system, South Africa, *PhD thesis, University of KwaZulu-Natal, South Africa*.

Cox Jr, J.H. and Phothitay, C., 2021. Surveys of the Siamese Crocodile *Crocodylus siamensis* in Savannakhet Province, Lao PDR 6 May–4 June 2008 Phase 1 Field Trip Report.

Crutsinger, G.M., Short, J. and Sollenberger, R., 2016. The future of UAVs in ecology: an insider perspective from the Silicon Valley drone industry. *Journal of Unmanned Vehicle Systems, 4*, 161-168.

Da Silveira, R., Magnusson, W.E. and Thorbjarnarson, J.B., 2008. Factors affecting the number of caimans seen during spotlight surveys in the Mamirauá Reserve, Brazilian Amazonia. *Copeia, 2008*, 425-430.

Dendi, D. and Luiselli, L., 2017. Population surveys of Nile crocodiles (*Crocodylus niloticus*) in the Murchison Falls National Park, Victoria Nile, Uganda. *European Journal of Ecology*, *3*, 67-76.

Detoeuf-Boulade, A.S., 2006. *Reproductive cycle and sexual size dimorphism of the Nile crocodile (Crocodylus niloticus) in the Okavango Delta, Botswana*. PhD thesis, Stellenbosch University, Stellenbosch.

DWS., 2021. Department of Water and Sanitation, South Africa. Online water quality data exploration tool available at: https://www.dws.gov.za/iwqs/wms/data/000key2data.asp accessed on 2021/02/23.

Elsey, R.M. and Trosclair, P.L., 2016. The use of an unmanned aerial vehicle to locate alligator nests. *Southeastern Naturalist*, *15*, 76-82.

Evans, L.J., Davies, A.B., Goossens, B. and Asner, G.P., 2017. Riparian vegetation structure ad the hunting behavior of adult estuarine crocodiles. *PloS One*, *12*, e0184804.

Ezat, M.A., Fritsch, C.J., and Downs, C.T., 2018. Use of an unmanned aerial vehicle (drone) to survey Nile crocodile populations: a case study at Lake Nyamithi, Ndumo Game Reserve, South Africa. *Biological Conservation*, *223*, 76-81.

Ferreira, S.M. and Pienaar, D., 2011. Degradation of the crocodile population in the Olifants River gorge of Kruger National Park, South Africa. *Aquatic Conservation: Marine and Freshwater Ecosystems, 21*, 155-164.

Flores-Escalona, C.I., Charruau, P., López-Luna, M.A., Zenteno-Ruiz, C.E., Rangel-Mendoza, J.A. and Peralta-Carreta, C., 2021. Population status and habitat preference of *Crocodylus moreletii* Duméril and Bibron, 1851 (Crocodilia: Crocodylidae) within the limits of two protected natural areas in southeastern Mexico. *Herpetology Notes, 14*, 55-62.

Fuller, S., Collier, P. and Seager, J. 2008. Assessing and reporting real-time data quality for GNSS reference stations. *Journal of Spatial Science*, *53*, 149-159.

Gangoso, L., Viana, D.S., Dokter, A.M., Shamoun-Baranes, J., Figuerola, J., Barbosa, S.A. and Bouten, W., 2020. Cascading effects of climate variability on the breeding success of an edge population of an apex predator. *Journal of Animal Ecology*, *89*, 2631-2643.

Gatziolis, D., Lienard, J.F., Vogs, A., and Strigul, N.S. (2015). 3D tree dimensionality assessment using photogrammetry and small unmanned aerial vehicles. *PloS One*, *10*, e0137765.

González-Desales, G.A., Sigler, L., García-Grajales, J., Charruau, P., Zarco-González, M.M., Balbuena-Serrano, Á. and Monroy-Vilchis, O., 2021. Factors influencing the occurrence of negative interactions between people and crocodilians in Mexico. *Oryx*, *55*, 791-799.

Guo, X., Shao, Q., Li, Y., Wang, Y., Wang, D., Liu, J., Fan, J. and Yang, F. 2018. Application of UAV remote sensing for a population census of large wild herbivores—taking the Headwater Region of the Yellow River as an example. *Remote Sensing*, *10*, 1041.

Grant, P.B. and Lewis, T.R., 2010. High speed boat traffic: a risk to crocodilian populations. *Herpetological Conservation and Biology*, *5*, 456-460.

Groos, A.R., Bertschinger, T.J., Kummer, C.M., Erlwein, S., Munz, L. and Philipp, A., 2019. The potential of low-cost UAVs and open-source photogrammetry software for high-resolution monitoring of Alpine glaciers: a case study from the Kanderfirn (Swiss Alps). *Geosciences*, *9*, 356.

Hodgson, J.C., Baylis, S.M., Mott, R., Herrod, A. and Clarke, R.H., 2016. Precision wildlife monitoring using unmanned aerial vehicles. *Scientific Reports*, *6*, 1-7.

Hodgson, J.C., Mott, R., Baylis, S.M., Pham, T.T., Wotherspoon, S., Kilpatrick, A.D., Raja Segaran, R., Reid, I., Terauds, A. and Koh, L.P., 2018. Drones count wildlife more accurately and precisely than humans. *Methods in Ecology and Evolution*, *9*, 1160-1167.

IUCN (International Union for Conservation of Nature) 2021. *Crocodylus niloticus*. The IUCN Red List of Threatened Species distribution map. Version 2021. https://www.iucnredlist.org. Downloaded on 20 January 2021 and again for verification on 10 October 2021.

Jacobsen, N.H.G. 1984. The distribution and status of crocodile populations in the Transvaal outside the Kruger National Park. *Biological Conservation*, *29*, 191-200.

Jordaan, P.R., 2021. The establishment of a multifaceted *Crocodylus niloticus* Laurenti 1768 monitoring programme on Maputo Special Reserve (Maputo Province, Mozambique) with preliminary notes on the population (Reptilia: Crocodylidae). *Herpetology Notes*, *14*, 1155-1162.

Lane, E.P., Huchzermeyer, F.W., Govender, D., Bengis, R.G., Buss, P.E., Hofmeyr, M., Myburgh, J.G., Steyl, J.C., Pienaar, D.J. and Kotze, A., 2013. Pansteatitis of unknown etiology associated with large-scale Nile crocodile (*Crocodylus niloticus*) mortality in Kruger National Park, South Africa: Pathologic findings. *Journal of Zoo and Wildlife Medicine*, *44*, 899-910.

Marais, J., 2014 *Crocodylus niloticus* (Laurenti, 1768). In: Bates, M.F., Branch, W.R., Bauer, A.M., Burger, M., Marais, J., Alexander, G.J. and de Villiers M.S., 2014. Atlas and Red List of the Reptiles of South Africa, Lesotho and Swaziland. Suricata 1. South African National Biodiversity Institute, Pretoria

Martin, S., 2007. Global diversity of crocodiles (Crocodilia, Reptilia) in freshwater. In Freshwater Animal Diversity Assessment. Springer, Dordrecht. pp. 587-591.

Morris, T. and Letnic, M., 2017. Removal of an apex predator initiates a trophic cascade that extends from herbivores to vegetation and the soil nutrient pool. *Proceedings of the Royal Society B: Biological Sciences*, *284*, 20170111.

Muniz, F.L., Ximenes, A.M., Bittencourt, P.S., Hernández-Rangel, S.M., Campos, Z., Hrbek, T. and Farias, I.P., 2019. Detecting population structure of *Paleosuchus trigonatus* (Alligatoridae: Caimaninae) through microsatellites markers developed by next generation sequencing. *Molecular Biology Reports*, *46*, 2473-2484.

Nair, T., Thorbjarnarson, J.B., Aust, P. and Krishnaswamy, J., 2012. Rigorous gharial population estimation in the Chambal: implications for conservation and management of a globally threatened crocodilian. *Journal of Applied Ecology*, *49*, 1046-1054.

Naveda-Rodríguez, A., Utreras, V. and Zapata-Ríos, G., 2020. A standardised monitoring protocol for the black caiman (*Melanosuchus niger*). *Wildlife Research*, *47*, 317-325.

Nowak, M.M., Dziób, K. and Bogawski, P., 2018. Unmanned Aerial Vehicles (UAVs) in environmental biology: A review. *European Journal of Ecology*, *4*, 56-74.

Ortega-León, A.M., Santos-Morales, A.H., Zamora-Abrego, J.G. and Pérez-Mendoza, H.A., 2020. Analysis of the population dynamics of the endangered American crocodile, *Crocodylus acutus* in Paramillo National Natural Park. *Marine and Freshwater Research*, *72*, 14-25.

Ortiz, D.A., Dueñas, J.F., Villamarín, F. and Ron, S.R., 2020. Long-term monitoring reveals population decline of spectacled caimans (*Caiman crocodilus*) at a black-water lake in Ecuadorian Amazon. *Journal of Herpetology*, *54*, 31-38.

Pan, T., Wang, H., Duan, S., Ali, I., Yan, P., Cai, R., Wang, M., Zhang, J., Zhang, H., Zhang, B. and Wu, X., 2019. Historical population decline and habitat loss in a critically endangered species, the Chinese alligator (*Alligator sinensis*). *Global Ecology and Conservation*, *20*, e00692

Perretti, C.T. and Munch, S.B., 2012. Regime shift indicators fail under noise levels commonly observed in ecological systems. *Ecological Applications*, *22*, 1772-1779.

Pooley, A.C., 1982. Discoveries of a Crocodile Man. William Collins Sons and Co Ltd: Johannesburg.

Pooley, A.C. and Gans, C., 1976. The Nile crocodile. *Scientific American*, *234*, 114-125.

Prasad, K.K., Srinivasulu, C., Srinivasulu, A., Rao, G.R.K. and Shivaiah, C., 2018. Reassessment of status and spatial analysis of the distribution of *Crocodylus palustris* in Manjeera Wildlife Sanctuary, Telangana State, India. *Herpetological Conservation and Biology*, *13*, 569-575.

Rees, J.D., Kingsford, R.T. and Letnic, M., 2017. In the absence of an apex predator, irruptive herbivores suppress grass seed production: implications for small granivores. *Biological Conservation*, *213*, 13-18.

Ren, H., Zhao, Y., Xiao, W. and Hu, Z., 2019. A review of UAV monitoring in mining areas: Current status and future perspectives. *International Journal of Coal Science and Technology*, *6*, 320–333.

Saldarriaga Gómez, A.M., 2021 Conservation genetics of the largest captive population of the critically endangered Orinoco crocodile (*Crocodylus intermedius*): a contribution for its survival. PhD thesis, Universidad Nacional de Colombia, Colombia.

Scarpa, L.J. and Pina, C.I., 2019. The use of drones for conservation: A methodological tool to survey caimans nests density. *Biological Conservation*, *238*, 108235.

Schmidt, J.H., McIntyre, C.L., Roland, C.A., MacCluskie, M.C. and Flamme, M.J., 2018. Bottom-up processes drive reproductive success in an apex predator. *Ecology and Evolution*, *8*, 1833-1841.

Shaney, K.J., Hamidy, A., Walsh, M., Arida, E., Arimbi, A. and Smith, E.N., 2019. Impacts of anthropogenic pressures on the contemporary biogeography of threatened crocodilians in Indonesia. *Oryx*, *53*, 570-581.

Strickland, B., Vilella, F. and Flyni, R., 2018. Long-term spotlight surveys of American alligators in Mississippi, USA. *Herpetological Conservation and Biology*, *13*, 331-340.

Su, H., Wang, R., Feng, Y., Li, Y., Li, Y., Chen, J., Xu, C., Wang, S., Fang, J. and Xie, P., 2021. Long-term empirical evidence, early warning signals and multiple drivers of regime shifts in a lake ecosystem. *Journal of Ecology*, *109*, 3182-3194.

Suharno, S., Kadir, A., Sembiring, E., Masiki, A.D., Mubarak, T., Ratnawati, L.D., Lessil, N., Idris, D. And Imbenai, J.G., 2021. Population estimation of freshwater crocodiles (*Crocodylus novaeguineae*) and tree vegetation diversity at wildlife reserve of Mamberamo Foja, Papua, Indonesia. *Biodiversitas Journal of Biological Diversity*, *22*, 2928-2936.

Swanepoel, D.G.J., 1999. *Movements, nesting and the effects of pollution on the Nile crocodile (Crocodylus niloticus) in the Olifants River, Kruger National Park*. PhD thesis, University of KwaZulu-Natal, South Africa.

Swanepoel, D.G.J., 2001. The Raising of the Arabie Dam Wall and the Impacts on the Nile Crocodile Population. Unpublished Report No. P.RSA/00/0699. Department of Water Affairs and Forestry: Pretoria, South Africa.

Swanepoel, D., Kriek, N.P.J. and Boomker, J.D.F., 2000. Selected chemical parameters in the blood and metals in the organs of the Nile crocodile, *Crocodylus niloticus*, in the Kruger National Park. *Onderstepoort Journal of Veterinary Research, 67*, 141-148.

Tanaka, K.R., Van Houtan, K.S., Mailander, E., Dias, B.S., Galginaitis, C., O'Sullivan, J., Lowe, C.G. and Jorgensen, S.J., 2021. North Pacific warming shifts the juvenile range of a marine apex predator. *Scientific Reports, 11*, 1-9.

Than, K.Z., Strine, C.T., Sritongchuay, T., Zaw, Z. and Hughes, A.C., 2020. Estimating population status and site occupancy of saltwater crocodiles *Crocodylus porosus* in the Ayeyarwady delta, Myanmar: Inferences from spatial modeling techniques. *Global Ecology and Conservation*, *24*, e01206.

Thapa, G.J., Thapa, K., Thapa, R., Jnawali, S.R., Wich, S.A., Poudyal, L.P. and Karki, S., 2018. Counting crocodiles from the sky: monitoring the critically endangered gharial (*Gavialis gangeticus*) population with an unmanned aerial vehicle (UAV). *Journal of Unmanned Vehicle Systems*, *6*, 71-82.

Tmušić, G., Manfreda, S., Aasen, H., James, M.R., Gonçalves, G., Ben-Dor, E., Brook, A., Polinova, M., Arranz, J.J., Mészáros, J. and Zhuang, R., 2020. Current practices in UAS-based environmental monitoring. *Remote Sensing, 12*, 1001.

Toffanin, P., 2019. OpenDroneMap: The Missing Guide. UAV4GEO, first edition.

Ventura, D., Bonifazi, A., Gravina, M.F., Belluscio, A. and Ardizzone, G. 2018. Mapping and classification of ecologically sensitive marine habitats using unmanned aerial vehicle (UAV) imagery and object-based image analysis (OBIA). *Remote Sensing*, *10*, 1331.

Wang, D., Shao, Q. and Yue, H., 2019. Surveying wild animals from satellites, manned aircraft and unmanned aerial systems (UASs): A review. *Remote Sensing*, *11*, 1308.

Wallace, K., Leslie, A. and Coulson, T., 2013. Re-evaluating the effect of harvesting regimes on Nile crocodiles using an integral projection model. *Journal of Animal Ecology*, *82*, 155-165.

Warner, J.K., Combrink, X., Calverley, P., Champion, G. and Downs, C.T., 2016. Morphometrics, sex ratio, sexual size dimorphism, biomass, and population size of the Nile crocodile (*Crocodylus niloticus*) at its southern range limit in KwaZulu-Natal, South Africa. *Zoomorphology*, *135*, 511-521.

Woodborne, S., Huchzermeyer, K.D.A., Govender, D., Pienaar, D.J., Hall, G., Myburgh, J.G., Deacon, A.R., Venter, J. and Lübcker, N., 2012. Ecosystem change and the Olifants River crocodile mass mortality events. *Ecosphere*, *3*, 1-17.

Woodward, A.R. and Moore, C.T., 1993. Use of crocodilian night count data for population trend estimation. In *Proc. 2nd Regional Conference of the Crocodile Specialist Group, Species Survival Commission, IUCN*. 12-13.

Xu, X., Zhang, Y., Chen, Q., Li, N., Shi, K. and Zhang, Y., 2020. Regime shifts in shallow lakes observed by remote sensing and the implications for management. *Ecological Indicators*, *113*, 106285.

Zucoloto, R.B., Bomfim, G.C., de Campos Fernandes, F.M., Schnadelbach, A.S., Piña, C.I. and Verdade, L.M., 2021. Effective population size of broad-snouted caiman (*Caiman latirostris*) in Brazil: A historical and spatial perspective. *Global Ecology and Conservation*, *28*, e01673.

CHAPTER 2

The application and limitations of a low-cost UAV platform and open source-software combination for ecological mapping and monitoring

Albert Myburgh[1,4], Hannes Botha [2,3], Colleen T. Downs[1*] and Stephan M. Woodborne[4]

[1]*Centre for Functional Biodiversity, School of Life Sciences, University of KwaZulu-Natal, Private Bag X01, Scottsville, Pietermaritzburg, 3209, South Africa*

[2]*Scientific Services, Mpumalanga Tourism and Parks Agency, Nelspruit, South Africa*

[3]*Department of Biodiversity, University of Limpopo, Limpopo, South Africa*

[4]*iThemba LABS, Private Bag 11, WITS, South Africa*

African Journal of Wildlife Research - published

African Journal of Wildlife Research 51: 166–177. https://doi.org/10.3957/056.051.0166

*** Corresponding Author:** Colleen T. Downs

Email: downs@ukzn.ac.za; **ORCID:** http://orcid.org/0000-0001-8334-1510

Other emails and ORCIDs:

A Myburgh Email: Albert.isotopes@gmail.com; ORCID: http://orcid.org/0000-0002-6891-1893

H Botha Email: nilecrocs@mweb.co.za; ORCID: https://orcid.org/0000-0001-6870-5494

SM Woodborne Email: Swoodborne@tlabs.ac.za; https://orcid.org/0000-0001-8573-8626

Running header: Low-cost drones for ecological monitoring

2.1 Abstract

Low-cost uncrewed aerial vehicles (UAVs) have become ubiquitous, and advanced UAV systems are affordable for many field ecologists and wildlife managers. Many hobbyist UAVs have been applied to ecological studies, but proprietary software limits their widespread application with little quantification with regards to their accuracy and efficiency in the creation of maps through photogrammetry. Our study addressed these concerns by evaluating a combination of an entry-level UAV and open-source photogrammetry drone mapping software as a low-budget mapping solution for ecologists. Geometrically accurate orthophotograph maps were created from flights at altitudes below 70 m with and without differential global positioning system (d-GPS) ground control points. Object measurement errors were constrained below 30 mm for altitudes up to 70 m, and errors fell below 10 mm at 30 m altitudes with d-GPS points and below 20 mm without the use of d-GPS ground control points. Our analyses provide guidelines that parameterise the requirements for the mapping of smaller areas. Ecological surveys that do not require <50 mm accuracy can benefit from the methods described here, and many ecological studies that are presently using costly software and UAV platforms could save when adopting this approach.

Keywords: Consumer-grade UAV; Drone; DJI; Ecological monitoring; Measurement accuracy; Mapping; Photogrammetry

2.2 INTRODUCTION

Effective ecological management requires accurate observational data that are not budget-dependent and have relevant timelines (Hodgson *et al*., 2018; Fust and Loos, 2020). Remote sensed ecological research based on optical sensors operating in the red-green-blue visible spectrum (hereafter RGB) traditionally use satellite imagery and, where higher resolution is required, relatively costly helicopter or fixed-wing aircraft surveys (Wang, Shao, and Yue, 2019). Ecological data (e.g., land use, plant phenotyping, habitat classification and wildlife counts) are accessible through emerging technologies such as higher resolution satellite imagery (e.g., Sentinel-2 imagery as compared with images from the older Landsat series of satellites) or unmanned aerial vehicles (UAVs), and the cost of ecological monitoring is generally decreasing dramatically (Christie, Gilbert, Brown, Hatfield, and Hanson 2016; Wang *et al*., 2019). UAVs, commonly referred to as "drones", are increasingly being used in ecological surveys to monitor, map and track wildlife populations, vegetation dynamics and resource quantities (Guo *et al*., 2018; Ventura, Bonifazi, Gravina, Belluscio, and Ardizzone, 2018; Ren, Zhao, Xiao, and Hu, 2019; Tmušić *et al*., 2020). Widespread use of UAV-based surveys has been limited by proprietary post-flight processing software and relatively costly UAVs and equipment (Anderson and Gaston 2013; Buters *et al*., 2019; Groos *et al*., 2019).

UAVs equipped with RGB sensors are being applied as tools for mapping areas when combined with photogrammetry software (Hodgson, Baylis, Mott, Herrod and Clarke, 2016; Crutsinger, Short, and Sollenberger, 2016; Hodgson *et al*., 2018; Ezat, Fritsch, and Downs, 2018; Groos *et al*., 2019; Scarpa and Pina 2019). Photogrammetry (taking measurements from photographs) relies on overlapping images of an area/object of interest, identifying key scene features through mostly proprietary scene recognition algorithms (Fuller, Collier, and Seager, 2011; Gatziolis, Lienard, Vogs, and Strigul, 2015). Most UAV focused photogrammetry software (e.g., Pix4D and DroneDeploy) are relatively costly subscription-based packages that

outprice many hobby-grade UAVs on an annual basis: at the time of writing (end-2021), a basic Pix4D package costs ~US$ 291.67 monthly (see https://www.pix4d.com/pricing) (~US$ 3492 annually) compared with the purchase price of a mid-range hobby UAV (DJI Mavic Air 2 at ±US$ 799; with slight variations in price depending on the supplier).

OpenDroneMap (ODM) is an open-source software package specifically for UAV based photogrammetry for mapping and three-dimensional modelling of large areas. Originally only available as a command-line interface-driven package, it now has an additional user interface (WebODM) that runs on a local system without an internet connection. ODM can use aerial images (whether georeferenced or not) to construct orthophotographs, terrain and surface models (digital elevation models (DEMs) and digital surface models (DSMs)) and 3-dimensional point clouds of large areas. It is a viable alternative to proprietary packages and has been applied to map and monitor Alpine glaciers with comparable accuracy with a commercial alternative (Pix4D) (Groos *et al*., 2019). Processed orthophotographs and elevation models are output in a raster file format. These can be directly imported into a geographic information system (GIS) environment. Depending on the available hardware (in terms of processing power and the UAV), it can facilitate geometrically accurate, georeferenced mapping of relatively large areas (Groos *et al*., 2019; Toffanin 2019).

Global demand for hobby-grade UAVs coupled with regulations governing maximum weights for unlicensed UAVs (sub-250 g UAVs, e.g., in the United States of America) has fuelled rapid advancement in the miniaturisation and capabilities of these platforms. Relatively small UAVs (such as the DJI® Mini-, the Autel® nano- or Hubsan® ZINO mini-series) are relatively low-cost pocket-sized platforms with range and wind tolerances comparable with their larger counterparts. These platforms have the necessary hardware and software required for obtaining aerial images that can be used to map relatively large areas. Although their

accuracy and efficiency have not been assessed, they may be a sustainable and low-cost option, especially in ecology where sub-centimetre level accuracy is not required.

DJI is a popular supplier of UAVs with a broad range of products that serve hobbyists and industry. The most widespread DJI sensor is a 12-megapixel (4.63 mm x 6.71 mm) complementary metal-oxide semiconductor (CMOS) RGB sensor that has been used in several UAV models for various ecological studies (Cruzan *et al*., 2016; Schofield, Katselidis, Lilley, Reina, and Hays, 2017; Marx, McFarlane, and Alzahrani, 2017; Ezat *et al*., 2018; Fritsch and Downs, 2020). The most affordable package from DJI that carries the 12-megapixel sensor on a three-axis gimbal is the DJI Mavic Mini (recently also as the DJI Mini SE and Mini 2). The Mavic Mini is equipped with a global positioning system (GPS) and three-axis gimbal to stabilise and georeference aerial imagery. It can be flown with third-party flight software applications that make provision for the requirements of mapping where flight variables can be controlled, reported and repeated. The DJI Mavic Mini represents the best compromise between ground sampling distance (GSD in cm/pixel) and price within the DJI range, with a GSD of 3.56cm/px at 100 m altitude and a retail price of ~$ 399 (variable by supplier) at the time of writing.

While well-funded companies, projects and the private sector can often afford to implement commercially available UAV techniques, equipment and service providers, many ecological studies, wildlife managers and field rangers, especially in the developing world, would benefit from low-cost UAV mapping and monitoring. In the present study, we assessed the applicability of DJI's 12mp sensor on the Mavic Mini for remote sensing by comparing the accuracy and efficiency of this UAV, coupled with ODM, under various scenarios. We compared the accuracy between maps created with and without the use of ground control points (GCP) and the effect of various altitudes by empirically measuring objects of known length and GCP offsets. We expected altitude to affect measurement accuracy as the GSD increased.

We expected that fewer photographs and fewer clear ground features would result in sparser point clouds during the photogrammetry process, affecting the geometric accuracy of the resulting models (Toffanin 2019).

2.3 METHODS

We conducted test flights at nine different altitudes (100 m, 90 m, 80 m, 70 m, 60 m, 50 m, 40 m, 30 m, and 20 m (throughout the manuscript, altitude refers to above take-off location)) at two locations using a DJI Mavic Mini flown with Dronelink (Dronelink, 2020) from a smartphone connected to the DJI controller. At both locations, non-altitude flight variables were constant between all flights (Table 2.1), and the UAV started all flights from the same location and flew a south to north orientated flight plan. After each flight mission was completed, the return to home command was automatically initiated, and the UAV returned to its take-off location.

At location 1, flights were pre-programmed to cover a 0.5 ha parking lot adjacent to the Engineering 4.0 building at the University of Pretoria, South Africa, with the Pierre van Reyneveld Memorial in the centre of the parking lot. Here we used a permanently installed low-cost GPS system (Real-time kinematic (RTK) system, accurate to 15 mm) recently developed by Broekman and Gräbe (2021) to define GCP's, which were marked as crosses with dark masking tape for easy identification from aerial imagery. We used a standard tape measure to record the distance (n = 10) between various points in the area (parking bays and signs marked with road paint) (Figure 2.1).

At location 2, flights were all pre-programmed to cover the same 1-ha plot. Land cover in the plot mainly consisted of scattered patches of grassy vegetation, shrubs and rocky outcrops, with minimal elevation changes across the plot. We distributed eight blue polyvinyl chloride (PVC) pipes (four straight 100 mm diameter PVC pipes of lengths: 2003 mm, 1279

mm, 1193 mm and 675 mm; and four flexible 50 mm diameter pipes each 1230 mm in length) within the 1 ha plot to test measurement accuracies. We recorded flight time, battery consumption, and the number of photographs taken for each flight mission. No GCP's were used at this location.

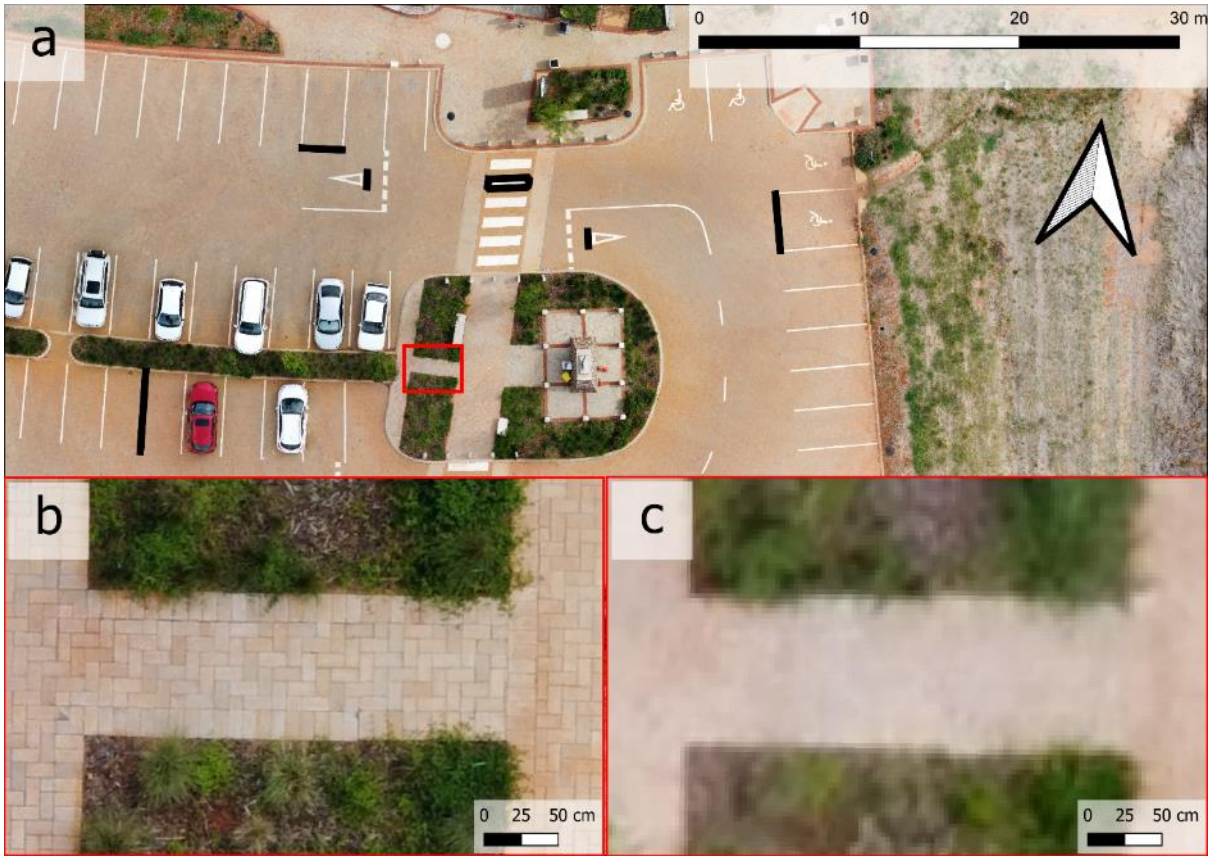

Fig. 2.1. Section of an orthophotograph (a) processed with ground control points (GCP's), with black bars indicating examples of measurements taken to assess accuracy during this study. Images b and c are extracts of the area outlined in red from photographs taken from 20 m and 100 m altitudes, respectively.

Table 2.1. Non-altitude specific flight parameters used in the present study.

Flight variables	**Level**
Image front overlap	80%
Image side overlap	70%
Maximum speed	16.1 km/h
Decent rate	-3 m.s
Ascent rate	3 m.s
Rotation rate	45°/second
Horizontal deceleration	-0.6 m/s^2
Horizontal acceleration	1.8m/s^2
Vertical acceleration	1.8m/s^2
Vertical deceleration	-0.9m/s^2
Rotational acceleration	10°/s^2
Rotational deceleration	-10°/s^2
Reference location	Take-off location
Flight pattern	Dronelink mode: Normal
Image capture angle pitch	-90° (nadir)

2.3.1 Image processing and analyses

We processed all image sets with ODM (version 1.9.2 build 28) through the Windows native WebODM interface on a desktop computer running a hexacore processor (4.2 GHz with 32 GB of DDR4 RAM). Images from flights at location 1 were processed using the default WebODM settings with the orthophotographs resolution set to the GSD of the sample images. These image sets were processed with and without GCP files (see Toffanin (2019) for instructions on using GCP's in ODM), resulting in a total of 18 orthophotographs from nine flights. Images from location 2 were processed using the default settings with the

orthophotograph resolution set to the resolution of the sample images except for those images from altitudes 60 m and above. These were rerun using the *High-Resolution* option in ODM, which increases the point density of generated point clouds and mesh resolution of 3-d models. It also increases orthophotograph resolution to 2 cm/ pixel, which determines the resolution of the output orthophotograph irrespective of the resolution of the original images. This was done as resolutions coarser than 2 cm/ pixel resulted in blurred edges, making it difficult to identify pixels representing the edges of the PVC pipes.

We imported all orthophotograph output from ODM into QGIS (QGIS 2021, version 3.18), and we measured objects by drawing a line (vector line/multiline layer) from the first to the last pixel representing the object/marking. Thereafter, we used the 'add geometry attributes' geoprocessing tool to measure the length of each line. We used the distance measurement tool in QGIS to assess the distance offset between the GCP markings in photographs processed with and without GCP files.

During photogrammetry in ODM, the first stage in the structure from motion (sfM) process is the recognition and matching of key features to produce a sparse point cloud. The density of this point cloud can yield a lot of information on the model's overall accuracy as more point recognitions are generally associated with more accurate models (Toffanin 2019). These sparse point cloud data were extracted from the .laz files, output from ODM using the fast orthophotograph mode (this mode skips point cloud densification), through Fugro™ viewer, and points per square meter were determined by dividing the total number of points in sparse point clouds by the total area represented by the orthophotograph. We determined the total area represented by each orthophotograph by extracting the geometry attributes of orthophotographs in QGIS.

We did not focus on the vertical error in the current approach as the focus was on two-dimensional map creation, but we assessed the vertical accuracy of models created in ODM by

comparing the height estimate of the Pierre van Reyeneveld Memorial and several other features (a concrete pillar/university sign/street lamp and speed ramp, n = 5) across altitudes using WebODM's built in 3D measurement tools and we included a sample terrain model and textured model created of the Pierre van Reyenveld Memorial for comparison with previous studies of the same structure (Appendix 2.1; Broekman and Gräbe (2021)).

We used a Student's t-test to compare measurement errors between those photograph sets processed with and without GCP's and an analysis of variance (ANOVA) to evaluate measurement errors across altitudes in R (R Core team (2021)) through the R studio interface (RStudio team, 2021). We used an ANOVA to test whether GCP's or altitude had the most significant effect on GPS offsets. If there is a significant difference between the offset of GCP's then ODM orthophotographs are not geometrically correct, whilst a relative offset across all GCP's would mean that ODM orthophotographs are geometrically correct but that the Mavic Mini's GPS is not as accurate as an RTK system. All graphs and regressions were derived in Microsoft Excel® (Office 2019).

2.4 RESULTS

At location 1, measurement errors of objects with known dimensions differed significantly between images processed with and without ground control points ($p < 0.05$, $n = 90$) across all flights combined, but there were no significant differences between absolute errors for altitudes 70 m and below between images processed with and without GCP's ($p > 0.1$, $n = 50$). Below 70 m altitude, GCP's had no measurable effect on measurement accuracy when using the present hardware. For those images processed with GCP's, altitude had no significant effect on measurement error (ANOVA, $F = 0.113$, $p > 0.5$), although the variance associated with mean absolute error increased with altitude (Figure 2.2).

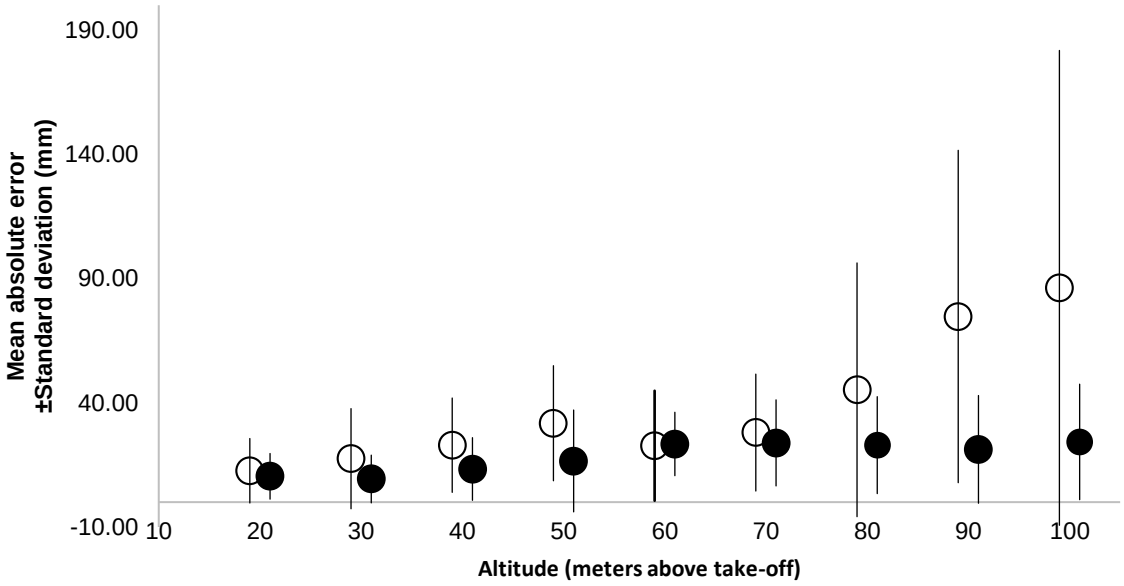

Fig. 2.2. Mean absolute error (MAE) of object measurements from orthophotographs processed with and without ground control points (GCP's) from various altitudes. (Solid circles represent mean errors from orthophotographs processed with GCP's. Open circles represent mean errors from orthophotographs processed without GCP's. Solid lines represent the standard deviation associated with MAE's).

Vertical accuracy did not differ significantly from actual height measurements ($p > 0.1$, $n = 5$) for all heights below 70 m. Above 70 m, it was impossible to measure the height of the desired objects as only two of the five objects had associated points in the rendered point clouds (Figure 2).

At location 2, flight times, number of photographs and battery consumption were all related to altitude (Table 2.2), whilst measurement errors of PVC pipes were significantly influenced by altitude (ANOVA, $F = 10.9$, $p < 0.01$) (Figure 2.4). Measurement errors at location 2 did not differ from measurement errors at the same altitudes from tests at location 1 ($p > 0.1$, $n = 9$). The derived measurement errors were thus constrained between different areas and were related to altitude.

Although flights were programmed to cover the same areas, we found when evaluating the size of the produced orthophotographs that flights at higher altitudes inevitably created larger orthophotograph maps as the camera's field of view included larger sections along the periphery of the area of interest. We used the area covered by the entire point cloud to derive point cloud densities, and plot these relative to mean absolute errors (Figure 2.5). There was an inverse relationship between the point cloud density and the accuracy of orthophotographs across all flights processed without GCP points where:

$a = 174.21\ p^{-0.417}$ $R^2 = 0.4131$

where p is the point cloud density (in pixels per square meter (px/m^2)), and a represents the geometric accuracy (expressed as mean absolute error of measurements (MAE)).

Table 2.2. Flight and processing parameters for a DJI Mavic Mini mapping a 1 ha plot flown with Dronelink and processed with OpenDroneMap photogrammetry software in the present study.

Altitude (m)	**100**	**90**	**80**	**70**	**60**	**50**	**40**	**30**	**20**
GSD (Ground sampling distance (cm/px)	3.56	3.2	2.84	2.49	2.13	1.78	1.42	1.07	0.71
Distance travelled (m)	424	402	685	599	694	770	753	1000	1400
Mission flight time (minutes:seconds)	02:02	01:59	02:28	02:23	02:50	03:21	03:44	05:53	11:07
Number of photographs	10	11	18	27	31	58	59	126	285
Battery consumption (%)	17	13	16	18	18	22	22	26	50

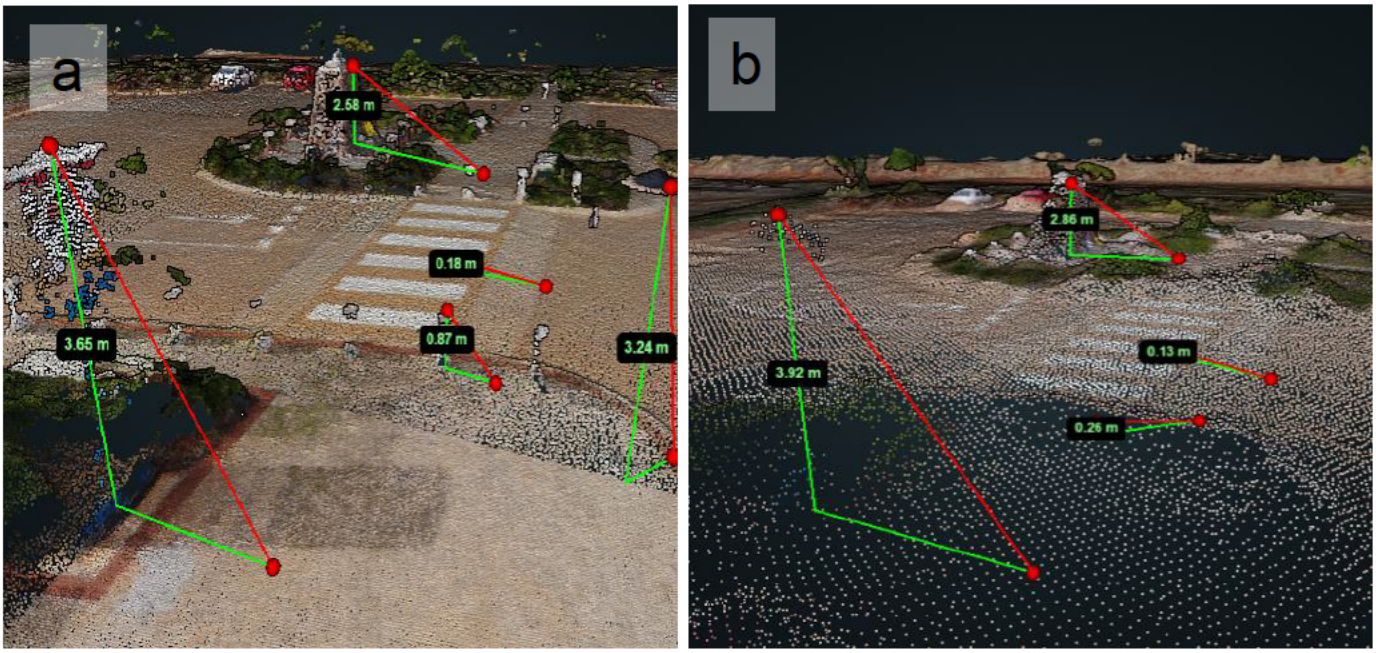

Fig. 2.3. Point clouds created in Open Drone Map (ODM) with height measurements using the built-in measurement tool in WebODM where a. is modelled from aerial images taken at 20 m altitude, while b. is modelled from aerial images taken from 90 m altitude. Some features such as the lampshade (on the right border of a) and the concrete pillar (centre of a, 0.87 m high) failed to produce key scene features needed for point cloud creation from 90 m altitude.

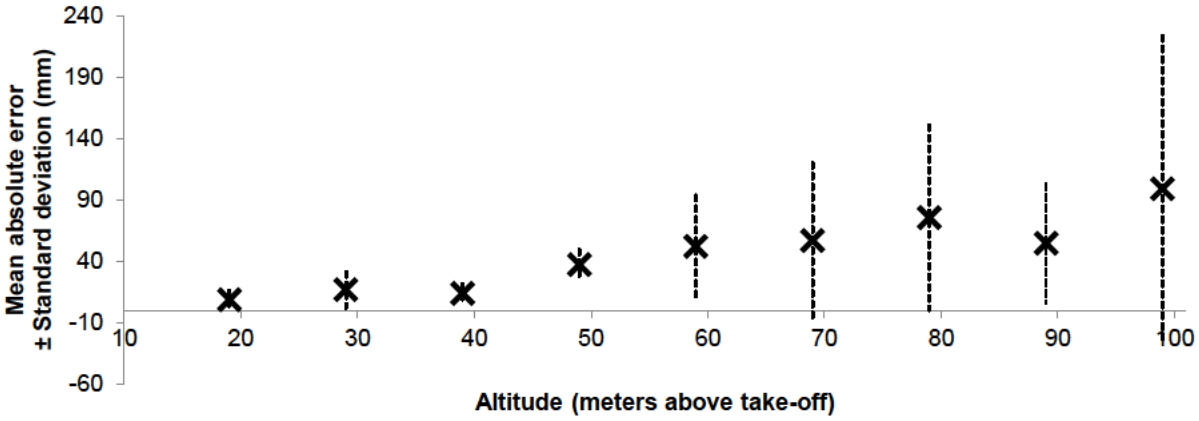

Fig. 2.4. Mean absolute error (MAE) related to PVC measurements from orthophotographs from each altitude at location 2 in the present study. (Dashed lines represent the standard deviation associated with the MAE at the respective altitude).

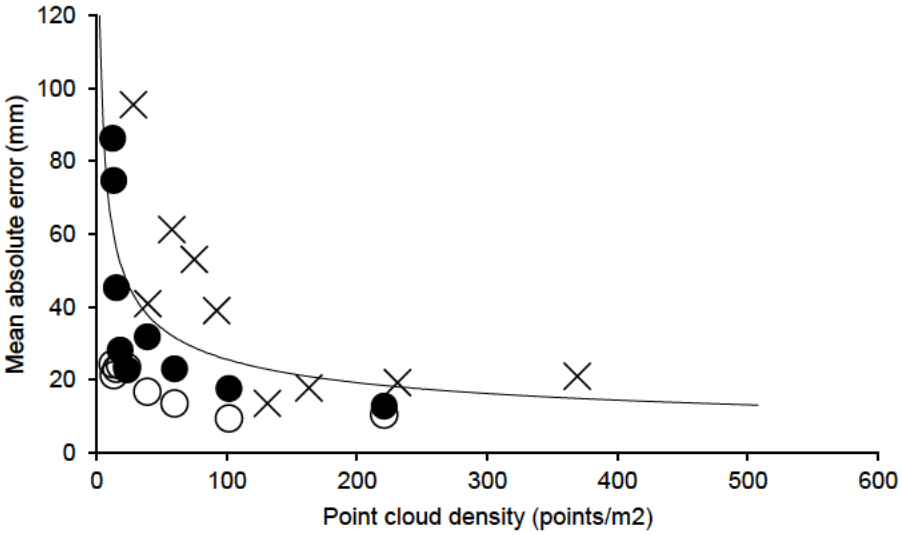

Fig. 2.5. Mean absolute errors across all flights plotted against the sparse point cloud density. (Open circles represent errors associated with images processed with GCP points. Solid circles represent errors from orthophotographs taken at location 1, while crosses are errors from orthophotographs taken at location 2 during the present study).

2.5 DISCUSSION

We found orthophotographs produced from DJI Mavic Mini images and processed through ODM photogrammetry software were geometrically accurate (errors constrained below 100mm) if the UAV was kept below 70 m altitude. Without GCP's for orthophotograph correction, altitude was the primary factor affecting the accuracy of measurements taken from orthophotographs output from ODM. The effect of orthophotograph correction through GCP use is evident at higher altitudes, where fewer key scene features are recognised, and sparse point clouds have lower densities. Above 70 m, GCP's compensate for lack of geometric accuracy, and so the Mavic Mini should not be used when accurate measurements are required without GCP's at altitudes higher than 70 m. Apart from the use of GCP's the orthophotograph resolution affected the pixilation of the start and end of objects of interest, especially in the case of the PVC pipes. There was a subjective assignment of an individual pixel as part of the object, as not part of the object, or that the object edge fell somewhere within the pixel because the pixel itself was neither distinctively the colour of the object, nor the colour of the background. This introduced variance, even with the use of GCP's, as coarser resolutions resulted in larger subjective pixel offsets.

The processing resolution and flight altitude should be tailored to the target measurement's desired accuracy, and oversampling should be avoided. In certain circumstances, the desired accuracy may be less than the default setting and processing time can be substantially reduced by increasing the orthophotograph resolution parameter (up to the GSD of the original sample images). This introduces issues of efficiency as improved resolution in the orthophotograph measurements is limited by GSD. Improved GSD implies a smaller footprint of the flight path for the same battery life of the UAV, and a substantial increase in the number of required photographs. This has a knock-on effect on processing demands on the system (both computing power and processing time) as processing times and

the maximum number of images increase linearly with cores, clock rate, as well as RAM and hard drive size and speed (Toffanin, 2019). Flight planning software provides estimates on GSD, number of photographs and flight times so that these factors can be considered beforehand. UAV systems with cameras capable of taking higher-resolution photographs should be used when greater accuracy is required, and flights are limited to minimum altitudes or when flight times are constrained.

When images are processed without GCP's, errors increase with altitude. To elucidate the underlying reasons for the unaccounted error, it is necessary to understand the photogrammetry process. It comprises two steps. Firstly is the production of a point cloud derived only from key scene features that the software identifies in successive photographs (due to photograph overlap), this is known as the "sparse point cloud". The point cloud density of sparse point cloud models is not affected by the processing resolution, and processed orthophotographs are produced after the initial point cloud is created, so that point counts do not vary between orthophotographs processed at different resolutions. Essentially, if the same set of photographs are processed at various resolutions, the sparse point cloud density remains constant. The sparse point cloud informs the second step of the photogrammetry process. This interpolation process (point cloud densification, meshing and texturing), from each point in the sparse point cloud, produces the final orthophotograph and three-dimensional model (see Toffanin (2019) for a breakdown of the photogrammetry process in ODM). The sparse point cloud's point density was a good proxy for the empirical accuracy of orthophotographs, and in this study, point cloud densities of >100 points per m2 were associated with measurement errors below 20 mm. The sparse point cloud density was calculated at the scale of the entire orthophotograph, so the accuracy of the dimensions of a target feature will be affected by the number of points in that vicinity of the orthophotograph.

To increase the number of key scene features, and therefore, the number of points in the sparse point cloud model, the following should be considered. Firstly, flying lower and slower. Decreasing the altitude of flights increases the clarity of objects in images resulting in more point recognitions. Some researchers have suggested stopping and hovering the UAV in order to capture images (Cruzan et al., 2016), but this increases flight times and decreases the area that could potentially be surveyed. Furthermore, UAVs are more efficient (require less energy per unit time) during constant forward flight (Hwang et al., 2018). Secondly, image overlap can be adjusted to increase the number of key scene features that could potentially be identified between images. Increasing image overlap will result in more images and greater processing times. Thirdly, landscape heterogeneity also influences accuracy as more heterogonous areas yield more key scene features in a landscape. This is a known shortfall of the photogrammetry process when compared with alternatives such as LIDAR (Adams and Chandler, 2002). Extremely reflective surfaces often result in large open patches in point clouds where the software fails to recognise key scene features between photographs; these include photographs taken over water where alternative methods should be considered (Nocerino and Menna, 2020). Deployment of reference targets is an alternative but can be troublesome in some environments (e.g. when surveying remote river reaches for crocodilian population census (Ezat et al., 2018)). The accuracy/density of the sparse point cloud is also affected by other factors that should be considered in ecological studies. The effect of wind on vegetation is an example. Any movement of vegetation between photographs results in recognition of fewer key features with a reduction in orthophotographs' accuracy and clarity (Probst, Gatziolis, and Strigul, 2018).

Although low-cost UAV's have been broadly applied in ecological studies (Cruzan et al., 2016; Schofield et al., 2017; Marx et al., 2017; Ezat et al., 2018; Fritsch and Downs, 2020), none have considered the use of open-source software and sub 250 g UAVs as an alternative

to proprietary packages and larger, more expensive UAV platforms. For example, Cruzan et al. (2016) used a DJI Phantom Vision 2+ (12mp CMOS RGB sensor) to map small plots (1 - 16 ha) to produce vegetation cover maps. They used the proprietary software package, AgiSoft PhotoScan (AgiSoft LLC, St. Petersburg, Russia), priced at ~US$ 3499 (see https://www.agisoft.com/buy/online-store/) at the time of writing, almost ten times the price of their UAV. They further flew the UAV manually at 40 m altitude, hovering in place to capture an image every 15 m, covering a total of 16 ha in 4 h over a span of 2 days, using 10 UAV batteries. Although they did not make any reference to their final accuracy or their required accuracy, the techniques evaluated in the present study could produce an orthophotograph of their study area at a fraction of the cost with 30 min of flying time (2 batteries) and a quantified absolute error of 13 - 40 ± 10 mm (depending on the use of d-GPS, GCP's).

Although we did not evaluate the accuracy of complete elevation models output from ODM in this study, Cruzan et al. (2016) required DEM's capable of differentiating trees from shrubs, something which ODM should be capable of at altitudes up to 100 m, provided that the vegetation yields key scene feature points (Toffanin, 2019). Ezat et al. (2018) used a DJI Phantom 3 (12mp CMOS RGB sensor) and the proprietary software package DroneDeploy (~US$ 299 per month) to produce orthophotographs of Lake Nyamithi, Ndumo Game Reserve, South Africa. The required flight height for the detection and measurement of Nile crocodiles (Crocodylus niloticus) in their study was 55 m altitude. Using the current methods would provide an absolute measurement accuracy of 37.2 ± 12 mm at 50 m altitude, a considerable improvement over typical techniques for crocodilian monitoring (Ferreira and Pienaar, 2011). Fritsch and Downs (2020) surveyed narrow river reaches and lakes using a DJI Phantom 3 and used unprocessed images to conduct counts of common hippopotamus (*Hippopotamus amphibius*) populations through manual flight control without any image post-processing. The

current techniques could be applied to their study to maintain consistency in flight and processing parameters. This could add value to their study in that hippopotamus locations could be accurately determined (with ± 4 m geographic accuracy) for space use analyses when combined with georeferenced orthophotographs produced by ODM. Manual control of UAVs is also subject to fluctuations in flight speed and direction, and pre-planned flight plans can improve efficiency and flight distance and enable accurate method repetition (Hwang et al., 2018).

The present study quantified the empirical errors obtained from a relatively low-cost UAV to perform photogrammetry missions. Although we used ground control points (GCP's), the aim was to determine the accuracy of a low-cost approach to photogrammetry and the open-source software ODM, and we showed that accurate measurements could be obtained at altitudes up to 70 m without the need for GCP's. GPS offsets recorded in this study showed that UAV based mapping that requires accurate spatial information (<4 m accuracy) should identify several GCP's that can be used to align and georeference aerial imagery to ensure repeatability and replicability between surveys. For a low-cost alternative, the orthophotographs generated in ODM could be imported into a global information system (GIS) system where a georeferencing tool and satellite imagery can provide GCP points if no GCP points were pre-defined or as a last resort if no other sources of geo-correction are available. The approach used in this study should enable researchers that are not currently applying UAV based mapping or monitoring as part of their study design to apply the technique at relatively low costs with quantifiable error. The errors presented here should enable researchers that are not familiar with UAV mapping to make an informed decision on the required accuracy for their research and the corresponding flight and processing parameters.

Examples of where the present technique may be applied include: Small scale land-use change analyses, vegetation cover mapping and monitoring, and wildlife surveys, especially in

small reserves and constrained habitats (such as waterways for amphibious vertebrate counts and size estimates). The technique can also be used to supplement current ecological monitoring, such as habitat classification for small mammal studies (Herrera et al., 2020). For these studies, flights at 50 m altitudes or below can be used to quantify (in square meters) habitat types associated with small mammal trap positions. Another use could be determining the percentage of canopy cover in small forest patches in studies investigating forest regeneration (Rolo, Olivier, and van Aarde, 2017) or the effects of fire (Veenendaal et al., 2018). Here higher altitude flights would be sufficient as ground-truthing can identify tree species, whilst orthophotographs can be used to quantify canopy cover.

2.6 CONCLUSIONS

We found that DJI's 12-megapixel sensor on the Mavic Mini can be used to effectively measure objects with definable accuracy when combined with open-source photogrammetry, GIS software and flight planning packages. This can allow accurate size quantification from maps of relatively large areas at an extremely low cost compared with previous studies (Cruzan et al., 2016; Ezat et al., 2018). The GSD and processing resolution and the initial point cloud density generated by ODM can be used to indicate model accuracy. The methods used in the present study provide an inexpensive approach to UAV based mapping that is orders of magnitude more affordable than commercial alternatives. It requires a single initial investment and does not need monthly software subscriptions nor high maintenance costs. There is no need for any assembly of self-built UAV platforms, and can be adapted and used with any "out of the box" UAV with quantifiable errors. The UAV used in this study was both low-cost and comparatively small (245 x 289 mm as measured from the tips of the propellers when open and 140 x 81 mm when folded for packing). This makes its use ideal in situations where a low-profile UAV with minimal disturbance is required or for research in remote areas where UAV

surveys are not the primary research objective, and packing space is limited. While the budget approach may be perfectly adequate for certain ecological applications, it remains clear that more expensive systems, including RTK, PPK or d-GPS technologies, mechanical shutter cameras, and high pixel density sensors, will always yield the best precision and accuracy that the technique offers.

2.7 ACKNOWLEDGEMENTS

We are grateful to the National Research Foundation (ZA, Grant 98404) and the University of KwaZulu-Natal (ZA) for funding.

2.8 REFERENCES

Adams, J., and Chandler, J. (2002). Evaluation of LIDAR and medium scale photogrammetry for detecting soft-cliff coastal change. *Photogrammetric Record*, *17*, 405-418. https://doi.org/10.1111/0031-868x.00195

Anderson, K., and Gaston, K.J., (2013). Lightweight unmanned aerial vehicles will revolutionize spatial ecology. *Frontiers in Ecology and the Environment*, *11*, 138-146. https://doi.org/10.1890/120150

Buters, T.M., Bateman, P.W., Robinson, T., Belton, D., Dixon, K.W., and Cross, A.T. (2019). Methodological ambiguity and inconsistency constrain unmanned aerial vehicles as a silver bullet for monitoring ecological restoration. *Remote Sensing*, *11*, 1180. https://doi.org/10.3390/rs11101180

Broekman, A. and Gräbe, P.J. (2021). A Low-Cost, Mobile Real-Time Kinematic Geolocation Service for Engineering and Research Applications. HardwareX, e00203. https://doi.org/10.1016/j.ohx.2021.e00203

Christie, K.S., Gilbert, S.L., Brown, C.L., Hatfield, M., and Hanson, L. (2016). Unmanned aircraft systems in wildlife research: current and future applications of a transformative technology. *Frontiers in Ecology and the Environment*, *14*, 241-251. https://doi.org/10.1002/fee.1281

Crutsinger, G.M., Short, J., and Sollenberger, R. (2016). The future of UAVs in ecology: an insider perspective from the Silicon Valley drone industry. *Journal of Unmanned Vehicle Systems*, *4*, 161-168. https://doi.org/10.1139/juvs-2016-0008

Cruzan, M.B., Weinstein, B.G., Grasty, M.R., Kohrn, B.F., Hendrickson, E.C., Arredondo, T.M., and Thompson, P.G. (2016). Small unmanned aerial vehicles (micro-UAVs, drones) in plant ecology. *Applications in Plant Sciences*, *4*, 1600041. https://doi.org/10.3732/apps.1600041

Ezat, M.A., Fritsch, C.J., and Downs, C.T. (2018). Use of an unmanned aerial vehicle (drone) to survey Nile crocodile populations: a case study at Lake Nyamithi, Ndumo Game Reserve, South Africa. *Biological Conservation*, *223*, 76-81. https://doi.org/10.1016/j.biocon.2018.04.032

Ferreira, S.M. and Pienaar, D. (2011). Degradation of the crocodile population in the Olifants River gorge of Kruger National Park, South Africa. *Aquatic Conservation: Marine and Freshwater Ecosystems*, 21, 155-164. https://doi.org/10.1002/aqc.1175

Fust, P., and Loos, J. (2020). Development perspectives for the application of autonomous, unmanned aerial systems (UASs) in wildlife conservation. *Biological Conservation*, *241*, 108380. https://doi.org/10.1016/j.biocon.2019.108380

Fritsch, C., and Downs, C.T. (2020). Evaluation of low-cost consumer-grade UAVs for conducting comprehensive high frequency population censuses of hippopotamus populations. *Conservation Science and Practice*, *2*, e281. https://doi.org/10.1111/csp2.281.

Fuller, S., Collier, P., and Seager, J. (2008). Assessing and reporting real-time data quality for GNSS reference stations. *Journal of Spatial Science*, *53*, 149-159. https://doi.org/10.1080/14498596.2008.9635155

Gatziolis, D., Lienard, J.F., Vogs, A., and Strigul, N.S. (2015). 3D tree dimensionality assessment using photogrammetry and small unmanned aerial vehicles. *PloS One*, *10*, e0137765. https://doi.org/10.1371/journal.pone.0137765

Groos, A.R., Bertschinger, T.J., Kummer, C.M., Erlwein, S., Munz, L., and Philipp, A. (2019). The potential of low-cost UAVs and open-source photogrammetry software for high-resolution monitoring of Alpine glaciers: a case study from the Kanderfirn (Swiss Alps). *Geosciences*, *9*, 356. https://doi.org/10.3390/geosciences9080356

Guo, X., Shao, Q., Li, Y., Wang, Y., Wang, D., Liu, J., Fan, J., and Yang, F. (2018). Application of UAV remote sensing for a population census of large wild herbivores—taking the Headwater Region of the Yellow River as an example. *Remote Sensing*, *10*, 1041. https://doi.org/10.3390/rs10071041

Herrera, J.P., Wickenkamp, N.R., Turpin, M., Baudino, F., Tortosa, P., Goodman, S.M., Soarimalala, V., Ranaivoson, T.N., and Nunn, C.L. (2020). Effects of land use, habitat characteristics, and small mammal community composition on Leptospira prevalence in northeast Madagascar. *PLOS Neglected Tropical Diseases*, *14*, e0008946. https://doi.org/10.1371/journal.pntd.0008946

Hodgson, J.C., Baylis, S.M., Mott, R., Herrod, A., and Clarke, R.H. (2016). Precision wildlife monitoring using unmanned aerial vehicles. *Scientific Reports*, *6*, 1-7. https://doi.org/10.1038/srep22574

Hodgson, J.C., Mott, R., Baylis, S.M., Pham, T.T., Wotherspoon, S., Kilpatrick, A.D., Raja Segaran, R., Reid, I., Terauds, A., and Koh, L.P. (2018). Drones count wildlife more accurately and precisely than humans. *Methods in Ecology and Evolution*, *9*, 1160-1167. https://doi.org/10.1101/165019

Hwang, M.H., Cha, H.R., and Jung, S.Y. (2018). Practical endurance estimation for minimizing energy consumption of multirotor unmanned aerial vehicles. *Energies*, 11, 2221. https://doi.or/10.3390/en11092221

Marx, A., McFarlane, D., and Alzahrani, A. (2017). UAV data for multi-temporal Landsat analysis of historic reforestation: a case study in Costa Rica. *International Journal of Remote Sensing*, *38*, 2331-2348. https://doi.org/10.1080/01431161.2017.1280637

Nocerino, E., and Menna, F. (2020). Photogrammetry: linking the world across the water surface. *Journal of Marine Science and Engineering*, *8*, 128. https://doi.org/10.3390/jmse8020128

Probst, A., Gatziolis, D., and Strigul, N. (2018). Intercomparison of photogrammetry software for three-dimensional vegetation modelling. *Royal Society Open Science*, *5*, 172192. https://doi.org/10.1098/rsos.172192

QGIS Development Team (2021). QGIS Geographic Information System. Open Source Geospatial Foundation Project. http://qgis.osgeo.org

R Core Team (2021). R: A language and environment for statistical computing. R Foundation for Statistical Computing, Vienna, Austria. URL https://www.R-project.org

RStudio Team (2021). RStudio: Integrated Development for R. RStudio, PBC, Boston, MA. http://www.rstudio.com/.

Ren, H., Zhao, Y., Xiao, W., and Hu, Z. (2019). A review of UAV monitoring in mining areas: Current status and future perspectives. *International Journal of Coal Science and Technology*, *6*, 320–333. https://doi.org/10.1007/s40789-019-00264-5

Rolo, V., Olivier, P.I., and van Aarde, R. (2017). Tree and bird functional groups as indicators of recovery of regenerating subtropical coastal dune forests. *Restoration Ecology*, *25*, 788-797. https://doi.org/10.1111/rec.12501

Scarpa, L.J., and Pina, C.I. (2019). The use of drones for conservation: A methodological tool to survey caimans nests density. *Biological Conservation*, *238*, 108235. https://doi.org/10.1016/j.biocon.2019.108235

Schofield, G., Katselidis, K.A., Lilley, M.K., Reina, R.D., and Hays, G.C. (2017). Detecting elusive aspects of wildlife ecology using drones: new insights on the mating dynamics and operational sex ratios of sea turtles. *Functional Ecology*, *31*, 2310-2319. https://doi.org/10.1111/1365-2435.12930

Tmušić, G., Manfreda, S., Aasen, H., James, M.R., Gonçalves, G., Ben-Dor, E., Brook, A., Polinova, M., Arranz, J.J., Mészáros, J., and Zhuang, R. (2020). Current practices in UAS-based environmental monitoring. *Remote Sensing*, *12*, 1001. https://doi.org/10.3390/rs12061001

Toffanin, P. (2019). OpenDroneMap: The Missing Guide. UAV4GEO, first edition. https://odmbook.com/

Veenendaal, E.M., Torello-Raventos, M., Miranda, H.S., Sato, N.M., Oliveras, I., van Langevelde, F., Asner, G.P., and Lloyd, J. (2018). On the relationship between fire regime and vegetation structure in the tropics. *New Phytologist*, *218*, 153-166. https://doi.org/10.1111/nph.14940

Ventura, D., Bonifazi, A., Gravina, M.F., Belluscio, A., and Ardizzone, G. (2018). Mapping and classification of ecologically sensitive marine habitats using unmanned aerial vehicle (UAV) imagery and object-based image analysis (OBIA). *Remote Sensing*, *10*, 1331. https://doi.org/10.3390/rs10091331

Wang, D., Shao, Q. and Yue, H., (2019). Surveying wild animals from satellites, manned aircraft and unmanned aerial systems (UASs): A review. *Remote Sensing*, *11*, 1308. https://doi.org/10.3390/rs11111308

2.9 SUPPLEMENTARY INFORMATION

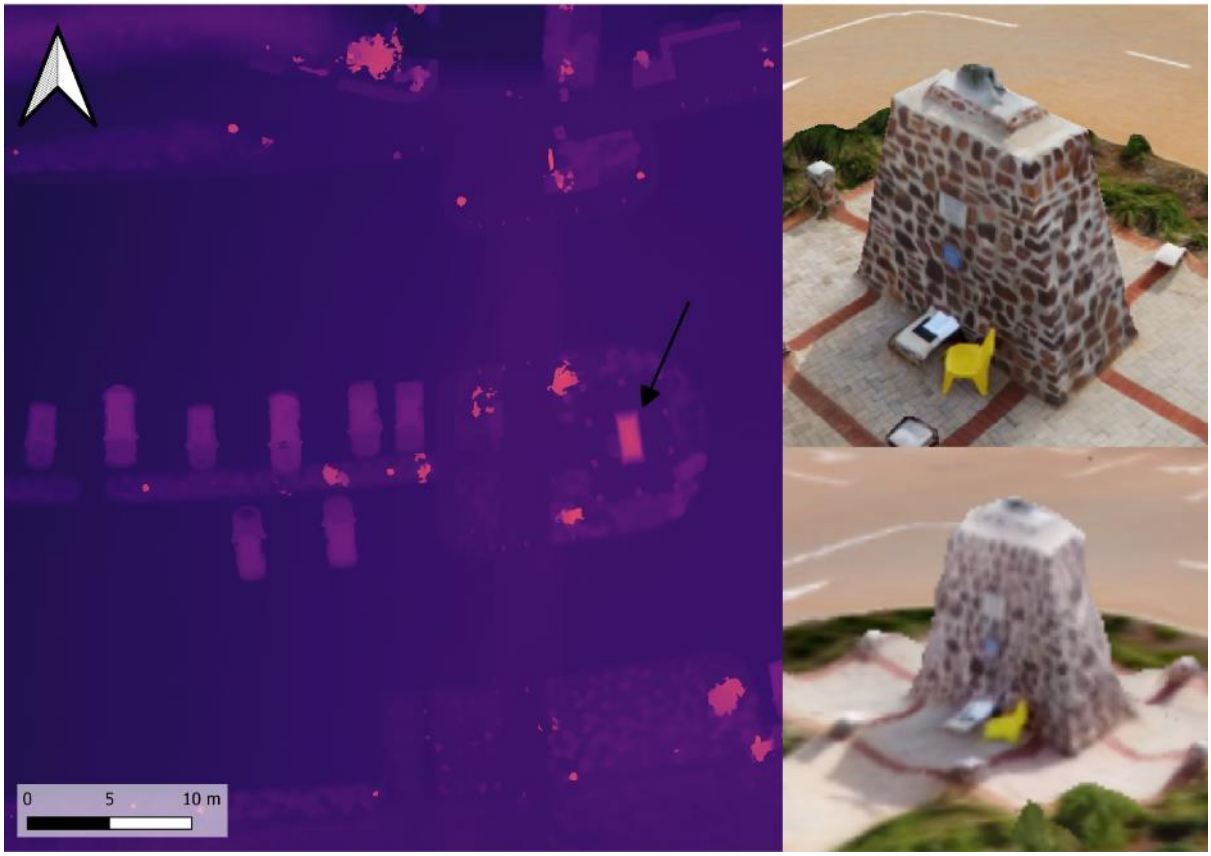

Appendix 2.1. Digital surface model of the Pierre van Reyneveld memorial (arrow in main figure) and surrounding parking lot at the Engineering 4 building, University of Pretoria, South Africa, created with ODM and a DJI Mavic Mini flown at 20 m altitude, with a depiction of the 3-d models that ODM can create from photographs taken at nadir from 2 different altitudes (20 m and 100 m respectively).

CHAPTER 3

Quantifying crocodile welfare in open pens on commercial crocodile farms in South Africa using a UAV and open-source software

A Myburgh[1,4], DM Veldsman[2], JG Myburgh[3], CT Downs[1], EC Webb[2] and S Woodborne[4]

[1]Centre for Functional Biodiversity, School of Life Sciences, University of KwaZulu-Natal, Private Bag X01, Scottsville, Pietermaritzburg, 3209, South Africa

[2]Department of Animal and Wildlife Sciences, Faculty of Natural and Agricultural Sciences, University of Pretoria, Private Bag X20, Hatfield, 0028, South Africa

[3]Department of Paraclinical Sciences, Faculty of Veterinary Science, University of Pretoria, Private Bag X04, Onderstepoort, 0110, South Africa

[4]iThemba LABS, Private Bag 11, WITS, South Africa

Formatted for and submitted to Animal Welfare

3.1 Abstract

Relatively few techniques exist for evaluating parameters related to the welfare of commercially farmed Nile crocodiles *Crocodylus niloticus* in open pens in South Africa. Here, we present a novel technique for quantifying several parameters associated with the welfare of farmed Nile crocodiles. We used a low-cost consumer UAV ("drone") and open-source photogrammetry software to survey/map several crocodile pens and determine stocking densities, indices of biomass and several other pen and pond related parameters at two relatively large Nile crocodile farms in South Africa. Nile crocodile counts were then compared with farmer estimates and differed significantly. We show how these parameters can be used to evaluate the welfare of farmed crocodiles and provide suggestions for future applications of the technique.

Keywords: Animal welfare; crocodilians; *Crocodylus niloticus;* Drones; Nile crocodile; Stocking density; Welfare parameters

3.2 Introduction

Specialists working on commercial farms usually focus on animal health and production as indicators of good animal welfare (Mellor et al. 2020). Optimal animal welfare also includes consideration of the animal's affective state (i.e. how the animal feels or sentience), as well as an emphasis on natural living (i.e. consideration of whether the animal can express natural behaviours that are specific to that species, and whether they have what they need and want) (Mellor et al. 2020).

Increased stocking densities can affect stress levels and increase agonistic interactions between captive animals, reducing the general health of the animals (e.g., immune resistance, fertility, growth rate) (Elsey et al. 1990; Davis 2001; Bothma and Van Rooyen 2005; Brien et al. 2007; Brien 2015; Veldsman 2019; Webb et al. 2021). Reduced growth rates result in a greater investment of resources per unit product (meat or skin) and lower product quality, providing less income per animal reared (Shilton et al. 2014; Webb et al. 2021). The available area per animal/animals per unit area has been one of the main factors determining animal welfare on commercial crocodilian farming operations (Spoolder et al. 2000; Thomas et al. 2004; North et al. 2006; Weeks et al. 2008; Webb et al. 2021). Apart from benefits to profitability, the monitoring of the welfare and "well-being" of crocodilians in captivity (e.g. commercial farms) is becoming more important (Manolis and Webb 2016) as buyers of crocodilian products (skins and meat) increasingly demand that individual farm's husbandry, welfare and management practices be regularly evaluated through a certification process that is re-evaluated annually.

Crocodilians are amphibious, ectothermic reptiles that require heterogeneous environments for survival, growth and reproduction on commercial farms (Huchzermeyer 2003). Crocodiles spend many daylight hours close to water, which serves as refuge areas and is crucial for thermoregulation as crocodiles generally shuttle between the land and water to

maintain their body temperatures (Bothma and Van Rooyen 2005; Downs et al. 2008). In general, there is a lack of reliable and often a complete absence of evidence-based welfare parameters for commercial crocodile farm managers and external evaluators to use (Elsey et al. 1990; Davis 2001; Poletta et al. 2008; Ganswindt et al. 2014; Webb et al. 2021). Although the faecal corticosterone testing method was validated in the Nile crocodile (*Crocodylus niloticus*) (Ganswindt et al. 2014), more methods (more tools in the toolbox) are needed to be able to effectively and objectively evaluate intensive farming operations in southern Africa (J G Myburgh, unpublished data 2021).

The number of crocodiles per pen (stocking density) on a commercial farm is sometimes not known. Similarly, total pen size (m^2) and related pen parameters (waterbody size, length of water-line, etc.) are often not precisely measured. If a crocodile farmer does not use a specific recording system, especially in breeder pens, the number of animals per pen could easily be misrepresented. Furthermore, it is also important to always indicate the size of the individual crocodiles (TL), whenever the stocking density of animals per m^2 is considered (Webb et al. 2021). This is better expressed as biomass per m^2 because crocodiles have a fast growth rate, especially during the first year. In most cases, stocking density and other welfare parameters for larger Nile crocodiles are only objective estimates (T Carpenter, unpublished data 2021).

In South Africa, communal and single pen systems are used on Nile crocodile commercial farms, usually with one water body for each pen; and these water bodies generally have different designs, shapes, sizes and water depths (Carpenter, unpublished data 2021). Whilst pen design determines the available area per animal (total pen m^2 / number of animals in the open), water body design is multifaceted. It includes considerations of water-line length (the length of beach line or water's edge and the zone of interaction between crocodiles), water surface area to water-line ratios and the distance to the water from any point within the pen.

The water-line is considered extremely important from a management and welfare perspective; shorter water-lines (high number of animals per meter of water-line) have more intense movement of animals in and out of the water per specific length (m). This interaction between animals crossing the water-line may lead to more interaction between animals and damage to skins (Veldsman 2019). In South Africa, most commercial farms use one waterbody (usually square or elongated) per pen for the growers (T Carpenter, unpublished data 2021). In the case of adult breeders, the water-line is usually much longer because of the more natural shapes (bays and undulating water-lines) of some of the waterbodies in their enclosures (T Carpenter, unpublished data 2021). On commercial crocodile farms, it is possible to have optimal crocodile stocking densities (number of crocodiles per total pen m^2) with inadequate water area or water-lines if waterbodies are too far apart (in case of multiple waterbodies per pen), or too small, potentially hindering the crocodiles' thermoregulatory capabilities (T Carpenter, unpublished data 2021).

A review of literature evaluating proposed crocodilian stocking densities exists, but there is generally a lack of consistency between proposed stocking densities for various crocodilian species (Veldsman 2019; Webb et al. 2021). In South Africa and Zimbabwe, crocodile farms presently rely on regulations set out by the South African Bureau of Standards (SANS 2009) and the Crocodile Farmers Association of Zimbabwe (CFAZ): Codes of Practise (CFAZ, 2012), which are general guidelines based on *The Code of Practice on the Humane Treatment of Wild and Farmed Australian Crocodiles* (NRMMC 2009). These guidelines are based on historical research and acknowledge the need for improved methods of determining and evaluating stocking densities and other welfare parameters on commercial crocodile farms (Manolis and Webb 2016). Although generalised numerical values serving as guidelines for stocking densities of Nile crocodiles on commercials farms are still important, a more holistic

approach for the evaluation of farm crocodile welfare and "well-being" is becoming more relevant (G E Swan, unpublished data 2021; Mellor et al. 2020).

The use of unmanned aerial vehicles (UAV's) or drones for mapping and monitoring has been limited to larger commercial operations with access to proprietary software packages and high-cost commercial UAV's. Recently, consumer-grade UAV's have been applied to various ecological studies and are capable of producing georeferenced and geometrically corrected orthophotographs of relatively large areas when combined with photogrammetry software packages (Anderson et al. 2013; Hodgson et al. 2016; Ezat et al. 2018; Buters et al. 2019; Scarpa and Pina 2019; Fritsch and Downs 2020). Consumer-grade UAV's and open-source software with comparable accuracy to proprietary commercial alternatives present a novel approach to mapping and monitoring of smaller areas and are well suited for commercial crocodile farming operations.

In the present study, we assessed two relatively large-scale commercial crocodile farms in South Africa. We evaluated the potential of using a low-cost consumer-grade UAV and open-source software packages to determine crocodile stocking densities and several other environmental parameters in open-air grower communal pens and breeder holding facilities. We predicted that the UAV counts would be higher than the farmer estimates of the number of Nile crocodiles per pen and that the stocking densities would be misrepresented, especially in grower pens where stocking densities are relatively difficult to estimate because of the smaller size (usually 0.5 to 1.8m total length or TL) of the animals. We further assumed that more naturally shaped ponds and those with islands would provide longer waterline lengths.

3.3 Materials and methods

3.3.1 UAV flights

Three flights over two non-consecutive days at two commercial crocodile farms were required to cover all the pens on both farms. All flights were conducted in early winter between 10h00 and 11h00, as per Downs et al. (2008) and Calverley and Downs (2014), when most/all animals are basking and are clearly visible. All flights were conducted using a DJI Mavic Mini (Da Jiang Innovations, Shenzhen, China) (available for ± R 7500 / US$550 from most South African suppliers e.g. Takealot (https://www.takealot.com/dji-mavic-mini-drone/PLID59285407)) flown with Dronelink flight planning software (available for US$ 24,99 from Dronelink (Dronelink, Austin, Texas)) installed on a smartphone connected to the DJI Smart controller. All flights were pre-programmed through the Dronelink web interface and were constrained to the flight variables listed in Table 3.1. Flight altitude was constant for all flights at 40 m relative to the take-off location. During flights, the UAV took a series of photographs with specified overlap that were used to construct orthophotograph mosaics of the areas of interest. Farm A was small enough to be covered entirely by one flight lasting approximately 12 min, and farm B required two flights of five and nine min, respectively. Combined, we surveyed a total of 10.5 ha and took 455 photographs.

3.3.2 Image processing

We processed all images with OpenDroneMap (ODM) through the WebODM interface on a notebook computer running an AMD® Ryzen™ 7 3700U quad-core processor with a maximum clock speed of 2.3 GHz with 20 GB of DDR4 RAM and an Intel® 512 GB solid-state drive (SSD). Orthophotograph resolution was constrained to the GSD (ground sampling distance; in cm/pixel) of the original images at 1.42 cm/pixel. We converted processed orthophotographs as georeferenced Tag Image File Format (.tif) files. We imported these into

QGIS (QGIS Development Team (2021)) and aligned them with satellite imagery of the study locations through the raster georeferencing tool in QGIS. Although tiff files from ODM are already georeferenced, we used the alignment with key features in satellite imagery as a tool to standardise the position of the orthophotographs should future flights of the same area be conducted. Since we were not attempting to measure any object precisely but rather looking at broad patterns, we did not require sub-centimetre level accuracy.

Table 3.1: Flight variables used in this study

Flight variables	Level
Image frontal overlap	80%
Image side overlap	70%
Maximum speed	16.1 km/h
Decent rate	-3 m/s
Ascent rate	3 m/s
Rotation rate	45°/second
Horizontal deceleration	-0.6 m/s^2
Horizontal acceleration	1.8m/s^2
Vertical acceleration	1.8m/s^2
Vertical deceleration	-0.9m/s^2
Rotational acceleration	10°/s^2
Rotational deceleration	-10°/s^2
Reference location	Take-off location
Flight pattern	Normal
Image capture angle pitch	-90° (nadir)

3.3.3 Determination of crocodile and pen related variables

We counted Nile crocodiles by creating a vector (Point) layer in QGIS where a point could be placed on each crocodile head that was visible in orthophotographs (Fig. 3.1a) and obtained data on the number of Nile crocodiles per pen as documented by the respective farming operations. Nile crocodile lengths were determined by creating a vector (LineString/CompoundCurve) layer, from the first pixel representing the crocodile's snout

following the curve of its back to the last pixel representing the tip of the crocodile's tail, and extracting the geometry attributes thereof (Fig. 3.1b). Crocodile sizes were then divided into size classes of 10 cm increments to investigate size class distributions within pens. Breeder pens were relatively easy to count when compared with grower pens, where crocodiles were much smaller and often clumped, making the identification of individuals difficult (Fig. 3.1c).

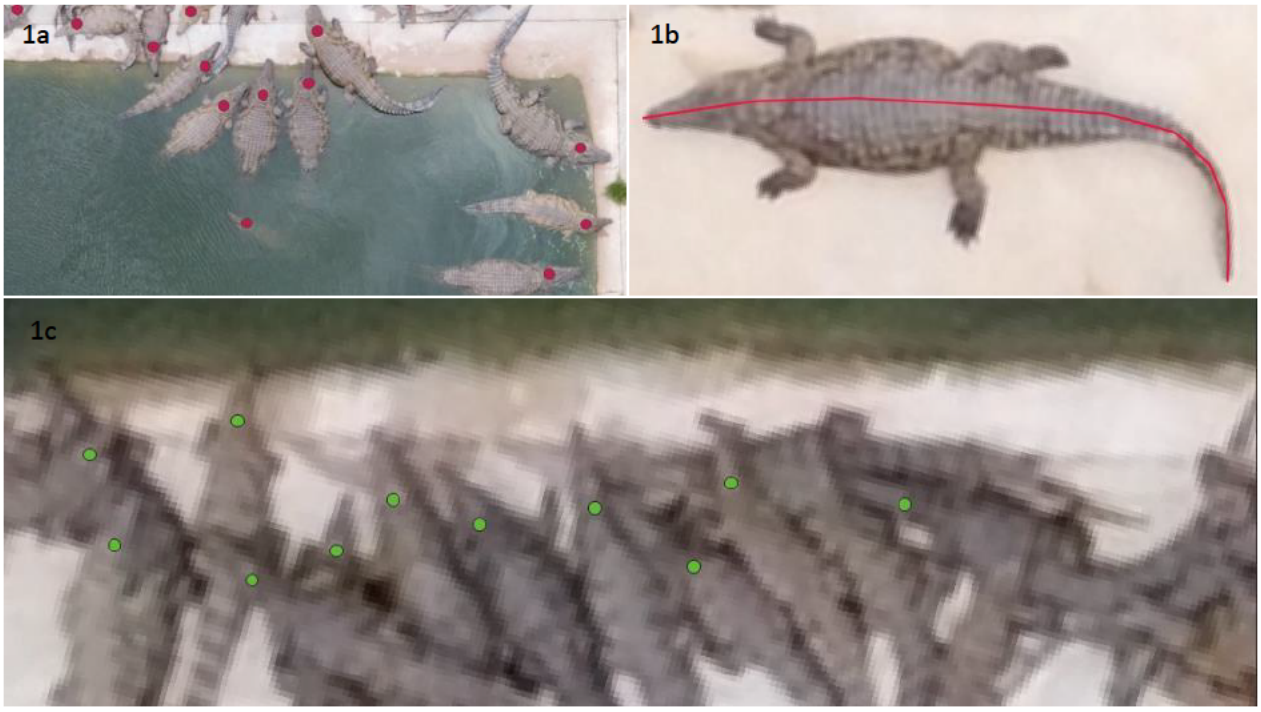

Figure 3.1: An illustration of a. how breeder and c. grower Nile crocodiles in orthophotographs were counted, and b. measured using point and line layers in QGIS. Breeder crocodiles are approx. 3 m in length and growers approx. 1.5 m. Note the difficulty in identifying the head of a grower crocodile in c.

We created geo-package (polygon/multi polygon) layers for all Nile crocodile pens and ponds observed in the orthophotographs and derived their geometry attributes in QGIS. We omit illustrations of the pen and pond designs to preserve farm anonymity. Crocodile holding pens are divided into breeder (B) and grower (G) pens for both farms A and B (e.g. breeder

and grower pens on farm A were designated AB and AG, respectively, managers pers. comm.). The coordinate reference system (CRS) for all images and associated layers was EPSG: 32735 - WGS 84 / UTM zone 35S. We used the Nile crocodile count to infer stocking density, expressed as a function of various other parameters (animals per unit area), while we used crocodile length as an indicator of biomass (length in m per unit area or length).

For all open-air pens and ponds, we were able to derive the area and circumference, enabling estimations of water-line length and total water area, as well as the percentage water area in the respective pens (Table 3.2). Stocking densities could then be determined as the number of animals per unit area (pen/pond). We expressed water efficiency per pen as the total water area (m^2) as a function of water-line length (m) in each pen. We expressed water availability per pen as the total percentage of pen area covered by water in each pen.

Statistical analyses

We used a Student's t-test to compare farmer estimates with UAV derived Nile crocodile counts, and used a linear regression to evaluate the relationship between the number of crocodiles per unit area and meters of crocodile per unit area. We used a Shapiro-Wilk normality test for size class estimates to compare crocodile size distributions in pens with high and low stocking densities.

3.4 Results

We counted a total of 7147 Nile crocodiles in 16 pens on the two commercial crocodile farms (Farm A and B), and we determined TLs for a total of 1887 Nile crocodiles. We found a linear relationship between the number of crocodiles per unit area and meters of crocodile per unit area, conforming to the equation:

$$A = 1.115b + 0.0644$$

where *A* represented the number of crocodiles per unit area, and *b* represented the length of crocodiles per unit area with an R^2 of 0.98 when considering all pens across both farms.

For all open-air pens and ponds, the area and circumference could be derived, enabling estimations of waterline length and total water area, as well as percentage water area in pens (Table 3.2). Water efficiency (m/m^2) was expressed as total water area (m^2) as a function of water-line length (m). Water availability was expressed as the total percentage of pen area covered by water. Note that only pen BB2 has a water area >50%. Pen BG4 had the greatest water efficiency with 1.42 m of water line per m^2 of water and the highest biomass load at 3.84 m of crocodile/m^2 of water. The ponds in this pen were merely three furrows, approximately 1.5 m across, whilst the average crocodile length in this pen was 1.2 m. Pen BB2 had the lowest water efficiency at 0.14 m of water line per m^2 of water, and the pond in this pen covered approximately 60% of the total pen area with 0.17 m of crocodile/m^2 of water. The crocodiles in this pen were notably more clumped, with few animals in the middle of the pond.

For some Nile crocodile breeder pens, significant size discrepancies distinguished between males and females (Figure 3.2). We used length estimates to derive size distributions (Figure 3.3) and split these into size classes (designated every 10 cm; e.g. 100 - 110 cm; 111 - 120cm, etc.) to compare size distributions across pens. For example, in pen AG9, size classes were bivariate and non-normally distributed (Shapiro-Wilk test; $P = 0.01329$), and in pen BG3 with a lower stocking density, size classes were normally distributed (Shapiro-Wilk test; $P = 0.6467$).

Table 3.2: Pen and pond characteristics derived from drone images combined with photogrammetry and GIS software for 16 pens across two commercial crocodile farms (A and B) hosting both breeder (xB#) and grower (xG#) stock. (See definitions in text).

Pen variables			Pond variables			
Pen code	**Pen area**	**Pen circumference**	**Water area (m^2)**	**Waterline (WL)(m)**	**Water efficiency (m/m^2)**	**Water availability (% of total pen area)**
AB1	5446	317	1139	284	0.25	20.91
AB2	8490	390	3003	492	0.16	35.37
AG1	1420	149	486	91	0.19	34.23
AG2	607	115	252	88	0.35	41.52
AG3	426	82	186	74	0.40	43.66
AG4	643	99	285	98	0.34	44.32
AG5	767	108	321	102	0.32	41.85
AG6	1031	129	359	101	0.28	34.82
AG7	932	122	356	103	0.29	38.20
AG8	842	124	291	92	0.32	34.56
AG9	504	90	205	78	0.38	40.67
BB1	12565	513	4018	850	0.21	31.98
BB2	4835	299	2760	393	0.14	57.08
BG1	6908	335	3411	543	0.16	49.38
BG3	2843	214	531	222	0.42	18.68
BG4	134	46	50	70	1.40	37.31

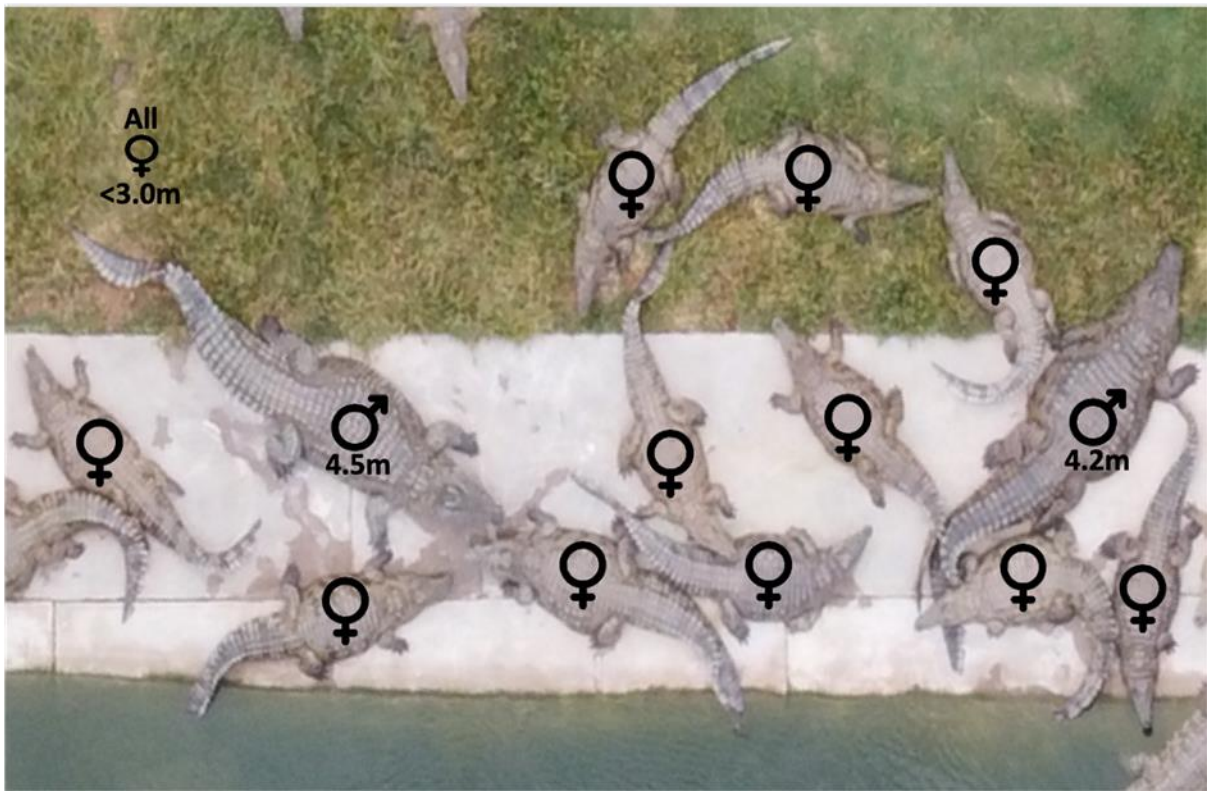

Figure 3.2: A cohort of crocodiles in an established breeder pen with significant size discrepancy allowing the differentiation of sexes.

The number of Nile crocodiles per pen counted from orthophotographs differed significantly from farmer estimates (n = 15, $P < 0.05$). When compared with farm owners' estimates of Nile crocodile stocking densities, orthophotograph counts were almost exclusively lower, with the exception of pen AG9. In some cases, like pen AB2, the farmer estimated 2000 animals whilst counts from orthophotos were much lower at 398. Nile crocodile pen and pond characteristics were combined with crocodile counts and length measurements to derive several indicators of crocodile welfare (Table 3.3).

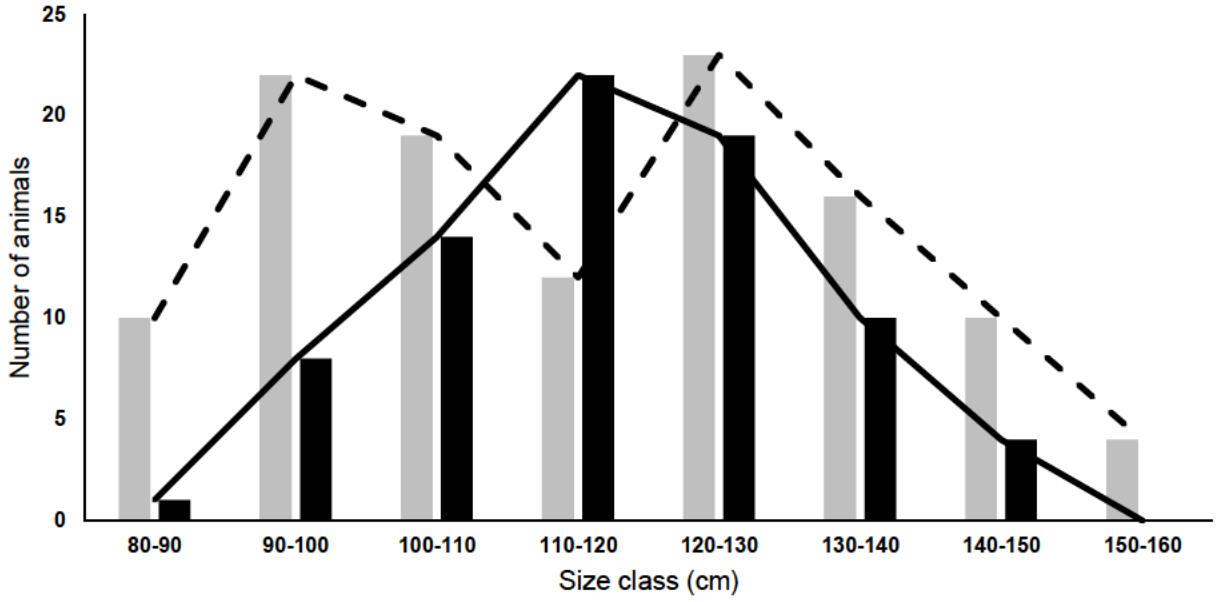

Figure 3.3: An example of two size distribution curves derived from length measurements of Nile crocodiles from two separate grower pens where the black bars and solid line represent pen BG3 with a stocking density of 0.17 animals/m^2 and the shaded bars and dashed line represent pen AG9 with a stocking density of 0.83 animals/m^2.

Table 3.3: Welfare parameters for 16 pens across two commercial crocodile farms (A and B) hosting both breeder (xB#) and grower (xG#) stock derived from UAV imagery combined with photogrammetry and GIS software.

Crocodile count and lengths					Density and biomass indicators				
Pen code	**Farm estimate**	**UAV derived count**	**Length measured (n)**	**Mean length (cm)**	**Absolute density (animals/m²)**	**Water line density (animals/mWL)**	**Absolute biomass (m of crocodile /m²)**	**Water-line biomass (m of crocodile/ mWL)**	**Water specific biomass (m of crocodile/m² of water)**
AB1	800	226	141	319	0.04	0.80	0.13	2.54	0.63
AB2	2000	398	268	307	0.05	0.81	0.14	2.48	0.41
AG1	3400	930	124	139	0.65	10.22	0.91	14.21	2.66
AG2	965	710	164	102	1.17	8.07	1.19	8.23	2.87
AG3	396	420	110	124	0.99	5.68	1.22	7.04	2.80
AG4	950	669	146	116	1.04	6.83	1.21	7.92	2.72
AG5	788	515	112	134	0.67	5.05	0.90	6.77	2.15
AG6	676	456	115	130	0.44	4.51	0.57	5.87	1.65
AG7	674	540	121	138	0.58	5.24	0.80	7.23	2.09
AG8	787	674	144	118	0.80	7.33	0.94	8.64	2.73
AG9	386	417	122	113	0.83	5.35	0.93	6.04	2.30
BB1	431	239	84	293	0.02	0.28	0.06	0.82	0.17
BB2	316	161	61	297	0.03	0.41	0.10	1.22	0.17
BG1	254	158	49	200	0.02	0.29	0.05	0.58	0.09
BG3	1000	474	78	78	0.17	2.14	0.13	1.67	0.70
BG4	400	160	48	120	1.19	2.29	1.43	2.74	3.84

3.5 Discussion

For the first time, several welfare parameters were derived for Nile crocodiles on commercial farming operations using a low-cost UAV and open-source photogrammetry software. Total counts derived from orthophotographs were most likely an underrepresentation of actual stocking densities, but the method ensured that total counts with the UAV could not exceed the actual number of crocodiles per pen. We found the farm owners' estimates of Nile crocodile stocking densities were significantly higher than the orthophotograph counts. Welfare organisations threatening farmers with prosecution because of overstocking will have to use, in future, more objective methods (e.g. UAV technology) to holistically determine the welfare parameters related to specific pens or farms. The relatively low-cost nature of this method, enabling flights at frequent (multiple flights per day) intervals and multiple counts per pen, would improve the accuracy of the different welfare-related investigations.

Whilst smaller crocodilians (<1 m TL) are often transferred between pens and can be counted with relative ease during handling, in bigger pens with larger animals (>1m TL), estimates of stocking densities are typically obtained by tracking deaths and additions to cohorts across multiple pens (T Carpenter, unpublished data 2021). In breeding pens, estimates of stocking densities rely on initial stocking records that can be as old as 30 years (T Carpenter, unpublished data 2021) and orthophotograph derived counts are well below the estimated numbers provided by farm owners. Breeder pens host the largest animals and, using the UAV technique, were counted with relative ease compared with grower pens, where crocodiles were considerably smaller and stocking densities higher (Figure 3.1c compared with Figure 3.1a). Breeder pens were also the largest pens on both farms, and farmers acknowledged that their estimates of stocking densities were most likely inaccurate owing to the difficulty of counting animals in such large enclosures (pers. comm.). Overestimation of actual stocking densities in

all but one pen bodes well for the welfare of animals on commercial crocodile farms as the correct stocking density is most likely smaller.

We found the minimum and maximum stocking densities derived from drone imagery on the two farms assessed in this study revealed a range of 0.02 - 0.05 animals/m^2 for the breeder pens, and 0.02 - 1.19 animals/m^2 for the grower pens. When these values were compared with stocking densities recommended by the South African National Standards document (SANS 2009) and CFAZ (2012), the results showed that drone-derived densities for grower crocodiles fell within the recommended guideline ranges. In contrast, we found breeder crocodile densities did not fit the recommended norms, and our data showed that these pens were overstocked.

Pen and pond size are two significant factors to consider when assessing stocking densities in commercial crocodile farming since both land and water areas are important for thermoregulatory and breeding activities (SANS 2009; CFAZ 2012; Manolis and Webb 2016). Water area per animal is as important as land area per animal as crocodiles are ectotherms that thermoregulate behaviourally with basking, shuttling and posturing (Downs et al. 2008). With insufficient space per crocodile in a captive pen, not all animals can successfully regulate their body temperatures if access to water and land are limited (Seebacher 1999; Downs et al. 2008; Manolis and Webb 2016).

Breeding behaviours of crocodiles are also space-reliant, which means that sufficient space for breeding-territory formation and the act of mating in water bodies is necessary (SANS 2009; CFAZ 2012). Industry recommendations are that water bodies cover approximately 50-70% of the area of the pens and that all crocodiles in a captive pen should be able to submerge (Bothma and Van Rooyen 2005; Brien et al. 2008; Shilton et al. 2014). In the present study, we found only one pen (pen BB2) had a percentage water area above 50%, with some ponds covering as little as 18% of the total available area in the pens. Pond area could be increased

by decreasing the total pen area; however, such an approach would negatively affect stocking densities.

The density and biomass indicators detailed in Table 3.3 are all potentially useful parameters for assessing crocodile' welfare on farms. Absolute density and absolute biomass indicate current space allowances per crocodile, enabling stocking density adjustments. Waterline density could be a useful indicator of basking space per animal; ideally, all crocodiles should be able to bask near or on the water-line. Water specific biomass could show whether a pond is adequate in size per the number of crocodiles in the captive pen. For this last parameter, pond depths could be included, and water body volume can be considered. WebODM (the open-source photogrammetry software package interface) has a built-in tool for volumetric calculations (Toffanin 2019). Ponds are routinely drained and cleaned, so this could easily be achieved by conducting flights over pens whilst ponds are empty.

The ability to estimate crocodile sizes remotely provides a means of evaluating size class distributions within pens (size variance in same-age groups result from runting or FTTS (Failure To Thrive Syndrome) (Brien et al. 2014)). Overstocking introduces more chances for competition and results in preferential resource utilisation where larger animals (bullies) obtain more food, exacerbating the size variance within a pen (Veldsman 2019). This can be difficult to manage once it has occurred as larger operations have pens with many hundreds of animals, making it difficult to identify and remove smaller individuals. Once the effects of overstocking have occurred, it often remains within the cohort until slaughter (Brien et al. 2014). Runting and FTTS will result in bivariate (not normally distributed) size distributions within a pen, as seen in pen AG9 with a relatively high stocking density (Figure 3.3) when compared with pen BG3 with a lower stocking density and a normal size distribution. Therefore, the present technique provides a novel aspect to crocodile farm management through remote size

estimation and may be used in future studies to more accurately estimate the relationship between animal welfare and stocking density.

We found that measurements of both crocodile numbers and average length could be used to estimate biomass within a pen. Indices of biomass can potentially be used to inform feeding and medication regimes. Biomass indices based on TL should be used with caution as some crocodiles may lose part of their tails during agonistic interactions. Snout vent length (SVL) would be a more reliable parameter in such cases (Combrink et al. 2012). The SVL can accurately be determined in crocodiles lying on their bellies (as seen with orthophotographs); the vent's endpoint is closely associated with the third circumferential skin groove behind the back legs (Combrink et al. 2012). To derive SVL measurements using the current technique and hardware, flights would have to be conducted at a lower altitude to decrease the GSD (ground sampling distance in cm/px) and increase the clarity of orthophotographs.

Although Nile crocodile biomass could be estimated from SVL, the body condition of the animal should also be considered. During the present study, we found several pens had crocodiles that were notably wider (more obese) than others, and future studies may consider an SVL to width ratio to derive indices of both biomass and body condition. Such parameters could be used to optimise food and medication requirements, predict meat and skin yields and quality, and evaluate water replacement regimes for ponds.

One of the greatest expenses on a commercial crocodile farm is the treatment and replacement of water within ponds (T Carpenter, unpublished data 2021). Several pond and pen design variables exist, and the present technique could be used to compare the effectiveness of variations in pen and pond characteristics. Water replacement costs are directly correlated to water volume, while volume relies on the pond design. Pond design has several implications for both crocodile welfare and the profitability of the farm.

Industry recommendations are that water bodies should occupy 50-70% of crocodile enclosures. Water depth must allow the crocodiles to stand in the water comfortably, and the edges of water bodies should gradually ascend to allow easy haul out (Bothma and Van Rooyen 2005; Brien et al. 2007; Shilton et al. 2014). As such, ponds on commercial farms are often shallow with a constant depth and bank slope (>1m depth; slope >30°) (Bothma and Van Rooyen 2005; Brien et al. 2007), allowing for pond area to be the variable that determines water volume differences between ponds. In this study, pen BG4 has the greatest water efficiency with 1.42 m of water line per m^2 of water and the highest biomass load at 3.84 m of crocodile/m^2 of water. If the ponds in pen BG4 conform to the average bank slope and depth, it provides minimal water volume per animal, results in decreased water quality and increases possible agonistic interaction within the ponds.

Increasing the available water line per animal decreases the risk of agonistic interaction, benefiting both crocodile welfare and the quality of the animal skins. Pen BB2 had the lowest water efficiency at 0.14 m of water line per m^2 of water. Future studies may consider the distribution of animals within pens; pens like pen BB2 may increase agonistic interaction because of a lack of sufficient waterline, and pens like pen BG4 may require more frequent water replacements or more frequent water treatment. The pond in pen BG3 only covered 18% of the total pen area, and crocodiles in this pen were absent from large parts of the pen that were not close to the water's edge. Therefore, if crocodiles on commercial farms do not use some areas that are too far away from a water body, numerical stocking density values can falsely be reduced by making the pen (land area) larger without increasing the available water area or waterline length. In essence, when farmers make pens bigger (land portion) to reduce the stocking density, it does not contribute to welfare value because crocodiles often do not use areas far from the water. This gives a 'false' low stocking density (on paper), but the stocking density in the pen is still high relative to the amount of water available. UAV's can be a

valuable tool in determining the relationship between water and land availability. Future studies may consider using multiple flights to produce specific maps of space-use within pens to evaluate minimum and maximum water to land ratios within pens.

Although we did not generate 100% accurate counts in the present study, it would be necessary to avoid any confusion should the technique described here be widely implemented, especially as a law enforcement technique. To achieve absolute accuracy, the technique would have to be applied to multiple farms with multiple UAV derived counts taken just before slaughter to compare absolute counts with UAV derived estimates to determine the percentage error associated. Fortunately, the technique will always undercount and never overcount as all crocodiles are marked in orthophotographs when counted. This allows the UAV derived estimate to be used as a "minimum" estimate of stocking density. Another confounding factor is the counting of crocodiles that are submerged during flights. As ponds are relatively shallow, crocodiles can be counted underwater if the water is clear enough. However, it does become a problem in ponds with relatively turbid/algae prone water where visibility is limited. Future studies might consider using multiple flights during mid-winter mornings when crocodiles are typically all basking.

3.5.1 Animal welfare implications

The present study provides a novel technique for crocodile farm management and monitoring of crocodile well-being. It produces counts and size estimations for open-air crocodile pens that host larger animals (>1 m TL) and paves the way for several future studies that can better inform optimal stocking densities on commercial crocodile farms. The technique can be applied as an inexpensive method to monitor compliance with stocking density and welfare parameters and can be used in conjunction with other methods (e.g. faecal corticosterone analysis) to investigate stress levels on commercial crocodile farms. Compared

with commercial UAV mapping approaches, the present technique is orders of magnitude more affordable and can be especially useful in areas where funding is limited.

3.6 Acknowledgements

We would like to thank the National Research Foundation (ZA, Grant 98404) and the University of KwaZulu-Natal (ZA) for providing funding for this research. We would also like to thank the farm owners for providing permission to conduct the research on their properties.

3.7 References

Anderson K, Gaston KJ 2013 Lightweight unmanned aerial vehicles will revolutionize spatial ecology. *Frontiers in Ecology and the Environment 11:* 138-146

Bothma JDP and Van Rooyen N 2005 Intensive wildlife production in Southern Africa. Van Schaik Publishers: Pretoria, South Africa, pp. 268-300. ISBN 0627025498

Brien, M.L., Webb, G.J., McGuinness, K. and Christian, K.A., 2014. The relationship between early growth and survival of hatchling saltwater crocodiles (*Crocodylus porosus*) in captivity. *Plos One*, 9, e100276.

Brien ML 2015 Growth and survival of hatchling saltwater crocodiles (*Crocodylus porosus*) in captivity: the role of agonistic and thermal behaviour. *PhD dissertation, Charles Darwin University*: Darwin, Australia

Buters TM, Bateman PW, Robinson T, Belton D, Dixon KW and Cross AT 2019 Methodological ambiguity and inconsistency constrain unmanned aerial vehicles as a silver bullet for monitoring ecological restoration. *Remote Sensing 11:* 1180

CFAZ 2012 Crocodile Farmers Association of Zimbabwe: Codes of Practise (2012)

Calverley PM and Downs CT 2014 Population status of Nile crocodiles in Ndumo Game Reserve, Kwazulu-Natal, South Africa (1971–2012). *Herpetologica 70,* 417-425.

Combrink X, Warner JK, Hofmeyr M, Govender D and Ferreira SM 2012. Standard operating procedure for the monitoring, capture and sampling of Nile Crocodiles (*Crocodylus niloticus*). *South African National Parks* unpublished report, Skukuza, South Africa, pp.1-14

Davis BM 2001 Improved nutrition and management of farmed crocodiles: hatching to harvest. Rural Industries Research and Development Corporation. Project, (01/123), 102. ISBN 0642583455

Downs CT, Greaver C and Taylor R 2008 Body temperature and basking behaviour of Nile crocodiles (*Crocodylus niloticus*) during winter. *Journal of Thermal Biology 33*: 185-192

Elsey RM, Joanen T, McNease L and Lance V 1990 Stress and plasma corticosterone levels in the American alligator—relationships with stocking density and nesting success. *Comparative Biochemistry and Physiology Part A 95*: 55-63.

Elsey RM, Joanen T, McNease L and Lance V 1990 Growth rate and plasma corticosterone levels in juvenile alligators maintained at different stocking densities. *Journal of Experimental Zoology 255*: 30-36

Ezat MA, Fritsch CJ and Downs CT 2018 Use of an unmanned aerial vehicle (drone) to survey Nile crocodile populations: a case study at Lake Nyamithi, Ndumo game reserve, South Africa. *Biological Conservation 223*: 76-81

Fritsch CJ and Downs CT 2020 Evaluation of low-cost consumer-grade UAVs for conducting comprehensive high-frequency population censuses of hippopotamus populations. *Conservation Science and Practice 2*: e281

Ganswindt SB, Myburgh JG, Cameron EZ and Ganswindt A 2014 Non-invasive assessment of adrenocortical function in captive Nile crocodiles (*Crocodylus niloticus*). *Comparative Biochemistry and Physiology*, *Part A 177*: 11-17

Hodgson JC, Baylis SM, Mott R, Herrod A and Clarke RH 2016 Precision wildlife monitoring using unmanned aerial vehicles. *Scientific Reports 6*: 1-7

Huchzermeyer FW 2003 Crocodiles: biology, husbandry and diseases. *CABI*; Oxford, UK

Manolis SC and Webb GJW 2016 Best Management Practices for Crocodilian Farming. Version 1. *IUCN-SSC Crocodile Specialist Group*: Darwin, Australia

Mellor D, Beausoleil N, Littlewood K, McLean A, McGreevy P, Jones B and Wilkins C 2020 The 2020 Five Domains Model: Including Human-Animal Interactions in Assessments of Animal Welfare. *Animals 10*: 1870

NMMRC 2009. Code of Practice on the Humane Treatment of Wild and Farmed Australian Crocodiles. Published by the *Natural Resource Management Ministerial Council*, Canberra, Australia.

North BP, Turnbull JF, Ellis T, Porter MJ, Migaud H, Bron J and Bromage NR 2006. The impact of stocking density on the welfare of rainbow trout (*Oncorhynchus mykiss*). *Aquaculture 255*: 466-479

Poletta GL, Larriera A and Siroski PA 2008 Broad snouted caiman (*Caiman latirostris*) growth under different rearing densities. *Aquaculture 280*: 264-266

QGIS Development Team 2021 QGIS Geographic Information System. Open Source Geospatial Foundation Project. http://qgis.osgeo.org

SANS 2009 SABS standards division. South African national standards, crocodiles in captivity. SANS 631:2009 Edition 1, ISBN 978-0-626-22294-9.

Scarpa LJ and Pina CI 2019 The use of drones for conservation: A methodological tool to survey caiman's nests density. *Biological Conservation 238*: 108235

Seebacher F 1999 Behavioural postures and the rate of body temperature change in wild freshwater crocodiles, *Crocodylus johnstoni*. *Physiological and Biochemical Zoology 72*: 57-63

Shilton C, Brown GP, Chambers L, Benedict S, Davis S, Aumann S and Isberg SR 2014 Pathology of runting in farmed saltwater crocodiles (*Crocodylus porosus*) in Australia. *Veterinary Pathology Online 51*: 1022-1034

Spoolder HAM, Edwards SA and Corning S 2000 Legislative methods for specifying stocking density and consequences for the welfare of finishing pigs. *Livestock Production Science 64*: 167-173

Thomas DG, Ravindran V, Thomas DV, Camden BJ, Cottam YH, Morel PCH and Cook CJ 2004 Influence of stocking density on the performance, carcass characteristics and selected welfare indicators of broiler chickens. *New Zealand Veterinary Journal 52*: 76-81.

Toffanin, P., 2019. OpenDroneMap: The Missing Guide. UAV4GEO, first edition.

Veldsman DM 2019 *Effects of stocking density on production and behaviour of farmed grower Nile crocodiles (Crocodylus niloticus)*. Masters dissertation, University of Pretoria: Pretoria, South Africa.

Webb EC, Veldsman DM, Myburgh JG and Swan GE 2021 Effects of stocking density on growth and skin quality of grower Nile crocodiles (*Crocodylus niloticus*). *South African Journal of Animal Science 51*: 142-150

Weeks CA 2008 A review of welfare in cattle, sheep and pig lairages, with emphasis on stocking rates, ventilation and noise. *Animal Welfare 17*: 275-284

CHAPTER 4

Morphometrics of Nile crocodiles and their use in UAV based crocodile population monitoring

Albert Myburgh[1], Stephan M. Woodborne[2] and Colleen T. Downs[1*]

[1]*Centre for Functional Biodiversity, School of Life Sciences, University of KwaZulu-Natal, Private Bag X01, Scottsville, Pietermaritzburg, 3209, South Africa*

[2]*iThemba LABS, Private Bag 11, WITS, South Africa*

Formatted for submission to *Zoomorphology*

*** Corresponding Author:** Colleen T. Downs

Email: downs@ukzn.ac.za; **ORCID:** http://orcid.org/0000-0001-8334-1510

Other emails and ORCIDs:

A Myburgh Email: Albert.isotopes@gmail.com; ORCID: http://orcid.org/0000-0002-6891-1893

SM Woodborne Email: Swoodborne@tlabs.ac.za; https://orcid.org/0000-0001-8573-8626

Running header: Morphometrics of Nile crocodiles using UAVs

4.1 Abstract

Drone imagery is increasingly used in the field of population ecology. Although the movement of animals often limits the application of photogrammetry for population dynamic modelling, exothermic organisms rely on periods of little to no movement as part of their natural thermoregulatory behaviour. Nile crocodiles are suited for population census from rectified aerial imagery as they are quiescent if photographed between 10h00 and 13h00 in winter when basking. Overlapping images can then be used to construct rectified orthophotographs through photogrammetry where crocodiles can be counted and measured. However, in their natural habitat and with low photographic resolutions, it is often difficult to estimate total crocodile lengths from aerial imagery as the tail is not always visible or easily defined due to low photograph resolution or the colour of the tail against darker backgrounds such as river pebbles/sand/mud. Here, we present two allometric factors for the estimation of Nile crocodile *Crocodylus niloticus* total lengths from newly defined morphometrics that were easily attainable from aerial imagery. We used rectified high-resolution drone orthophotographs to estimate factors for determining total lengths from snout to neck length (SNL) and snout to hind limb length (SHL). Crocodile total length was accurately predicted (137 ± 144 mm average errors) from both of these parameters enabling demographic population census of crocodiles even if the head is the only feature visible in the aerial imagery (e.g., when the animal is partly submerged). The correction factors presented here will enable the collection of sufficiently accurate demographic data for crocodile populations required to manage wild crocodile populations using emerging technologies.

Keywords: Crocodile population; UAV census; Open-source photogrammetry; correction factor

4.2 Introduction

Accurate demographic data at frequent intervals are required for the effective management of animal populations, especially in anthropogenically threatened aquatic systems (Utete 2021). Compared with large terrestrial vertebrates, Nile crocodile *Crocodylus niloticus* populations are difficult to monitor as they are cryptic, aquatic animals that often occur in relatively inaccessible areas (Dendi and Luiselli 2017). Traditional crocodile population census techniques include fixed-wing or helicopter-based surveys or counts from boats where waterways are accessible (Bayliss 1987; Combrink 2004; Ferreira and Pienaar 2011, Wallace et al. 2013). These techniques are costly, require expensive equipment, and group crocodiles into very broad classes based on the observer's opinion (Ezat et al. 2018). Furthermore, fixed-wing aircraft, helicopters and motorboats routinely used for crocodile population monitoring are relatively large, noisy and are known to cause disturbance to crocodiles during their use (Elsey and Trosclair 2016). Crocodilians are camouflaged aquatic organisms with high size dimorphism throughout their life span. The identification of smaller individuals is challenging in South Africa, especially from relatively fast-moving aerial platforms, and the result is that spotlight surveys often detect a greater quantity of smaller individuals, although many are recorded as “eyes only” with no information on the size of the animal (Wallace et al. 2013). Additionally, many smaller waterways do not allow for spotlight surveys by boat or on foot (Ferreira and Pienaar 2011).

Some attempts have been made to mathematically account for several factors that influence Nile crocodile population census data from traditional approaches (Ferreira and Pienaar 2011; Warner et al. 2016), but none have succeeded in providing population estimates with an accuracy comparable to that of unmanned aerial systems (UAV) based population censuses (Ezat et al. 2018; Hodgson et al. 2018; Aubert et al. 2021). The advantages of UAV based crocodile population monitoring greatly outweigh the necessity to continue monitoring

crocodile populations using traditional techniques (Aubert et al. 2021). Previously, sizes were subjective estimates, and they can now be obtained with centimetre accuracy, providing population demographic data unattainable through more traditional approaches (Hodgson et al. 2018).

Although the advantages of UAV-based crocodile population census are clear, factors limit the widespread application of the technique. With increased accuracy and the ability to estimate sizes from aerial images, there is a need to relate several morphometric parameters of crocodiles to one another as one or the other is often unavailable. Three of the most applicable standard morphometric parameters taken from captured or deceased Nile crocodiles include total length (TL; the distance from the tip of the snout, along the centreline of the animal's back, to the tip of the tail), snout vent length (SVL; the distance from the tip of the snout to the third circumcircle scute layer that corresponds to the opening of the cloaca) and head length (HL; maximum distance from the snout to the posterior ridge of the supraoccipital bone) (Warner et al. 2016).

From aerial imagery, the ground sampling distance or GSD (clarity of orthophotographs; measured in cm/pixel) is mainly determined by two factors: the altitude at which an image is taken and the resolution of the sensor (camera) that is used to take a photograph. Generally, lower altitudes and cameras with more megapixels, higher quality optics and/or larger sensors produce orthophotographs with greater clarity (Toffanin 2019). Orthophotographs with a GSD greater than 2cm/pixel make the identification of a crocodile's tail relatively difficult. Furthermore, this, coupled with the colouration of the tip of the tail (usually dark brown/green) against a dark background, such as river rocks or dark sand/gravel, makes length measurements difficult to obtain (Fig. 4.1).

Several parameters are used to estimate total crocodile length (TL) from other morphometric parameters as many crocodiles lose part of their tails during agonistic

interactions (Combrink et al. 2012; Fukuda et al. 2013). Previous studies have made use of the relationship between head length (HL) or snout-vent length (SVL) and total length derived from large datasets of captured individuals for which zoometric relationships are easily determined (Hutton 1987; Salem 2011; Warner et al. 2016). There are several problems using traditional zoometric relationships when conducting crocodile census with UAV based platforms: head lengths are traditionally measured by using a standard tape measure from the tip of the snout to the ridge created by supraoccipital bone's posterior edge (Warner et al. 2016). This measurement is difficult to replicate from UAV imagery as the required features are difficult to identify, particularly in low-resolution images. It becomes more feasible to estimate the length from the tip of the snout to the line created by the junction between the end of the dermal scute plates on the neck corresponding and the anterior of the front limbs of the crocodile (Fig. 4.2a) (Snout to Neck Length from here on referred to as SNL). This is easily measured from low-resolution UAV imagery as the front limbs are easily distinguishable (Fig. 4.2).

Another commonly used morphometric parameter is the snout-vent length (SVL): In orthophotographs with a GSD >3cm/pixel, some sections of the tail that are used for the identification of the third circumcircle scute layer associated with the opening of the cloacal vent can be difficult to see, and the last recognisable point on the crocodiles' body might be the hind legs (Fig. 4.2b). In such cases, the distance from the tip of the snout to the region of the body behind the hind legs (the circumcircle scute layer behind the hind legs (Fig. 4.2) can be relatively accurately identified (snout hind limb length, from here on referred to as SHL)

There is no correlation value in the present literature that can be used to estimate total length (TL) from SHL or SNL as these parameters are not standard measurements associated with the zoometrics of crocodilians. In this study, we used high-resolution rectified UAV imagery of Nile crocodiles taken at a commercial crocodile farm to derive a relationship

between the SNL, SHL and the TL for Nile crocodiles for use in future UAV based crocodilian population monitoring. We consider SNL for use in cases where the body of a crocodile is not visible (e.g. when an individual is partly submerged). We hypothesised that there would be a linear correlation between the SNL and TL and also between the SHL and the TL of a Nile crocodile when measured from UAV derived images. We derived and compared the relationship between the SNL, SHL and TL to previous studies on crocodilians' morphometrics.

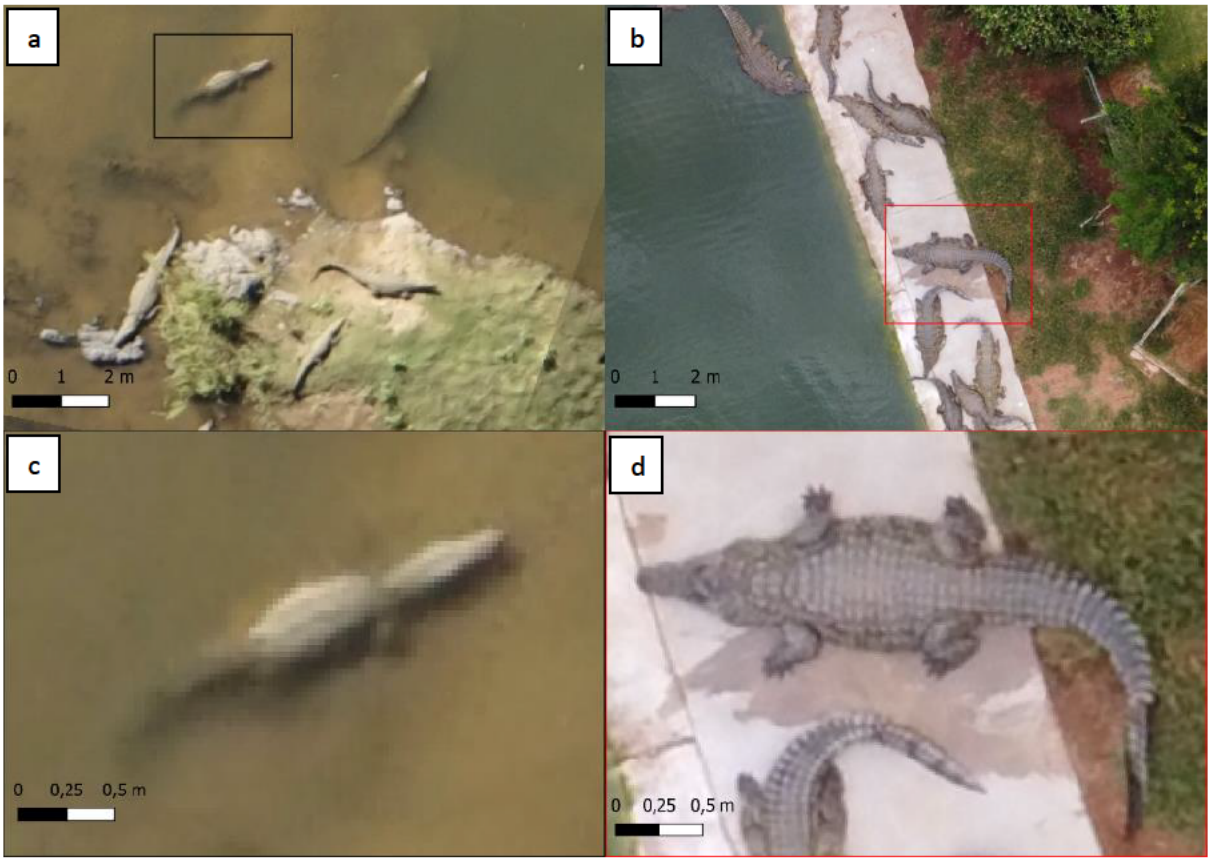

Figure 4.1: Nile crocodiles in orthophotographs with a GSD of 3cm/px (a) as opposed to one with a GSD of 1.4cm/px (b). (Note the difficulty in identifying the tip of the tail in the extract (c) of the first figure (a). At low resolution, the head and limbs are the only discernible features).

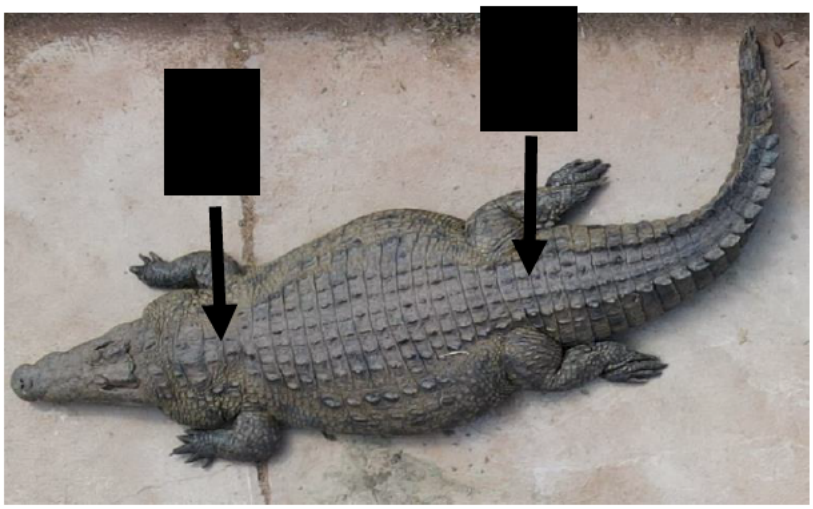

Figure 4.2: Depiction of morphological features that are easily recognisable from UAV imagery during a Nile crocodile census. 'A' depicts the end of the dermal neck scutes and 'B' refers to the circumcircle scute layer behind the hind legs. This crocodile is missing a region of the tail.

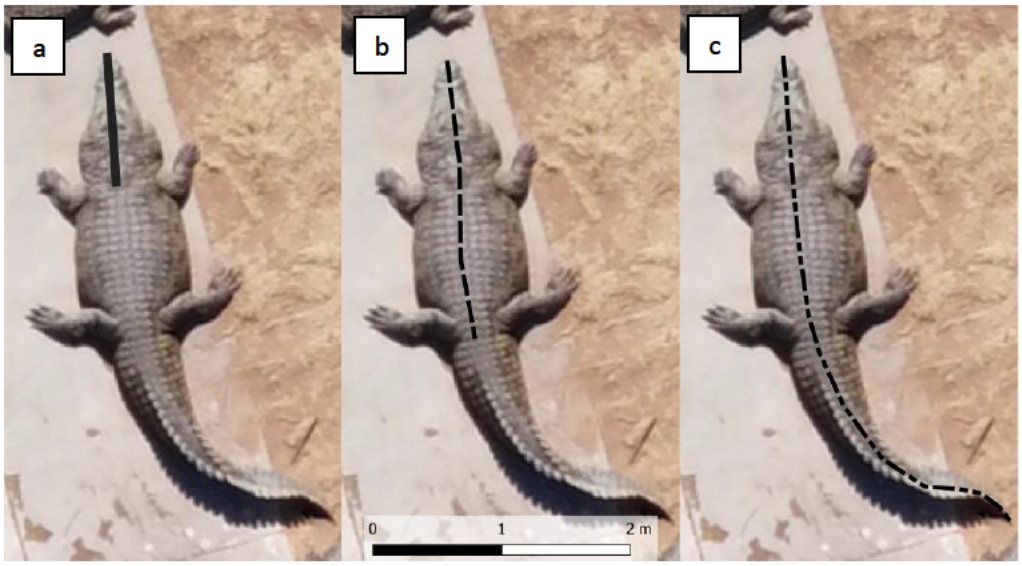

Figure 4.3: An illustration of how snout to neck length (SNL; solid line) (a), snout to hind leg length (SHL; dotted line) (b), and total length (TL; dot dash line) (c), were estimated using line-string layers on an orthophotograph derived from OpenDroneMap (ODM), in QGIS.

4.3 Methods

We used a DJI Mavic UAV with a 12-megapixel CMOS sensor to survey a 2.5-ha area containing 11 pens housing breeder and grower crocodile stock on a commercial Nile crocodile farm in South Africa during winter (we omit the name and location of the farm as they wish to remain anonymous). The UAV was programmed to follow a predetermined flight path at an altitude of 40 m covering the area in a grid pattern, taking images with approximately 80% frontal and 70% side overlap over the entire area as per the recommendations of Myburgh et al. (2021) (Chapter 2).

The flights were programmed in Dronelink using the default parameters and were similar to that of Myburgh et al. (2021) (Chapter 2), with estimated errors <40 mm. The flight was conducted between 10h00 and 11h00 on a relatively cold winter morning when most Nile crocodiles were basking and could be photographed out of the water (Downs et al. 2008).

The flight produced 177 images which we processed into a single orthophotograph at 1.42 cm resolution using OpenDroneMap (ODM) on a notebook with a quad-core processor (clock speed of 2.3 Ghz, 20 Gb of DDR3 RAM). The resulting orthophotograph from ODM was imported into QGIS (version 3.18.3-Zürich) (QGIS 2021), and SNL, TL and SHL were estimated using vector line layers and deriving their geometry attributes using the "add geometry attributes" function in QGIS.

We estimated SNL by drawing a line (line-string layer) from the tip of the Nile crocodile's snout to the position of the front limbs, which corresponds to the end of the nuchal cluster in Nile crocodiles. We measured TL by estimating the distance between the first pixel representing the snout, following the curve of the animals back to the tip of the tail for those individuals where the tip of the tail could be clearly distinguished from the background. We excluded crocodiles where the tail did not terminate in a clear tip (indicating loss of tail). SHL

was estimated by deriving the distance from the tip of the Nile crocodile's snout to the last scute layer behind its hind legs (Fig. 4.3).

We used a linear regression analysis to compare the relationship between TL, SHL and SNL in Microsoft Excel®. Using the same methods, we estimated the TL of an additional 50 crocodiles that were not used for the derivation of the correction models from SHL and SNL and compared their predicted TL's against measured TL's using a students t-test.

A further 10 crocodiles were measured from a UAV survey of a wild crocodile population (Myburgh et al. (in prep)) (Chapter 6). For these crocodiles, the same metrics were derived, but the tip of the tail on some animals was noticeably missing, and the TL's with a full tail from these animals are most likely underestimated when compared with their captive counterparts.

4.4 Results

We compared TL with SNL for 253 Nile crocodiles ranging in estimated TL from 710 mm to 4810 mm, and with estimated SHL for 151 Nile crocodiles across the same size range. An additional set of 50 crocodiles TL, SHL and SNL could be determined to estimate errors associated with the derived relationships, and these had a TL size range between 840 mm and 4310 mm. All measurements and regressions apply to lengths in mm.

There was a strong correlation (R^2 = 0.88) between the TL and the SNL (Fig. 4.4) conforming to the equation with a correlation coefficient of 0.94:

$$TL = SNL\ (5.829) + 54 \qquad \text{Equation 1}$$

There was a strong correlation (R^2 = 0.98) between TL and the SHL (Fig. 4.5) conforming to the equation with a correlation coefficient of 0.99:

$$TL = SHL\ (1.994) + 140 \qquad \text{Equation 2}$$

For the subsample of 50 Nile crocodiles, we found that the predicted lengths of TL from SNL had average errors of 103 ± 403 mm and a root mean square error of 341 ± 236 mm. Furthermore, the predicted TL's did not differ significantly from actual TL's (T-test; $t = 2$; $p > 0.1$; $n = 50$). For the same sample, predicted lengths of TL from SHL had average errors of 137 ± 144 mm, and a root mean square error of 159 ± 118 mm. Again the predicted TL's did not differ significantly from actual TL's (T-test; $t = 2$; $p > 0.1$; $n = 50$).

From equations 1 and 2, TL could be predicted using a conversion factor of ±1:6 for the estimation of TL from SNL and ±1:2 for the estimation of TL from SHL. Measurements from wild Nile crocodiles fell within one standard deviation of the relationships derived from farmed Nile crocodiles.

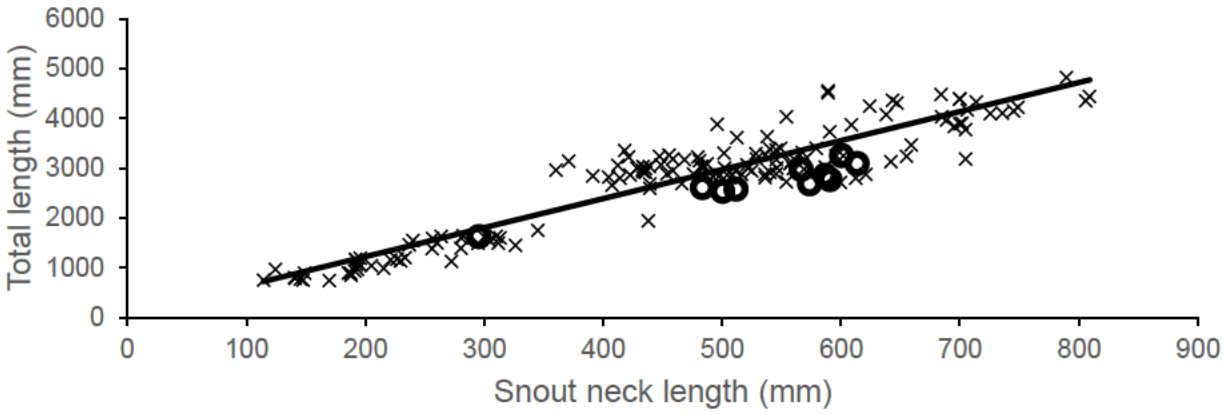

Figure 4.4: Relationship between the snout to neck length (SNL) and the total length (TL) of farmed Nile crocodiles (crosses) and wild Nile crocodiles (open circles) as measured from UAV derived imagery in the present study.

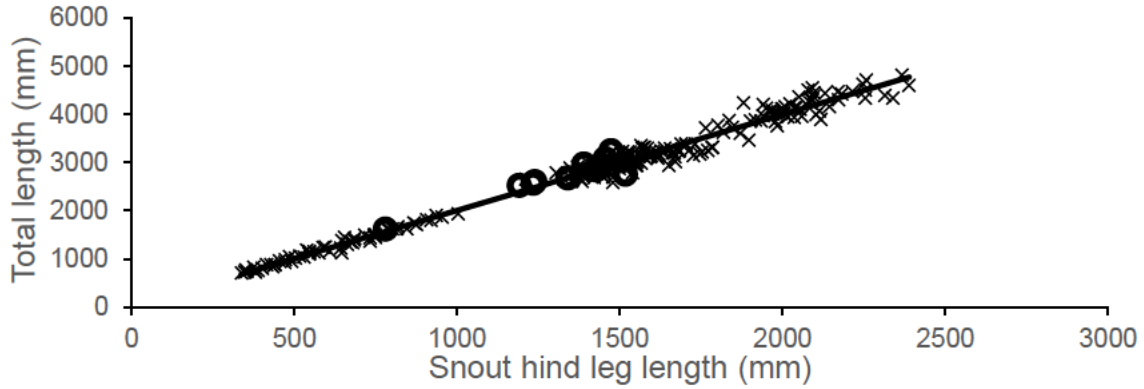

Figure 4.5: Relationship between the snout to hind leg length (SHL) and the total length (TL) of farmed Nile crocodiles (crosses) and wild Nile crocodiles (open circles) as measured from UAV derived imagery in the present study.

4.5 Discussion

In the present study, we defined two new parameters for estimating Nile crocodile total length from rectified imagery derived from UAV surveys of Nile crocodiles. The first parameter, snout to neck length (SNL), can predict the total length of a Nile crocodile, even when only the head, neck and front limbs are visible (as is the case when crocodiles are partly submerged). Lower absolute errors associated with TL predictions from snout to hind leg length (SHL) predict that it should be used to estimate TL when the animal's hind legs can be identified in an orthophotograph. The high degree of variance observed in the prediction of TL from SNL and SHL may be due to the effects of sexual dimorphism (Warner et al. 2016), and there are no current techniques capable of classifying the sex of an animal from UAV imagery. It is important to note that the estimation of SNL, and SHL have errors associated with the nature of the UAV technique and will differ based on the platform and the processing of images. In this study, these errors are constrained below 40mm as per Myburgh et al. (2021) and any measurements from orthophotographs using the ODM software will have errors between 0-37mm, however, this can be quantified using the point cloud density as outlined in Myburgh

et al. (2021). TL measurements from wild crocodiles were accurately determined from SHL and SNL. The underestimation of TL from SNL could be the result of either: 1. Low photograph resolution from the wild crocodile survey, confounding the estimation of SNL accurately, 2. That most wild Nile crocodiles lose a part of their tail during agonistic interactions (pers. obs.), which results in an underestimation of their possible TL or 3. Captive animals differ in their morphometrics due to the regularity of feeding, competition and activity. SHL should therefore be used whenever possible, and SNL should be reserved only for those instances where SHL cannot be confidently derived. Future UAV surveys of wild populations with lower GSD's could be used to constrain these relationships.

Several studies have investigated the relationship between various zoometric parameters related to crocodilians. These are all applicable to traditional survey and capture techniques and do not consider the requirements for surveys of crocodilians from UAV based imagery. Historically a conversion factor of 1:7 (Warner et al. 2016) was assumed to give a relative estimation of TL from HL, and this can be reduced to 1:5.8 (±1:6) when using the SNL as defined in the present study. Previously derived relationship between TL and SVL can be used to derive SVL from UAV predicted TL's and this can then be used to predict the morphometrics that are traditionally associated with Nile crocodiles (Warner et al. 2016).

Although length estimations from UAV imagery can theoretically be accurate to a few centimetres or even millimetres, depending on the available hardware, ecologists should use caution when deriving size classes from UAV imagery. The errors associated with the estimation of TL from SNL and SHL in the present study can be used as guidelines for assigning animals to separate size classes. Based on the derived margins of errors, we recommend placing crocodiles into size classes differentiated by at least 500 mm, especially when using SNL to predict TL. It is also worth considering simultaneously placing animals

into size classes that are compatible with more traditional census data so that historical data may still be applicable and correction factors for them determined.

Traditional crocodile surveys place crocodiles into relatively broad size classes based on subjective observer estimates of total length (Graham and Bell 1969; Ferreira and Pienaar 2011). Nile crocodiles are classed as yearlings, juveniles, subadults or adults (Wallace et al. 2013). UAV derived census data can improve on these or partition animals into various size classes more accurately. For general purposes of population modelling, the four size classes should be sufficient as they have been broadly defined in the literature, and the persistence and survivability parameters associated with them have been mathematically deduced (Wallace et al. 2013).

Once we have datasets derived through the UAV method spanning a few years, we can extract life history traits from these. It will be necessary to do UAV surveys in parallel with traditional approaches to derive corrections that can be used to preserve legacy datasets. Future studies should focus on the error associated with the true TL of an animal when compared with UAV derived TL's, and crocodilian capture should be combined with TL estimates of captured animals or animals of known length. Here, captured and marked animals could be resampled during UAV surveys, and true TL errors could be estimated. However, if the photogrammetry process is sufficiently accurate, the TL derived from UAV imagery negates the need to capture crocodilians for TL measurements, and UAVs represent a non-invasive method for crocodile population monitoring that should be used over more traditional methods wherever possible (Jordaan 2021). The ability to accurately predict TL from an accurate remote sensing platform also paves the way for biomass estimates at a much larger scale than traditional methods and can enable research questions that explore carrying capacity and population viability at large scales.

4.6 Acknowledgements

We would like to thank the National Research Foundation (ZA, Grant 98404) and the University of KwaZulu-Natal (ZA) for providing funding that supported this research. We would also like to thank the respective farm owners for allowing us to conduct this research on their property.

4.7 References

Aubert C, Le Moguédec G, Assio C, Blatrix R, Ahizi MN, Hedegbetan GC, Kpera NG, Lapeyre V, Martin D, Labbé P, Shirley MH (2021) Evaluation of the use of drones to monitor a diverse crocodylian assemblage in West Africa. Wildlife Research. https://doi.org/10.1071/WR20170

Bayliss P (1987) Survey methods and monitoring within crocodile management programmes. In: Webb, G.J.W., Manolis, S.C., Whitehead, P.J. (Eds), Wildlife Management: Crocodiles and Alligators. Sydney, Australia: Surrey Beatty and Sons, pp 157-175.

Combrink AS (2004) Population Survey of *Crocodylus niloticus* (Nile crocodile) at Lake Sibaya, Republic of South Africa. Doctoral dissertation, University of KwaZulu-Natal, South Africa.

Combrink X, Warner JK, Hofmeyr M, Govender D, Ferreira SM (2012) Standard operating procedure for the monitoring, capture and sampling of Nile Crocodiles (*Crocodylus niloticus*). South African National Parks, Skukuza, South Africa, unpublished report: 1-14.

Dendi, D, Luiselli L (2017) Population surveys of Nile crocodiles (*Crocodylus niloticus*) in the Murchison Falls National Park, Victoria Nile, Uganda. European Journal of Ecology 3:67-76.

Downs CT, Greaver C, Taylor R (2008) Body temperature and basking behaviour of Nile crocodiles (*Crocodylus niloticus*) during winter. Journal of Thermal Biology 33:185-192.

Elsey RM, Trosclair PL (2016) The use of an unmanned aerial vehicle to locate alligator nests. Southeastern Naturalist 15:76-82.

Ezat, MA, Fritsch CJ, Downs CT (2018) Use of an unmanned aerial vehicle (drone) to survey Nile crocodile populations: A case study at Lake Nyamithi, Ndumo game reserve, South Africa. Biological Conservation 223:76-81.

Ferreira SM, Pienaar D (2011) Degradation of the crocodile population in the Olifants River gorge of Kruger National Park, South Africa. Aquatic Conservation: Marine and Freshwater Ecosystems 21: 55-164.

Fukuda Y, Saalfeld K, Lindner G, Nichols T (2013) Estimation of total length from head length of saltwater crocodiles (*Crocodylus porosus*) in the Northern Territory, Australia. Journal of Herpetology 47:34–40

Graham A, Bell R (1969) Factors influencing the countability of animals. East African Agricultural and Forestry Journal 34 (supp 1): 38-43.

Hodgson JC, Mott R, Baylis SM, Pham TT, Wotherspoon S, Kilpatrick AD, Raja Segaran R, Reid I, Terauds A, Koh LP (2018) Drones count wildlife more accurately and precisely than humans. Methods in Ecology and Evolution 9:1160-1167.

Hutton JM (1987) Morphometrics and field estimation of the size of the Nile crocodile. African Journal of Ecology 25:225-230.

Jordaan PR (2021) The establishment of a multifaceted *Crocodylus niloticus* Laurenti 1768 monitoring programme on Maputo Special Reserve (Maputo Province, Mozambique) with preliminary notes on the population (Reptilia: Crocodylidae). Herpetology Notes 14:1155-1162.

Myburgh, A., Botha, H., Downs, C.T. and Woodborne, S., 2021. The application and limitations of a low-cost UAV platform and open-source software combination for ecological mapping and monitoring. *African Journal of Wildlife Research, 51*, 166-177.

QGIS Development Team (2021) QGIS Geographic Information System. Open Source Geospatial Foundation Project. http://qgis.osgeo.org

Salem A (2011) Morphometric measurement and field estimation of the size of Crocodylus niloticus in Lake Nasser (Egypt). Transylvanian Review of Systematical and Ecological Research 12:53–74

Toffanin P (2019). OpenDroneMap: The Missing Guide. UAV4GEO. https://odmbook.com/

Utete B, (2021) A review of the conservation status of the Nile crocodile (*Crocodylus niloticus* Laurenti, 1768) in aquatic systems of Zimbabwe. Global Ecology and Conservation. https://doi.org/10.1016/j.gecco.2021.e01743

Wallace KM, Leslie AJ, Coulson T, Wallace AS (2013) Population size and structure of the Nile crocodile *Crocodylus niloticus* in the lower Zambezi valley Oryx 47:457-465

Warner, J.K., Combrink, X., Calverley, P., Champion, G. and Downs, C.T. (2016) Morphometrics, sex ratio, sexual size dimorphism, biomass, and population size of the Nile crocodile (*Crocodylus niloticus*) at its southern range limit in KwaZulu-Natal, South Africa. Zoomorphology 135:511-521

CHAPTER 5

The histology and growth rate of Nile crocodile (*Crocodylus niloticus*) claws

ALBERT MYBURGH[1,4], JAN MYBURGH[3], JOHAN STEYL[3], COLLEEN T. DOWNS[1], HANNES BOTHA[4,5] AND STEPHAN WOODBORNE[4].

[1]*Centre for Functional Biodiversity, School of Life Sciences, University of KwaZulu-Natal, Private Bag X01, Scottsville, Pietermaritzburg, 3209, South Africa*

[2]*Department of Animal and Wildlife Sciences, Faculty of Natural and Agricultural Sciences, University of Pretoria, Private Bag X20, Hatfield, 0028, South Africa*

[3]*Department of Paraclinical Sciences, Faculty of Veterinary Science, University of Pretoria, Private Bag X04, Onderstepoort, 0110, South Africa*

4iThemba LABS, Private Bag 11, WITS, South Africa

[4]*Scientific Services, Mpumalanga Tourism and Parks Agency, Nelspruit, South Africa*

[5]*Department of Biodiversity, University of Limpopo, Limpopo, South Africa*

Formatted for submission to *Herpetologica* (Uses USA English)

*** Corresponding Author:** Colleen T. Downs, **Email:** downs@ukzn.ac.za; **ORCID:** http://orcid.org/0000-0001-8334-1510

A Myburgh Email: Albert.isotopes@gmail.com; ORCID: http://orcid.org/0000-0002-6891-1893

J Steyl Email: johan.steyl@up.ac.za; ORCID: 0000-0002-5940-6799

JG Myburgh Email: jan.myburgh@up.ac.za; ORCID: https://orcid.org/0000-0002-2132-7251

H Botha Email: nilecrocs@mweb.co.za; ORCID: https://orcid.org/0000-0001-6870-5494

SM Woodborne Email: Swoodborne@tlabs.ac.za; ORCID: https://orcid.org/0000-0001-8573-8626

5.1 Abstract

The histology and growth of reptilian and crocodilian claws, in particular, have been reported, but the claws of Nile crocodiles (*Crocodylus niloticus*) have not been assessed. Age estimations on reptilian claws have not been attempted, although the claws of Nile crocodiles have been used for long-term dietary reconstruction with assumptions regarding their age. In this study, we report the histology and claw growth patterns of Nile crocodile claws. We used the growth patterns to infer axes for sampling the cornified material for radiocarbon dating and to derive age estimations of crocodilian claws to evaluate assumptions made in previous dietary reconstruction studies. Nile crocodile claws revealed similar growth patterns to those observed in other reptilians, and claws were no older than a decade. Claws appeared as modified scutes/scales, revealing an age profile along the unguis from the base to the tip and dorsoventrally through the unguis near the tip of the claw. Radiocarbon dates support the assumptions of previous studies that abrasion of the claws means that the retained cornified material is typically relatively young (5-10 years old). Claws can be used for dietary reconstruction in this time range, and we support the assumptions regarding claw growth made in previous studies, but it cannot be used to estimate ontogenetic age.

Keywords: Crocodile; Claws; diet; histology; radiocarbon; reconstruction

5.2. Introduction

ECOLOGISTS use variations in naturally occurring isotopes to reveal dietary relationships among organisms (Boecklen et al. 2011; Layman et al. 2012), patterns of migration (Cerling et al. 2006; Hallworth et al. 2018; Hobson and Wassenaar 2018), and to investigate ecological change (Dawson and Siegwolf 2007). Shifts in food web dynamics (the relative trophic position of organisms in a food web) have become important indicators of ecosystem state, especially in aquatic systems (Vander Zanden 1999; Wang et al. 2014; Santos et al. 2018; Krause et al. 2019). Isotope analysis of temporally resolved tissues, such as claws, baleen, feathers and hair that grow ubiquitously while remaining inert after their formation, is particularly useful because it can be used to resolve temporal changes in dietary assimilation (Dalerum and Angerbjörn 2005; Barquete et al. 2013). It reveals trophic relationships as well as migration data that is otherwise difficult to determine using conventional behavioral observations or stomach lavaging (Layman et al. 2012; Hobson and Wassenaar 2018).

The Olifants River, in the northeastern region of South Africa, is the country's most utilized river system (Ashton 2010). At approximately 450 km in length, it is exposed to industrial utilization in its upper catchment, serves one of the country's largest irrigation schemes, hosts many of its coal-fired power plants, and is subject to untreated sewage discharge throughout (Myburgh 2019). The Olifants River flows east and exits South Africa into Mozambique through the Olifants River Gorge in the Kruger National Park. Here, more than 180 large Nile crocodiles (*Crocodylus niloticus*) succumbed to the dietary disease pansteatitis in the autumn and winters of 2008-2010 (Ferreira and Pienaar 2011). This disease was prevalent in catfish (*Clarias* spp.) and Nile crocodiles and was later detected in herons and Mozambique tilapia (*Oreochromis mossambicus*) in other regions of the catchment (Myburgh and Botha 2009; Huchzermeyer 2012; Dabrowski 2014; Sara et al. 2020). Initial investigations focused on water quality (Ashton 2010) as Lake Massingir (located across the border in

Mozambique) back floods into the Olifants River Gorge during high flows, converting the river from lentic to lotic, stagnating pollutant laden water and driving toxic algal blooms (Woodborne et al. 2012; Woodborne 2021 unpub. data).

Stable isotope analyses showed dietary aetiology to pansteatitis associated with nutrient pollution as filter-feeding fish in the Olifants River Gorge had elevated δ^{15}N values linked to pollutant driven algal blooms (Woodborne et al. 2012; Woodborne et al. in prep). Elevated δ^{15}N values in aquatic systems are normally associated with nutrient pollution. It was postulated that the crocodiles were being exposed to a dietary item (filter-feeding fish) that trophically linked them to nutrient pollution in the river (Woodborne et al. 2012). Changes in diet are often reflected in keratinous tissues and samples along the basal-distal axis of the unguis of Nile crocodile claws from post-mortem animals had patterned cycles in δ^{15}N attributed to episodic fish binge feeding, and it was proposed that this exposure pathway (to pollutants) was the cause of the mass mortalities (Woodborne et al. 2012; see https://youtu.be/7XiXPt6Ujgk?t=5584). These periodic elevations in δ^{15}N were assigned a nominal time axis in the absence of data on the growth and wear rates of Nile crocodile claws and lacked the time scale needed to link the disease outbreak to chronological changes in river morphology and nutrient/pollutant dynamics. Further investigations into the development and age of crocodilian claws were suggested as this would constrain the uncertainties around the temporal scales of this fish binge feeding hypothesis (Woodborne et al. 2012).

The chemical composition, as well as a detailed description of the development and structure of various reptilian claws, appear elsewhere (Alibardi 2021), but notable differences exist during reptilian claw development in comparison with other taxa. The cornification process is differentiated from that of other taxa; the region of cell proliferation and growth is not localized in a nail groove, and dividing cells are equally distributed along the epidermis on the last phalange from the proximal base to the tip (Maderson 1985; Landmann 1986; Alibardi

and Thompson 2002; Alibardi 2009; 2010; 2016; 2021). Claws appear as modified scales/scutes where growth patterns are retained, and cornification occurs along the length of the claw (Kreisa 1979; Wu et al. 2004; Alibardi 2008a,b; 2009; Chang et al. 2009; Rutland et al. 2019) as the cytoplasmic content of epidermal cells is replaced by filamentous proteins (Tomlinson et al. 2004; Alibardi 2021). The result is a transformation from living, functional cells to cornified structurally dead and chemically inert cells (Müllling et al. 2000; Ethier et al. 2013; Wang et al. 2016). The histology of reptilian and crocodilian claws, in particular, has been investigated (Alibardi and Thompson 2002; Alibardi 2009; 2010; 2021), but the histology of the claws of the Nile crocodile has not been reported, and age estimations of the cornified structures of crocodilian claws have not been attempted.

Radiocarbon dating provides age measurements of carbon-based materials with biological origins (Bowman 1990; Taylor 1997; Hajdas et al. 2021). Advances in the last three decades have helped produce measurements with greater accuracy on smaller samples (typically in the mg range), allowing researchers in a number of disciplines to address chronological questions that could not be dealt with 10 or 20 years ago (Bronk Ramsey 2008; Hajdas et al. 2021). Human hair was one of the first samples to be dated using the technique (Libby 1949; 1954). Large-scale above-ground nuclear bomb testing in the mid-20th century resulted in a rise in atmospheric ^{14}C concentrations (known as the bomb curve), and this can be used to resolve ages with an annual or intra-annual resolution for samples that incorporated atmospheric carbon from the last 70 years (Reimer et al. 2004; Hodge et al. 2011; Dutta 2016). Cornified tissues are considered appropriate material for radiocarbon dating (Nardoto et al. 2020; Hajdas et al. 2021), and for tissues grown in the last 70 years, the bomb carbon curve provides a novel way of estimating age and growth rates.

The distribution of the growth layers in the claws of crocodilians and other reptiles should yield a distinct age profile across the dorsal-basal axis of the claw. A time series of this

nature is potentially useful in growth rate or age determination, but it could be used in combination with stable isotopes or trace element analysis to investigate dietary histories or migrations. This was implied but not tested in the study of diet histories of Nile crocodiles in the Kruger National Park following the pansteatitis epidemic.

In this study, we investigated the histology of the claw of the Nile crocodile and used the structure to inform the sampling of cornified material for radiocarbon dating to estimate the retention time of cornified material along the claw. We hypothesized that the claws of Nile crocodiles retain keratin for relatively short periods of time (10 years or less) and that the patterned spikes in Woodborne et al. (2012) are annual spikes of δ^{15}N associated with fish binge feeding. Alternatively, whether the claws of Nile crocodiles are older than 20+ years can be tested using the radiocarbon associated with above-ground nuclear testing. If this is the case, then the δ^{15}N patterns of Woodborne et al. (2012) are not annual, and the fish binge feeding hypothesis is rejected.

5.3 Materials and Methods

5.3.1 Histology

Limbs from hatchling Nile crocodiles were obtained from natural mortalities at a crocodile farm through collaboration with the Exotic Leather Research Centre, Onderstepoort Veterinary Institute (Faculty of Veterinary Science, University of Pretoria, Pretoria, South Africa) under ethical clearance from the University of KwaZulu-Natal, protocol reference number 020/15/Animal.

All histological examinations were conducted at the Onderstepoort Veterinary Institute during 2021. Limbs were fixed in formalin for at least 48 h after sampling. Subsamples containing phalanges and claws were dehydrated through 70, 80, 96, and 2X 100 % ethanol solutions and then processed through 50:50 ethanol: xylol, 2X 100 % xylol and 2X paraffin

wax (60–120 min per step) using an automatic tissue processor. Tissue samples were then imbedded manually into paraffin wax in plastic moulds, and sections of between 6-10 µm were cut using a microtome, fixed, and stained using toluidine blue. The orientation of cornified layers was used to infer the directionality of growth and the axis for sampling for radiocarbon analyses.

5.3.2 Radiocarbon Dating

Claws from two wild Nile crocodile individuals (± 3 m total length (TL)) were obtained from carcasses found during aerial surveys of the Olifants River in the Kruger National Park, South Africa, and another from a post-mortem investigation of a large crocodile (5.05 m TL) in the middle regions of the Olifants River, under permit number MPB 9225/2 from the Mpumalanga Tourism and Parks Agency. Claws were removed from animals several days following their death. The Kruger National Park Nile crocodiles succumbed to unknown circumstances, whilst the larger individual starved to death after it had swallowed fishing nets (pers. obs.). Claws were removed by severing the phalanges with the largest claws from the back foot of the animal using a scalpel.

Claw preparation and radiocarbon dating was conducted at iThemba LABS, Johannesburg, South Africa. Soft tissue and cornified material were separated by boiling claws in distilled water for approximately 3 h. Thereafter, claws were cleaned with a sterile toothbrush and sectioned, dorsoventrally in half, using a diamond-edged cutting blade on a Dremel™ rotary tool. A photograph of the sectioned claw was taken under a dissection microscope, imported and outlined in Designspark (Designspark Mechanical 5.0 (ANSYS Inc. 2020)) for graphical representation.

From the Kruger National Park Nile crocodile claws, four samples were obtained from the unguis of the claw (the dorsal aspect of the claw pertaining to the keratinous layer)

following the methods of Woodborne et al. (2012). The claw from the larger crocodile was sampled similar to the others, but an additional sample set was obtained along the basal dorsal axis of the claw through the unguis at the claw tip. For this claw, both sampling directions included a common sample (asterisk in Fig. 5.1), for a total of seven radiocarbon samples from a single claw. Samples of ± 6 mg were obtained at the selected locations using a dental drill (Fig. 5.1). Four additional claw tip samples were obtained from living animals in the Olifants River, Kruger National Park, by scraping cornified material from the claw tip (asterisk in Fig. 5.1) during routine health assessments on captured Nile crocodiles in the Kruger National Park.

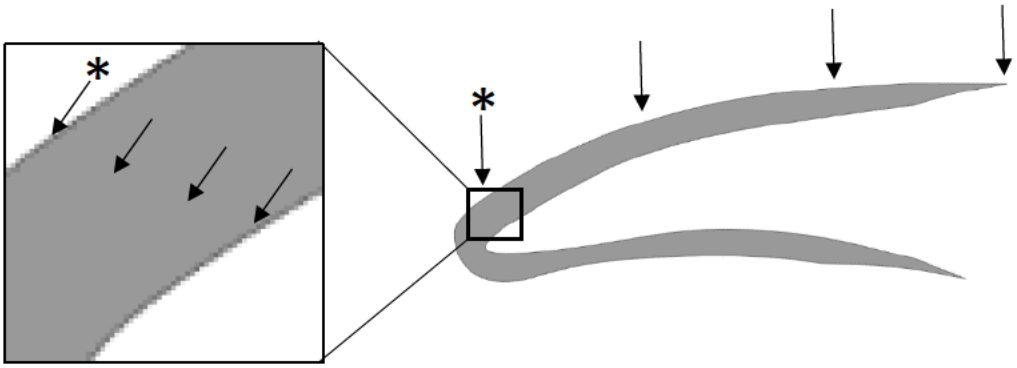

FIG. 5.1: A schematic outline of Figure 5.2(A). Sampling locations for radiocarbon dating along Nile crocodile claws in the present study. Arrows indicate sample locations, and those marked with an asterisk are from the same location. The Kruger National Park claws were only sampled on the dorsal aspect of the unguis.

The radiocarbon measurements were conducted at the AMS Facility of iThemba LABS, Johannesburg, Gauteng, South Africa, using the 6 MV Tandem AMS system (Mbele et al. 2017). The radiocarbon dates and errors were rounded to the nearest year. Radiocarbon dates were calibrated and converted into calendar ages with the OxCal v4.4 for Windows (Bronk Ramsey 2008) by using the SHCal20 atmospheric data set (Hogg et al. 2020).

FIG. 5.2: Histologically sectioned claws from hatchling Nile crocodiles (a, b, c) in the present study. The black bars indicate the areas where cross-sections were made b and c. Notice the uniform distribution of cornified tissue in b and the folded corneocytes on the dorsal surface in c. The black arrows are associated with the unguis (keratinous material) of the claw in all three images, with underlaying layers of keratinocytes stained in dark purple supported by the last phalange.

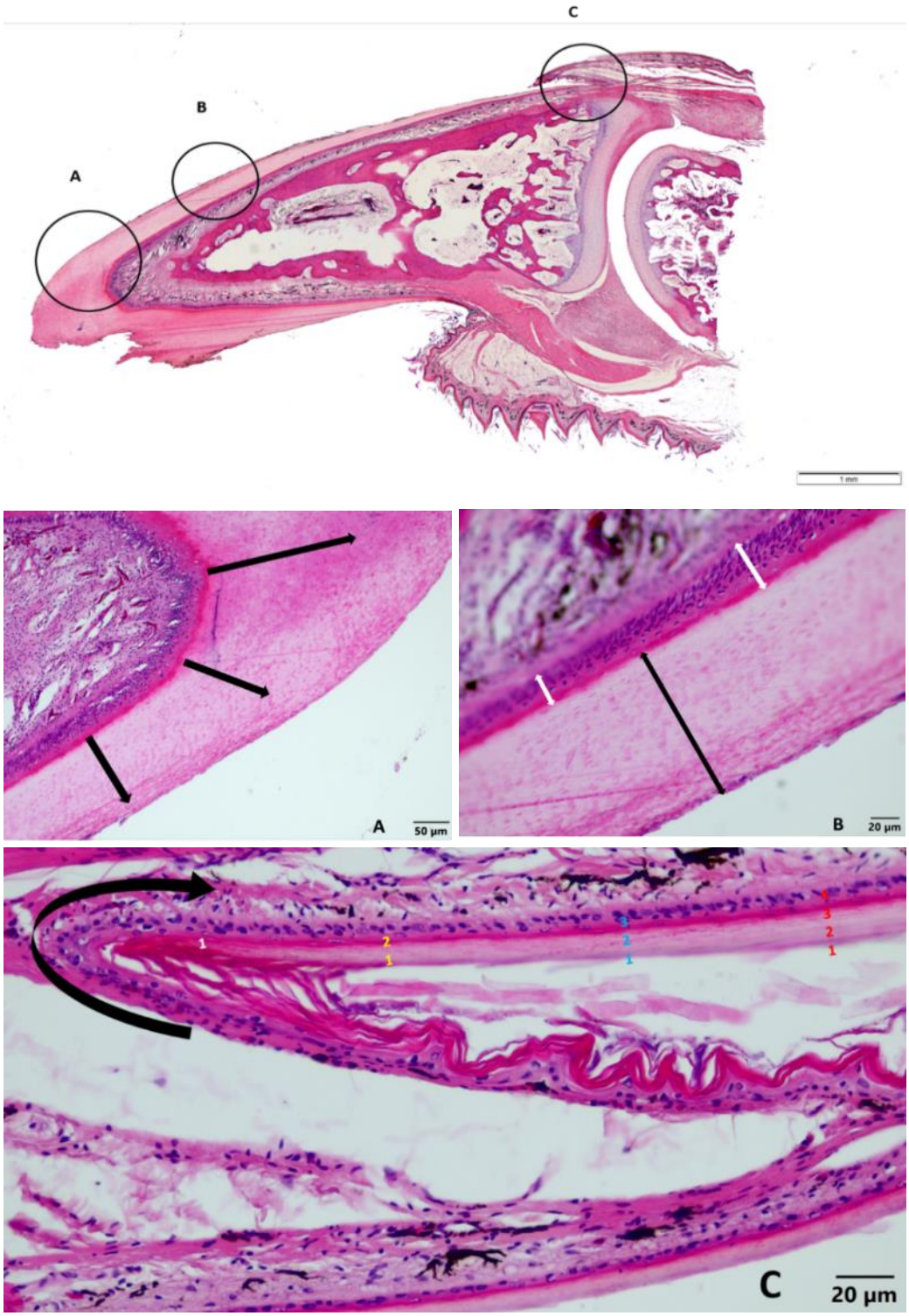

FIG. 5.3: Histologically **s**ectioned claws from hatchling Nile crocodiles in the present study. Circled areas indicate the areas associated with images a,b and c. The black arrows in a and b indicate the directionality of cornification, and the white arrows indicate regions of dividing corneocytes. The numbers in c correspond to individual layers of maturing corneocytes. The curved black arrow depicts the folded layer of keratinocytes at the dorsal side where the "skin" meets the claw.

5.4 Results

5.4.1 Histology

The claw of the Nile crocodile is similar in structure to that of the American alligator (*Alligator mississippiensis*) described in Alibardi (2009, 2021) (Fig. 5.2). In hatchlings where relatively low wear rates have not reduced the ventral surfaces, corneocytes formed stacked layers that were thickest on the dorsal, most curved part of the claw. Growth occurred uniformly around the last phalange (Fig. 5.2b) with folded layers of corneocytes where the claw and last scute layers differentiate (Fig. 5.3c). This results in elongation of the claw, and corneocyte layers thicken toward the tip (Fig. 5.2a and 5.3b).

Claws from adult Nile crocodiles had layers of cornification that conformed to the growth pattern seen in hatchling crocodiles. Corneocytes spread across the basal proximal axis of both the dorsal and ventral part of the last phalange and produce cornified sheaths that represent "stacked cones" so that an age profile existed along the length of the unguis and sub-unguis, as well as dorsoventrally through the unguis. This observation was fundamental to the use of claws as a proxy record (for example, diet history reconstruction through stable light isotope analyses) for behavioral changes through time. It also provided the growth framework that can be calibrated in terms of age using radiocarbon dating. The sub-unguis was more subject to wear and was relatively thin, and could not be sampled dorsoventrally to produce sufficient quantities of material for radiocarbon dating.

5.4.2 Radiocarbon dating

A total of 19 analyses were made from seven claws. It was anticipated that older corneocytes would have higher percent modern carbon (pMC) values as far back as about 1965, and so any cornified material that has formed in the last 70 years should reflect this peak (Hajdas et al.

2021). Results from both dorsal/ventral, and longitudinal sample transects showed no evidence of the elevated radiocarbon levels that occurred between 1960 and 1995 (Fig. 5.4). One result from Claw 3 fell within the range of the pre-1955 radiocarbon levels, but it also fell within 2 standard deviations of the post-2020 radiocarbon levels. Radiocarbon dating results are expressed with their associated errors in Table 5.1. Radiocarbon dates revealed variable ages from the three sectioned claws, with Claw 2 producing the oldest age estimation and a calibrated cornification date of around 2010 (± 5-10 years old).

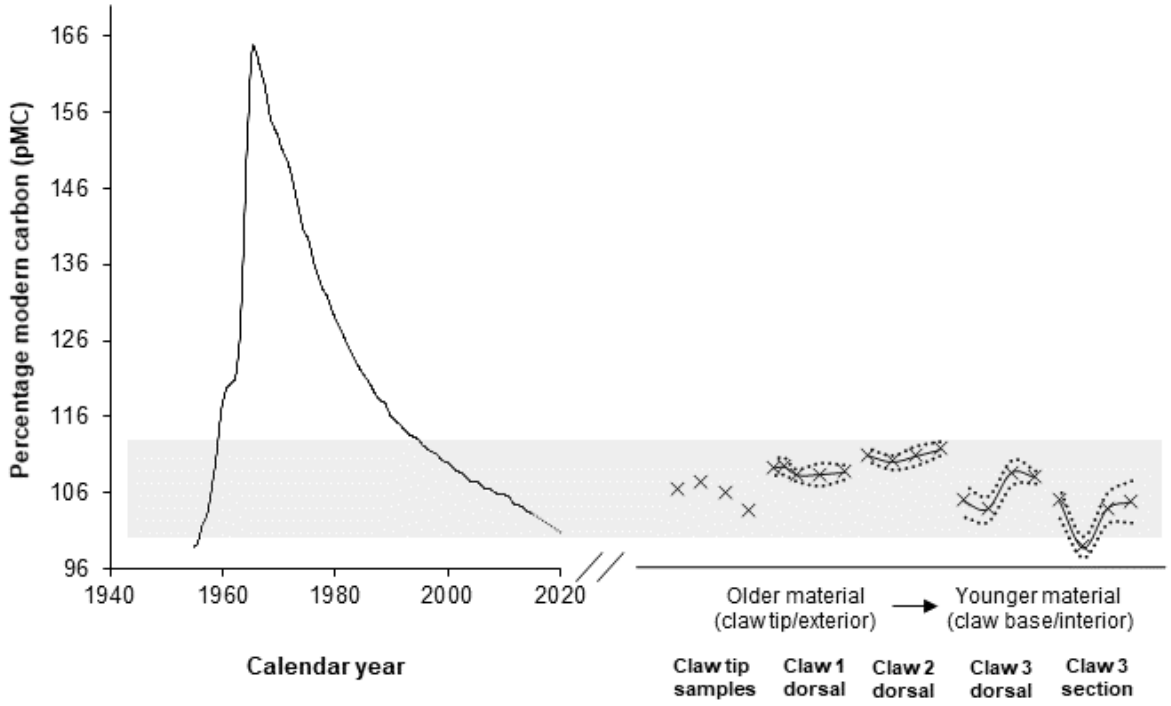

FIG. 5.4: Radiocarbon values (expressed as pMC) of Nile crocodile claws (represented by X's) compared with the atmospheric radiocarbon model of Turnbull et al. (2017) for the southern hemisphere zone 1-2. The shaded bar represents the area covered by the upper limits of the errors associated with one standard deviation (which are in turn individually represented by dashed lines). The solid lines indicate the pMC trends across pMC average values. The claw tip samples are from four individual animals whilst the claw samples for claw 1, 2 and 3 are sectioned claws from three different animals.

Table 5.1: Summary of radiocarbon results from Nile crocodile claws in the present study. Claws a-d indicate single claw tip scrapings taken from four different adult living animals whilst claws 1-3 are associated with deceased individual animals.

Sample/series ID	Sample location	pMC	pMC error
Claw a	Tip	103.36	0.34
Claw b	Tip	103.92	0.35
Claw c	Tip	102.99	0.35
Claw d	Tip	101.43	0.38
Claw 1	Tip	105.25	0.70
	Mid 1	105.36	0.71
	Mid 2	104.56	0.50
	Base	104.82	0.62
Claw 2	Tip	106.35	0.57
	Mid 1	105.74	0.60
	Mid 2	106.29	0.84
	Base	106.88	0.61
Claw 3	Tip	102.30	1.38
	Mid 1	101.63	1.12
	Mid 2	104.77	1.07
	Base	104.39	0.53
Claw 3 section	Outer surface/tip	102.30	1.38
	Inner 1	98.27	0.90
	Inner2	101.67	1.40
	Inner surface	102.27	1.90

5.5 Discussion

Histological evidence (Fig. 5.3) suggested that the growth of Nile crocodile claws led to an inherent age profile along two axes: one, along the dorsal surface of the unguis from the base to the tip of the claw, and another dorsoventrally through the unguis. As the epidermis grew distally (moved distally by the underlying phalangeal growth), cornification was continuous, and the hyper eosinophilic layer immediately adjacent to the last living corneocyte was the same age throughout the claw. Therefore the "inner" layer (first layer/region of cornification) of the claw is the same age. Following this, the claw's very "outer" layer retained the oldest corneocytes for that specific segment. It related that the "outer / dorsal" region of the very tip

of the claw would retain the oldest region of cornified material in a claw that was not subject to wear. This growth model, coupled with similar patterns in the radiocarbon analyses of claw 3 through these two axes, supports the growth patterns described here and elsewhere (Alibardi 2021).

Radiocarbon dates revealed variable ages for the three claws (Fig 5.4. and Table 5.1). None of the claws revealed any elevated radiocarbon associated with above-ground nuclear testing in the range 1960 to 1995. Considering the related errors in measurements, the absence of any evidence for keratin secreted in the 1960 to 1995 range in any of the samples suggests that it is doubtful that the Claw 3 result fell in the pre-1955 era, and the evidence indicated that all of the samples formed in the post-1995 era, i.e. these particular claws do not retain any material from the pre-1955 era and are all relatively young. All of the claws have estimated ages of <10 years (Fig. 5.3).

The anticipated temporal trends from the dorsal/ventral and interior/exterior sample sequences of Claws 1, 2 and 3 were not noted, and there may be an indication of an inverted sequence, but the results reported in Table 2.1 show that all results from these transects are statistically indistinguishable from each other when the errors are considered. The lack of a trend suggests that wear and ongoing claw growth lead to a relatively short temporal representation in the claw and that the notion of ageing Nile crocodiles by dating their claws was confounded by abrasion.

These radiocarbon results suggest that there was little or no claw material that persisted for more than ~10 years in wild Nile crocodiles. It is almost certain that all of the crocodiles in this study were older than 10 years, and the issue becomes a balance between the growth of new cornified layers versus the rate at which abrasion removes older material from the claws. The cornified layers that are retained have an inherent age structure, but are not reflective of the entire lifespan of the animal.

The fish binge feeding hypothesis used by Woodborne et al. (2012) to explain "annual" δ^{15}N excursions along the unguis of Kruger National Park Nile crocodile claws may actually be a conflation of a progressively older signature, moving distally from the base of the claw when wear exposes older corneocytes successively towards the tip of the claw in the area where the claw is thickest. Whether or not there is a duplication of the δ^{15}N pulses in a transect of the unguis does not affect the argument presented by Woodborne et al. (2012), as the overall number of pulses falls within the age range of claws, and they could conceivably reflect annual events. The evidence is consistent with the link between the river dynamics and the pansteatitis pandemics previously proposed. That the events are fish-eating binges cannot be unequivocally supported as self-metabolism (e.g., during starvation) is known to cause increases in δ^{15}N values of animal tissues (Doi et al. 2017). However, limited research suggests that periods of fasting do not significantly affect the δ^{15}N values of reptilian claws (McCue and Pollock 2008).

The methods described in Woodborne et al. (2012) for time series dietary reconstruction from crocodilian claws could be applied to living animals to infer trophic dynamics of the aquatic/terrestrial interface at an annual scale. This has larger implications for managing crocodilians as dietary changes can be compared with changes in land use, water quality etc., but future research should focus on elucidating the effects of seasonality, breeding and fasting in order to increase the resolution of trophic effects on crocodilian claw keratin isotope values. Unfortunately, the impact of claw wear means that they are not suitable for establishing the ontogenetic age of crocodiles.

5.6 Acknowledgements

We thank the IUCN Crocodile specialist group and the National Research Foundation (ZA, Grant 98404) for providing funding that supported this research.

5.7 Literature Cited

Alibardi, L. and Thompson, M.B., 2002. Keratinization and ultrastructure of the epidermis of late embryonic stages in the alligator (*Alligator mississippiensis*). *Journal of Anatomy*, *201*, 71-84.

Alibardi, L., 2009. Development, comparative morphology and cornification of reptilian claws in relation to claws evolution in tetrapods. *Contributions to Zoology*, *78*, 25-42.

Alibardi, L., 2010. Autoradiographic observations on developing and growing claws of reptiles. *Acta Zoologica*, *91*, 233-241.

Alibardi, L. (2016). Sauropsid cornification is based on corneous beta-proteins, a special type of proteins of the epidermis. *Journal of Experimental Zoology*, *326B*, 338–351.

Alibardi, L., 2021. Development, structure, and protein composition of reptilian claws and hypotheses of their evolution. *Anatomical Record*, *304*, 732-757

Ashton, P.J., 2010. Demise of the Nile crocodile (*Crocodylus niloticus*) as a keystone species for aquatic ecosystem conservation in South Africa: the case of the Olifants River. *Aquatic Conservation: Marine and Freshwater Ecosystems*, *20*, 489-493.

Barquete, V., Strauss, V. and Ryan, P.G., 2013. Stable isotope turnover in blood and claws: a case study in captive African penguins. *Journal of Experimental Marine Biology and Ecology*, 448, 121-127.

Boecklen, W.J., Yarnes, C.T., Cook, B.A. and James, A.C., 2011. On the use of stable isotopes in trophic ecology. *Annual Review of Ecology, Evolution, and Systematics*, *42*, 411-440.

Bowman, S., 1990. *Radiocarbon dating* (Vol. 1). Univ of California Press, Ca.

Bronk Ramsey, C., 2008. Radiocarbon dating: revolutions in understanding. *Archaeometry*, *50*, 249-275.

Chang, C., Wu, P., Baker, R.E., Maini, P.K., Alibardi, L. and Chuong, C.M., 2009. Reptile scale paradigm: Evo-Devo, pattern formation and regeneration. *International Journal of Developmental Biology*, *53*, 813.

Cerling, T.E., Wittemyer, G., Rasmussen, H.B., Vollrath, F., Cerling, C.E., Robinson, T.J. and Douglas-Hamilton, I., 2006. Stable isotopes in elephant hair document migration patterns and diet changes. *Proceedings of the National Academy of Sciences*, *103*, 371-373.

Dabrowski, J., 2014. *Pansteatitis in tilapia (Oreochromis mossambicus) from Loskop Dam, South Africa: links between the environment, diet and thyroid status*. PhD thesis, University of Pretoria, Pretoria, South Africa.

Dalerum, F. and Angerbjörn, A., 2005. Resolving temporal variation in vertebrate diets using naturally occurring stable isotopes. *Oecologia*, *144*, 647-658.

Dawson, T.E. and Siegwolf, R.T., 2007. Using stable isotopes as indicators, tracers, and recorders of ecological change: some context and background. *Terrestrial Ecology*, *1*, 1-18.

Doi, H., Akamatsu, F. and González, A.L., 2017. Starvation effects on nitrogen and carbon stable isotopes of animals: an insight from meta-analysis of fasting experiments. *Royal Society Open Science*, *4*, 170633.

Dutta, K., 2016. Sun, ocean, nuclear bombs, and fossil fuels: radiocarbon variations and implications for high-resolution dating. *Annual Review of Earth and Planetary Sciences*, *44*, 239-275.

Ethier, D.M., Kyle, C.J., Kyser, T.K. and Nocera, J.J., 2013, April. Trace elements in claw keratin as temporally explicit indicators of geographic origin in terrestrial mammals. *Annales Zoologici Fennici*, *50*, 89-99.

Ferreira, S.M. and Pienaar, D., 2011. Degradation of the crocodile population in the Olifants River gorge of Kruger National Park, South Africa. *Aquatic Conservation: Marine and Freshwater Ecosystems*, *21*, 155-164.

Gorman, D., Turra, A., Connolly, R.M., Olds, A.D. and Schlacher, T.A., 2017. Monitoring nitrogen pollution in seasonally-pulsed coastal waters require judicious choice of indicator species. *Marine Pollution Bulletin*, *122*, 149-155.

Hajdas, I., Ascough, P., Garnett, M.H., Fallon, S.J., Pearson, C.L., Quarta, G., Spalding, K.L., Yamaguchi, H. and Yoneda, M., 2021. Radiocarbon dating. *Nature Reviews Methods Primers*, *1*, 1-26.

Hallworth, M.T., Marra, P.P., McFarland, K.P., Zahendra, S. and Studds, C.E., 2018. Tracking dragons: stable isotopes reveal the annual cycle of a long-distance migratory insect. *Biology Letters*, *14*, 20180741.

Hobson, K.A. and Wassenaar, L.I. eds., 2018. *Tracking animal migration with stable isotopes*. Academic Press, London.

Hodge, E., McDonald, J., Fischer, M., Redwood, D., Hua, Q., Levchenko, V., Drysdale, R., Waring, C. and Fink, D., 2011. Using the 14 C bomb pulse to date young speleothems. *Radiocarbon*, *53*, 345-357.

Hogg, A.G., Heaton, T.J., Hua, Q., Palmer, J.G., Turney, C.S., Southon, J., Bayliss, A., Blackwell, P.G., Boswijk, G., Ramsey, C.B. and Pearson, C., 2020. SHCal20 Southern Hemisphere calibration, 0–55,000 years cal BP. *Radiocarbon*, *62*,759-778.

Huchzermeyer, K.D.A., 2012. Prevalence of pansteatitis in African sharptooth catfish, *Clarias gariepinus* (Burchell), in the Kruger National Park, South Africa. *Journal of the South African Veterinary Association*, *83*, 1-9.

Krause, A., Sandmann, D., Bluhm, S.L., Ermilov, S., Widyastuti, R., Haneda, N.F., Scheu, S. and Maraun, M., 2019. Shift in trophic niches of soil microarthropods with conversion of tropical rainforest into plantations as indicated by stable isotopes (15N, 13C). *PLoS One*, *14*, e0224520.

Landmann, L., 1986. Epidermis and dermis. In *Biology of the Integument*, 150-187, Springer, Berlin, Heidelberg.

Layman, C.A., Araujo, M.S., Boucek, R., Hammerschlag-Peyer, C.M., Harrison, E., Jud, Z.R., Matich, P., Rosenblatt, A.E., Vaudo, J.J., Yeager, L.A. and Post, D.M., 2012. Applying stable isotopes to examine food-web structure: an overview of analytical tools. *Biological Reviews*, *87*, 545-562.

Libby, W.F., Anderson, E.C. and Arnold, J.R., 1949. Age determination by radiocarbon content: world-wide assay of natural radiocarbon. *Science*, *109*, 227-228.

Libby, W.F., 1954. Chicago radiocarbon dates V. *Science*, *120*, 733-742.

Maderson, P.F., 1985. Some developmental problems of the reptilian integument. *Biology of the Reptilia*, *14*, 525-598.

McCue, M.D. and Pollock, E.D., 2008. Stable isotopes may provide evidence for starvation in reptiles. *Rapid Communications in Mass Spectrometry*, *22*, 2307-2314.

Mülling, C.K., 2000. Three-dimensional appearance of bovine epidermal keratinocytes in different stages of differentiation revealed by cell maceration and scanning electron microscopic investigation. *Folia Morphologica*, *59*, 239-246.

Myburgh, J. and Botha, A., 2009. Decline in herons along the lower Olifants River–could pansteatitis be a contributing factor. *Vet News*, *3*, 20-23.

Myburgh, A. 2019. Ecological responses to the nutrient gradient in the middle Olifants River, Limpopo Province, South Africa, MSc Thesis, University of Pretoria, Pretoria, South Africa

Nardoto, G.B., Sena-Souza, J.P., Chesson, L.A. and Martinelli, L.A., 2020. Tracking geographical patterns of contemporary human diet in Brazil using stable isotopes of nail keratin. In: Parra R.C., Zapico, S.C., Ubelaker, D.H., (Eds), *Forensic Science and Humanitarian Action: Interacting with the Dead and the Living*, Wiley, London, pp 441-455.

Rutland, C.S., Cigler, P. and Kubale Dvojmoč, V., 2019. Reptilian skin and its special histological structures. In: Rutland, C., Kubale, V. (Eds), *Veterinary Anatomy and Physiology*. InTech. https://www.intechopen.com/books/7144

Reimer, P.J., Brown, T.A. and Reimer, R.W., 2004. Discussion: reporting and calibration of post-bomb 14C data. *Radiocarbon*, *46*, 1299-1304.

Santos, X., Navarro, S., Campos, J.C., Sanpera, C. and Brito, J.C., 2018. Stable isotopes uncover trophic ecology of the West African crocodile (*Crocodylus suchus*). *Journal of Arid Environments*, *148*, 6-13.

Sara, J.R., Luus-Powell, W.J., Fogelson, S.B., Botha, H., Guillette, T.C., Smit, W.J., Hoffman, A., Kunutu, K.D., Koelmel, J.P. and Bowden, J.A., 2020. A histological evaluation of pansteatitis-affected Mozambique tilapia, *Oreochromis mossambicus* (Peters 1852), from different geographical locations in South Africa. *Journal of Fish Diseases*, *43*, 1185-1199.

Taylor, R.E., 1997. Radiocarbon dating. In: Taylor, R.E., Aitken, M.J. (Eds), *Chronometric dating in archaeology*, Springer, Boston, MA, pp 65-96.

Tomlinson, D.J., Mülling, C.H. and Fakler, T.M., 2004. Invited review: formation of keratins in the bovine claw: roles of hormones, minerals, and vitamins in functional claw integrity. *Journal of Dairy Science*, *87*, 797-809.

Turnbull, J.C., Mikaloff Fletcher, S.E., Brailsford, G.W., Moss, R.C., Norris, M.W. and Steinkamp, K., 2017. Sixty years of radiocarbon dioxide measurements at Wellington, New Zealand: 1954–2014. *Atmospheric Chemistry and Physics*, *17*, 14771-14784.

Vander Zanden, M.J., Casselman, J.M. and Rasmussen, J.B., 1999. Stable isotope evidence for the food web consequences of species invasions in lakes. *Nature*, *401*, 464-467.

Wang, Y., Gu, B., Lee, M.K., Jiang, S. and Xu, Y., 2014. Isotopic evidence for anthropogenic impacts on aquatic food web dynamics and mercury cycling in a subtropical wetland ecosystem in the US. *Science of the Total Environment*, *487*, 557-564.

Wang, B., Yang, W., McKittrick, J. and Meyers, M.A., 2016. Keratin: Structure, mechanical properties, occurrence in biological organisms, and efforts at bioinspiration. *Progress in Materials Science*, *76*, 229-318.

Woodborne, S., Botha, H., Huchzermeyer, D., Myburgh, J., Hall, G. and Myburgh, A., 2021. Ontogenetic dependence of Nile crocodile (*Crocodylus niloticus*) isotope diet-to-tissue discrimination factors. *Rapid Communications in Mass Spectrometry*, *35*, e9159.

Woodborne, S., Huchzermeyer, K.D.A., Govender, D., Pienaar, D.J., Hall, G., Myburgh, J.G., Deacon, A.R., Venter, J. and Lübcker, N., 2012. Ecosystem change and the Olifants River crocodile mass mortality events. *Ecosphere*, *3*, 1-17.

CHAPTER 6

Elucidating the population demographics of the Kruger National Park Olifants River Gorge Nile crocodile population: a case study using a large multirotor UAV

Albert Myburgh[1], Sam Ferreira[2], Danie Pienaar[2], Colleen T. Downs[1], Stephan Woodborne[3], and Andrew B. Davies[4]

[1]*Centre for Functional Biodiversity, School of Life Sciences, University of KwaZulu-Natal, South Africa*

[2]*Scientific Services, South African National Parks, Private Bag X402, Skukuza, 1350, South Africa*

[3]*NRF, iThemba LABS, University of the Witwatersrand, Wits, South Africa*

[4]*Organismic and Evolutionary Biology, Harvard University*

Formatted for submission to *Journal of Herpetology*

*** Corresponding Author:** Colleen T. Downs

Email: downs@ukzn.ac.za; **ORCID:** http://orcid.org/0000-0001-8334-1510

Other emails and ORCIDs:

A Myburgh Email: Albert.isotopes@gmail.com; ORCID: http://orcid.org/0000-0002-6891-1893

S. Ferreira Email: sam.ferreira@sanparks.org; ORCID:

D. Pienaar Email: danie.pienaar@sanparks.org; ORCID:

SM Woodborne Email: sm.woodborne@ilabs.nrf.ac.za; ORCID: https://orcid.org/0000-0001-8573-8626

A. Davies Email: andrew_davies@g.harvard.edu; ORCID: 0000-0002-0003-1435

6.1 Abstract

The Nile crocodile *Crocodylus niloticus* population in the Olifants River Gorge, Kruger National Park, South Africa, was decimated by a pansteatitis outbreak between 2008 and 2011. Since then, several helicopter and fixed-wing manned surveys have been conducted, but unmanned aerial vehicles (UAVs) offer the opportunity to evaluate the demographics of this population with greater resolution. Here, we present the first UAV based survey of this Nile crocodile population. In June 2021 we surveyed the entirety of the South African section of the Olifants River Gorge over two days using a large multirotor UAV with a high-resolution camera and PPK global positioning system (GPS) capability. We counted a total of 450 crocodiles, compared with 101 from a manned aerial survey. We derived accurate demographic data based on crocodile sizes and evaluated the population structure of this Nile crocodile population in what is considered a stronghold for the species in South Africa. Our results reflect a disproportionate number of large crocodiles in this reach and support the importance of the Olifants River Gorge as a breeding area. This work lays the foundation for future monitoring that aids in conserving the largest crocodilian in Africa.

Keywords: Drone; Olifants River Gorge; Kruger national park; Nile crocodile; Population demographics; Unmanned aerial vehicle

6.2 Introduction

The frequency at which ecosystems reach tipping points is expected to increase in the coming decades (Perretti and Munch 2012; Su et al. 2021), but it may be possible to prevent unwanted or degradative changes to ecological systems if they are detected in time (Biggs et al. 2009). Apex predators are good indicators of change as they provide an integrated view of the system state (Sergio et al. 2008; Gangoso et al. 2020), and large vertebrate predators reflect important top-down effects on ecosystems (Dobson et al. 2006; Morris and Letnic 2017). Crocodiles are part of the terrestrial aquatic interface, and their population dynamics may reflect broad changes in both of these systems (Evans et al. 2016, 2017, Woodborne et al. 2021). Their demise may be indicative of cascading effects, and the resilience of a system could be assessed by elucidating their population dynamics at a fine scale (Swanepoel 1999; Ashton 2010; Woodborne et al. 2021).

The Nile crocodile *Crocodylus niloticus* population of the Olifants River Gorge in the Kruger National Park, South Africa, has received much attention in the last 13 years (Ashton 2010; Ferreira and Pienaar 2011; Woodborne et al. 2012; Lane et al. 2013; Woodborne et al. (unpublished data); D. Pienaar (unpublished data)). In the autumn and winter of 2008, this population reached a tipping point when more than 180 (out of an estimated 780 (95% CI: 637–1222) (Ferreira and Pienaar 2011) large Nile crocodiles succumbed to pansteatitis, a dietary disease linked to chronic pollution and river dynamics in the catchment (Ashton 2010; Ferreira and Pienaar 2011; Woodborne et al. 2012).

The Olifants River Gorge (Figure 6.1) crosses the country border between South Africa and Mozambique and consists of the region of the Olifants River (‘Rio Dos Elefantes’ in Mozambican) from the confluence of the Letaba and Olifants Rivers (hereafter ‘the confluence’) in the Kruger National Park, to the mouth of Lake Massingir in Mozambique (a stretch of 15 km when measured along the river's course during low flow) (Figure 6.1). This

area is considered a stronghold for Nile crocodiles and one of the most important breeding areas for the species in the Kruger National Park, where crocodiles have remained relatively undisturbed since the proclamation of the park in 1926 (Joubert 1986; Swanepoel et al. 2000). The ± 8 km of the Olifants River Gorge in South Africa (20 to 100 m wide) is characterised by steep rock faces with intermittent sandy bays ideal as nesting sites for Nile crocodiles (Swanepoel 1999; Swanepoel et al. 2000). In Mozambique, the Rio Dos Elefantes Gorge flattens out, and here the river is wider with sandy beaches sparsely covered by vegetation on both banks. The reaches of the Olifants and Letaba Rivers upstream of the confluence within the Kruger National Park host a large number of Nile crocodiles, but the Olifants River Gorge is a relatively small region where crocodiles concentrate (Ferreira and Pienaar 2011). Here, the largest and most dominant animals maintain breeding territories, and it plays an important role in the source-sink dynamics of the Nile crocodile populations of the Olifants and Letaba Rivers (Swanepoel 2000; Ferreira and Pienaar 2011).

Accurate demographic data with an applicable resolution are required at timely intervals to detect possible manifestations of ecosystem degradation, which is specifically difficult to obtain for crocodilians as they exhibit traits of both fast and slow-growing species (Briggs Gonzalez et al. 2017). The estimation of crocodile population demographics using traditional survey techniques (aerial and spotlight counts) may be subject to greater bias and variability (Caughly 1974; Pollock and Kendall 1987; Pacheco 1996; Redfern et al. 2002; Da Silveira et al. 2008). Previous surveys of the Nile crocodile population of the Olifants River Gorge from 1989 to 2008 (N = 14) relied on helicopters, and crocodiles were counted additionally during the annual common hippopotamus *Hippopotamus amphibius* census (Ferreira and Pienaar 2011). Dedicated Nile crocodile monitoring (2008-2009, N = 4) was only undertaken once the population was in decline as a result of pansteatitis (Ferreira and Pienaar 2011).

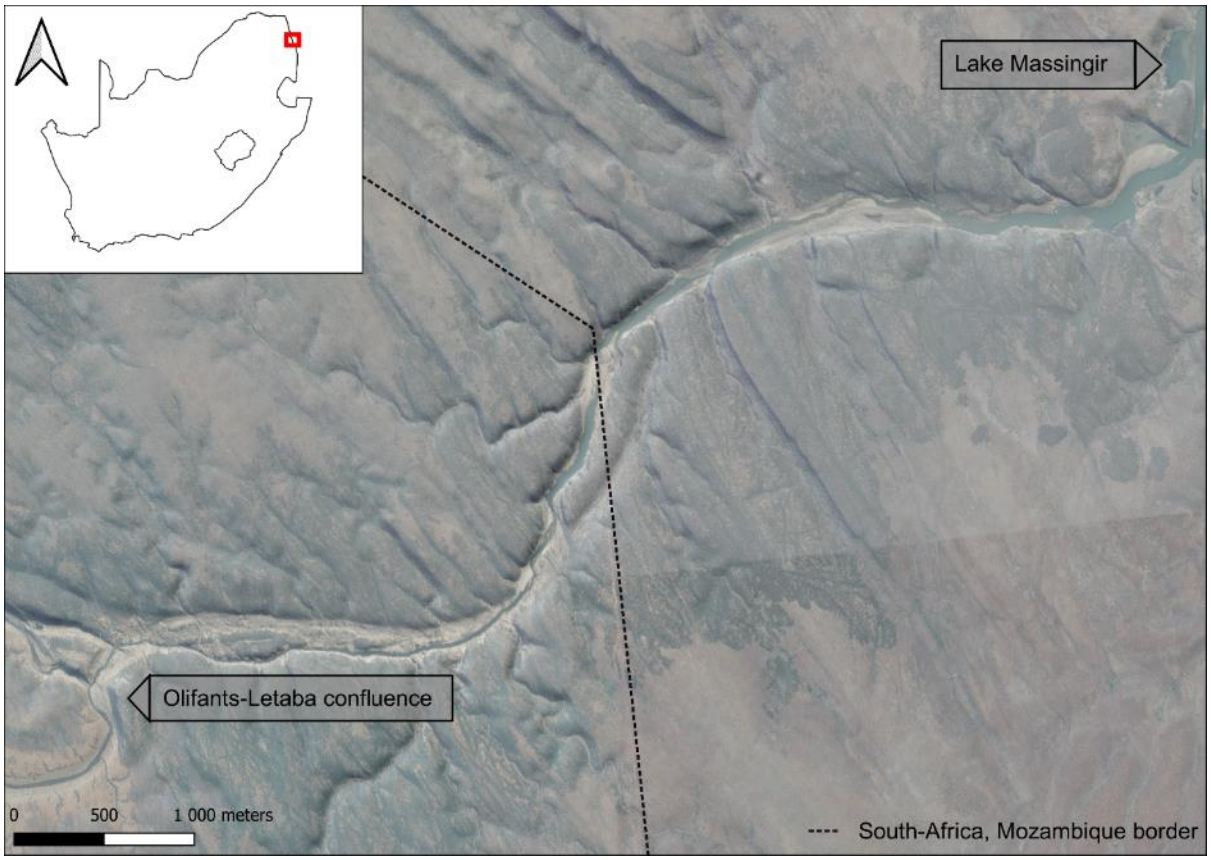

Figure 6.1: Hybrid satellite photograph and elevation model view of the Olifants River Gorge, Kruger National Park, South Africa. The Olifants River enters the gorge from the south and the gorge extends from the confluence to the mouth of Lake Massingir. (Satellite imagery: Google Earth) (Digital elevation model: SUDEM 2020 available at https://geosmart.space/products/sudem.html)

Traditional survey techniques categorise crocodiles into very broad size classes based on the observer's perspective (Ezat et al. 2018; Jordaan 2021). Comparisons between various techniques and unmanned aerial vehicle (UAV) based approaches highlight the benefits of UAVs over more traditional survey techniques (Aubert et al. 2021; Jordaan 2021). These outweigh the need for traditional survey techniques if the UAV can cover the desired area (Ezat et al. 2018; Nowak et al. 2018; Thapa et al. 2018; Jordaan 2021). One of the greatest advantages

of a UAV survey is eliminating bias in size class categorisation because rectified aerial imagery can be used to accurately measure crocodiles (Ezat et al. 2018; Myburgh et al. in prep). Additionally, survey frequencies can be increased, allowing for annual or intra-annual surveys at a fraction of what they would cost using traditional methods (Ezat et al. 2018; Jordaan 2021). The acquisition of population demographic data that are not subject to observer bias, where size classes can be easily defined, enriches demographic models with the resolution required to elucidate ecosystem change.

In this study, we evaluate the population demographics of the Nile crocodile population of the Olifants River Gorge using a large multirotor UAV equipped with a high-resolution camera. We compare the derived crocodile demographics with those obtained from a fixed-wing manned count a few weeks prior and discuss the differences between these methods. We evaluate the population using previously defined stage structure demographic models. We predicted the biomass of the population based on previous studies of total length (TL) body mass ratios and predicted that the biomass of the Nile crocodile population in the Olifants River Gorge exceeded that of other areas that are not considered breeding "hotspots". The Olifants River Gorge is expected to host a proportionally large number of adult crocodiles with relatively few smaller (<1.5 m TL) crocodiles that are not large enough to breed or compete for breeding territories.

6.3 Methods

6.3.1 Flights And Photograph Processing

We conducted UAV flights over the South African section (as delineated in Ferreira and Pienaar (2011)) of the Olifants River Gorge (415 ha) over a period of 2 days. We included a section of the Olifants River upstream of the confluence of the Olifants, and Letaba Rivers (70 ha) that stretches from the Olifants Trails Camp to the confluence (3.2 km) (see Ferreira and

Pienaar (2011) for descriptions of the survey reaches). The take-off location of the UAV meant that a small section of the Letaba river is also included in the density analyses of the area, but these animals are omitted from comparative counts between this and the fixed wing survey. The UAV flights were conducted on winter mornings (mid-June) over two days (flying between 10h00 and 14h00) when Nile crocodiles typically bask (Downs et al. 2008). All flights were approved by the South African Civil Aviation Authority and South African National Parks.

A Freefly Alta-XFlight quadcopter was piloted on automated routes using Alta Q Ground control flight planning software at an average altitude of 100m above the river, flying in grids perpendicular to the direction of the river with a ground sampling distance of ±3cm/pixel. A Stonex STX900 GNSS global positioning system (GPS) base station and AusPos (an online GPS processing service) for base station GNSS post-processing were used for UAV positional data. Inertial Explorer (v8.80) was used for trajectory processing, and Terraphoto (a product of Terrasolid; https://terrasolid.com/products/terraphoto) for image rectification and mosaicking. Mosaiced orthophotographs were output as .tiff files.

Orthophotographs were imported into QGIS (version 3.18.3), and Nile crocodiles were identified manually. Three independent observers identified Nile crocodiles from orthophotographs and verified them as single animals from original aerial imagery. In some cases (e.g., crocodiles that were swimming), individuals were rendered twice (due to movement between successive photographs), and were counted as single animals in our analyses. We counted Nile crocodiles by creating a vector point on the location of each identified crocodile head. Where the crocodile's tail was visible, a line string layer was created from the tip of the animal's snout, to the first circumcircle scute layer behind the animals' hind legs (snout to hind limb length (SHL)) as per Myburgh et al. (in prep)). We used standard geometry attribute derivations of line layers in QGIS to derive estimates of SHL. The correction equations derived

in Myburgh et al. (in prep) (Chapter 4) were used to estimate total length (TL) from snout to hind leg length (SHL).

We compared the Nile crocodile counts to the most recent fixed-wing survey (following the SOP of the Kruger National Park as per Ferreira and Pienaar (2011)) of the population (end-April 2021, 40 days earlier), which classified crocodiles as small, medium, large or extra-large as per the standard operating procedures of the Kruger National Park (Ferreira and Pienaar 2011). The observers during this flight were two experienced SANParks personnel that were involved in previous surveys of the same reach (Ferreira and Pienaar 2011). For comparison with other studies, Nile crocodile life stages (stage structure) were classified according to the size categories of Fergusson et al. (2006), and the population was divided on the basis of TL estimates into yearlings (< 50 cm), juveniles (50-100 cm), sub-adults (101-250 cm) and adults (>250 cm). To illustrate population demographics that are possible to obtain using UAV derived size estimations, we divided the estimated TL's into size classes at 10 cm increments and counted the number of individuals in each size class.

6.3.2 Population Models

We use the stage structure Leftkovich-matrix defined in Wallace et al. (2013) for the life stages of Nile crocodiles defined above to evaluate the stage structure of a crocodile population under stable growth (as in Wallace et al. 2013).

These results are expressed as a percentage of the total population when the yearling/hatchling size was omitted, similar to Wallace et al. (2013). To estimate biomass, we used the average length of Nile crocodiles that could be measured and multiplied this by the total number of crocodiles detected in this survey and used the biomass estimation equations of Warner et al. (2016). The biomass is related to shoreline length and total water area in the study region.

6.3.3 Software and Statistical Analyses

We used a Shapiro-Wilk normality test to evaluate the size class distribution of the Nile Crocodile population and a two-tailed students t-test to compare the UAV derived estimations to a previous survey of the population. We produced all regression and relationship graphs in Microsoft Excel© (Microsoft Office 2019) and created all maps with QGIS (version 3.18). Nile crocodile density distributions were generated using a kernel density heatmap calculated with a quartic kernel shape at a radius of 100 m. The population model was run in R through the RStudio interface (RStudio team, 2021).

6.4 Results

Orthophotograph resolutions were relatively low (3-5cm/px), and only the major features of crocodiles (head, limbs, tail etc.) could be identified (Figure 6.2). We counted 450 Nile crocodiles with UAV derived imagery and derived SHL for 351 of these. Some animals were submerged/partially submerged, making a size derivation difficult, and so we excluded these from the size class analyses. The ground sampling distance (GSD) of orthophotographs in this study was 3cm/pixel, hindering the identification of smaller individuals (hatchlings and smaller juveniles).

Estimated total lengths (N = 351) ranged from 123 to 544 cm, with a mean (± SD) of 284 ± 70 cm. When compared with the most recent population survey of the Olifants River Gorge using traditional methods, UAV derived counts were significantly higher across all five survey regions (two-tailed students t-test, $p > 0.05$) (Figure 6.3a). Within the survey region, crocodiles were most concentrated around the Olifants Trails Camp as well as at the South Africa/Mozambique border (Figure 6.3b).

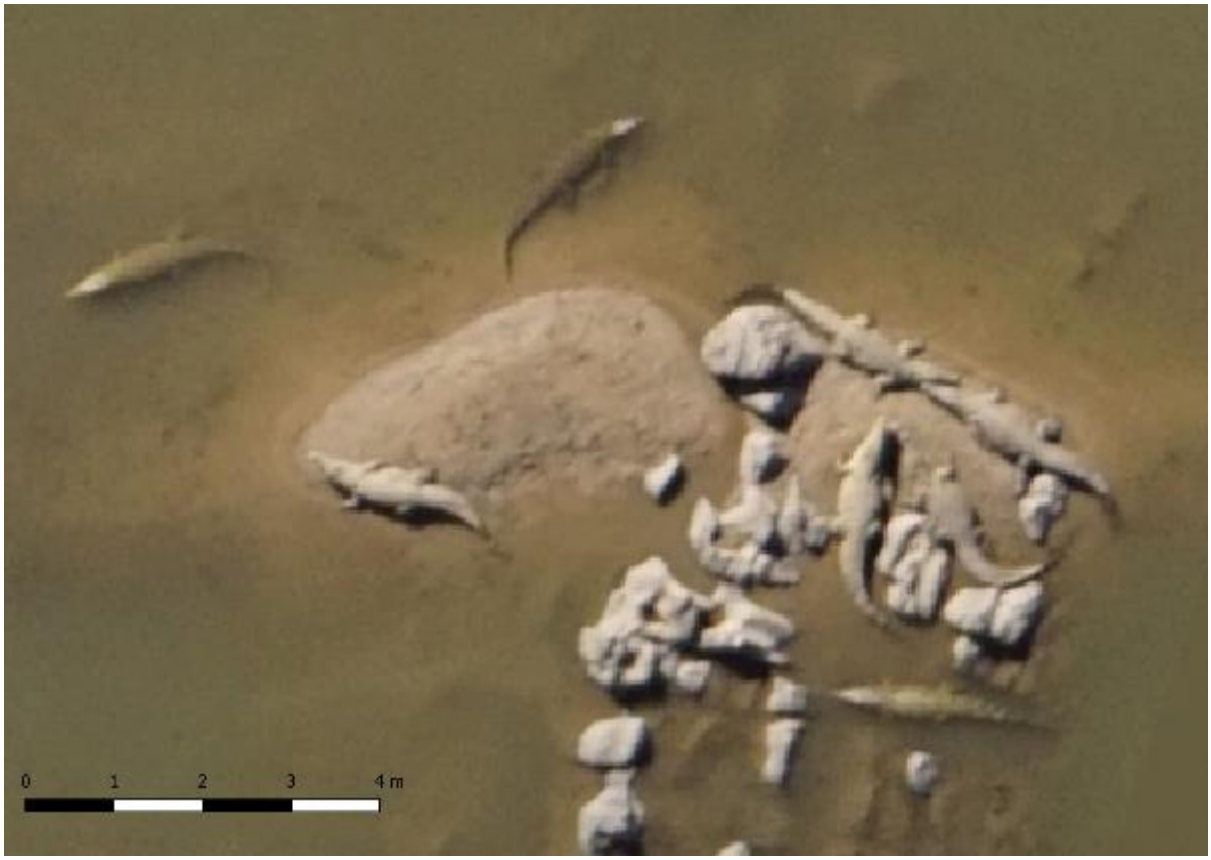

Figure 6.2: An extract from a processed orthophotograph depicting Nile crocodiles basking near a sandbank in the middle of the Olifants River. The resolution of 3 cm/pixel negated the ability to identify several morphometric features.

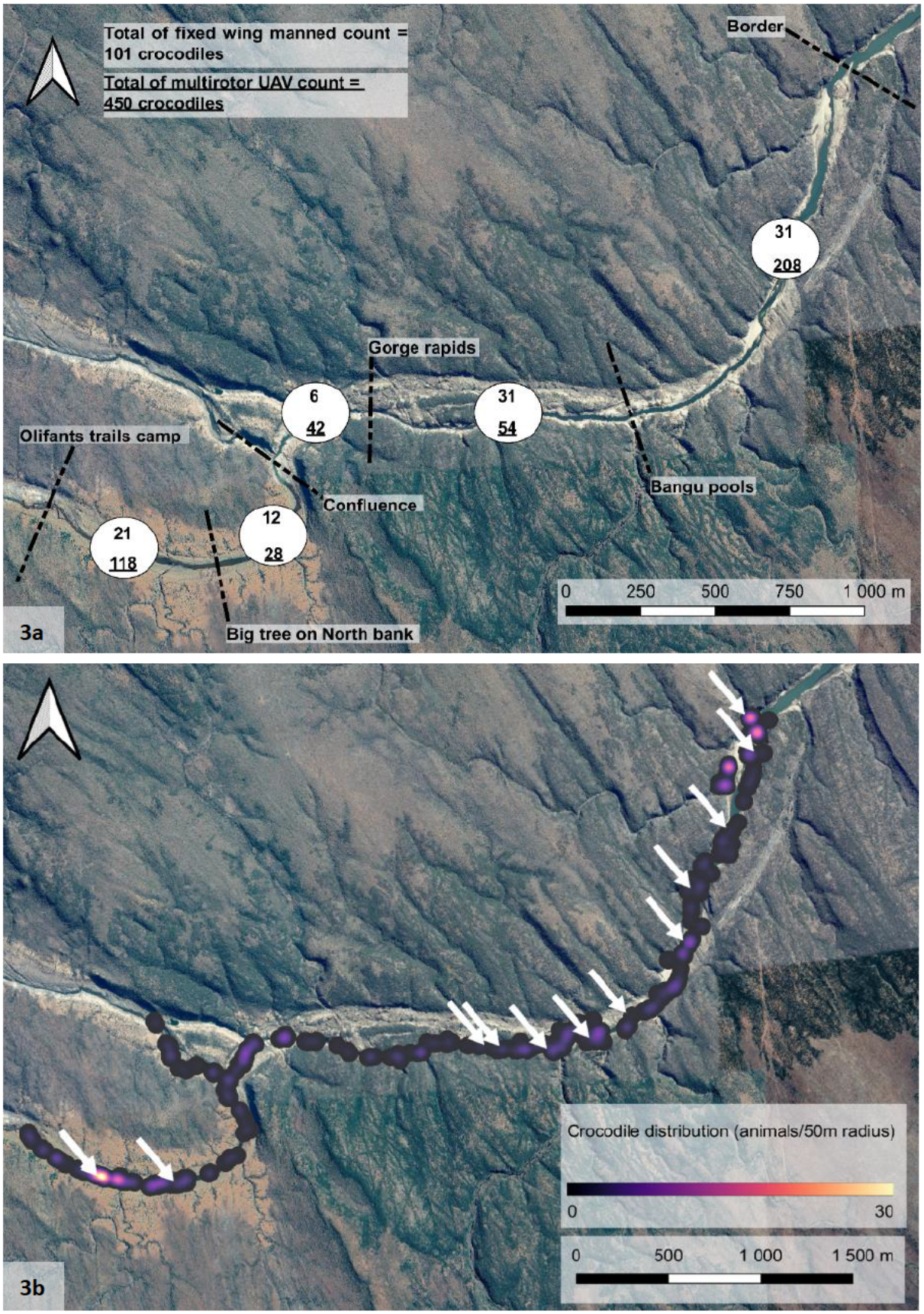

Figure 6.3: The South African reach of the Olifants River Gorge, divided into the five survey

regions (3a dotted lines) defined by the Kruger National Park Nile crocodile census operating procedures. 3a. the numbers in ellipses depict the count of Nile crocodiles from the manned fixed-wing and UAV platforms (UAV numbers are underlined). (Satellite image: Google Earth). 3b. the density of Nile crocodiles in the survey region, where white arrows indicate the position of crocodiles larger than 4.5 m total length.

The demographics of the Nile crocodile population of the Olifants River Gorge were not normally distributed but were skewed toward larger individuals (Shapiro-Wilk normality test, $w = 0.96$, $p < 0.01$; Figure 6.4). Consideration of the population without animals larger than 4m TL resulted in a normally distributed population (Shapiro-Wilk normality test, $w = 0.99$, $p > 0.05$), and animals >4 m were often individually distributed among groups of smaller animals (Figures 6.4 and 6.5).

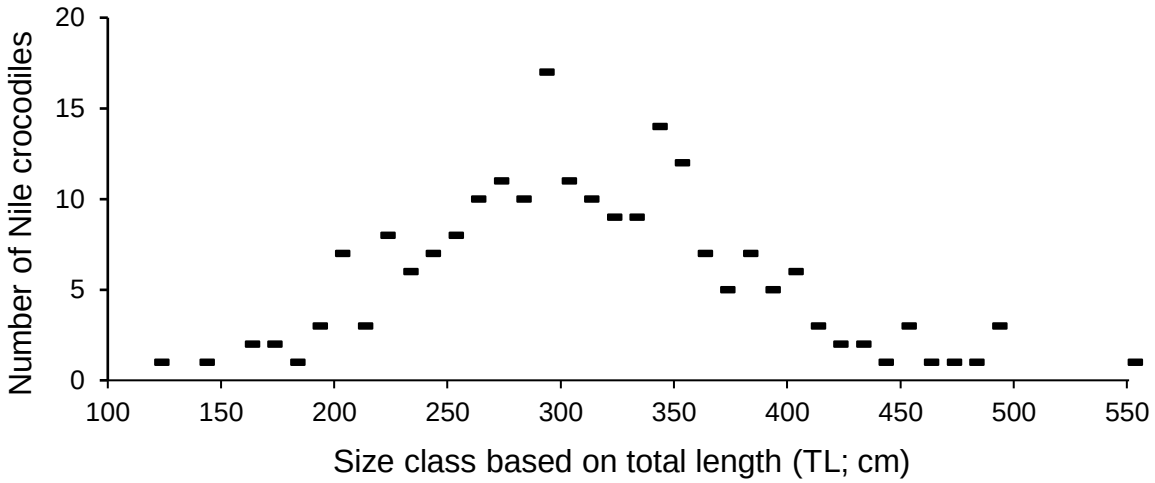

Figure 6.4: Size class distribution of the Nile crocodile population of the Olifants River Gorge (June 2021) derived from the UAV survey.

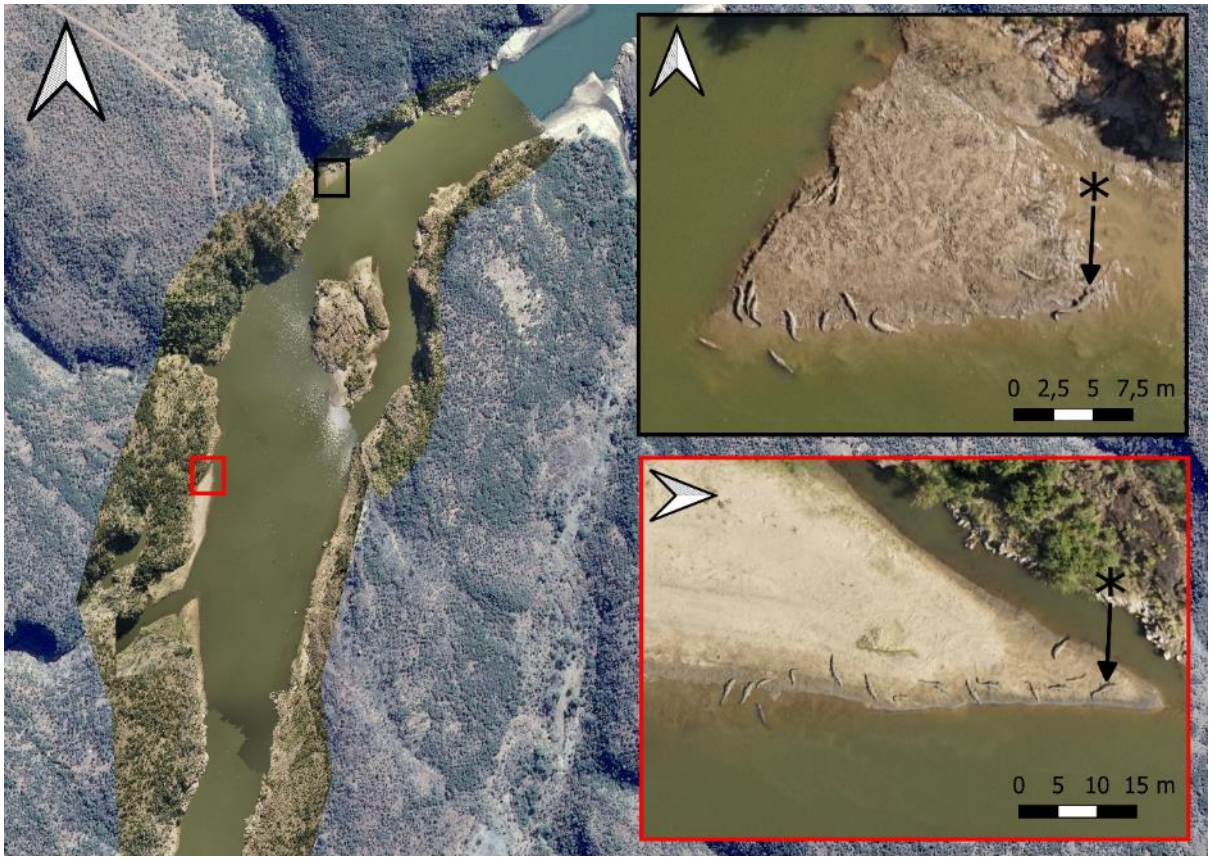

Figure 6.5: Rectified UAV orthophotographs overlaid on satellite imagery of the northern section of the Olifants River Gorge near the Mozambique border with extracts depicting groups of Nile crocodiles basking on sandbanks. Nile crocodiles marked with an asterisk were >4 m TL.

When divided into the size classes of Fergusson (2006), the Olifants River Gorge Nile crocodile population yielded 0% hatchlings and juveniles, 21.7% subadults and 78.3% adults. The stage structure of the Leftkovich-matrix defined for Nile crocodiles following Wallace et al. (2013) predicted a stage structure of 33.4% juveniles, 47.1% subadults and 19.5% adults.

Using the equations of Warner et al. (2016) and the average total length predicted by this study, the total biomass of Nile crocodiles in the surveyed sections equates to 34257.55 kg, which is 1.25 kg/km of jagged shoreline if the northern and southern shorelines are combined or to 2.7 kg/km if only if the southern shoreline is considered. The biomass per

hectare of water is 345.07 kg/ha. Following the river thalweg the equated biomass is ± 3 tons per km.

6.5 Discussion

The UAV-based survey detected more than four times as many Nile crocodiles in the survey area of the Olifants River Gorge compared with a fixed-wing manned aerial survey 40 days prior. Previous comparisons between a traditional survey technique (spotlight count) and a UAV approach found relatively similar numbers between those methods (Ezat et al. 2018), but that particular survey was done in a lentic system that was navigable by boat. In contrast, the Olifants River Gorge is only partially navigable by boat, even if Lake Massingir is back-flooded.

The number of crocodiles detected in the present study was comparable to that of Ferreira and Pienaar (2011), who estimated that the crocodile population in the Olifants River Gorge decreased from 760 (95% CI: 637-1222) to 460 (95% CI: 375-665) during the pansteatitis epidemic of 2008-2009 but differed from their 2010 estimate of 726 crocodiles (95% CI:559-1746). Repeated UAV surveys could be done in conjunction with helicopter and spotlight surveys for comparative estimations so that traditional survey techniques could be backtracked and population sizes more accurately defined. Nile crocodiles present a unique opportunity as optimal survey regimes for this species have been defined (Downs et al. 2008) and close correlation between UAV and traditional survey counts have been demonstrated (Ezat et al. 2018).

There was a clear lack of juveniles in the present study, which could be attributed to either a lack of juveniles or the inability to detect them as a result of a lack of orthophotograph clarity. A lower GSD is required for images with greater clarity, enabling the identification of smaller individuals, although smaller individuals should have been detected using the present

resolution, i.e. at ± 3 cm/pixel an 80 cm crocodile is still discernible. The data implies that they might be missing from the region during the survey period or that previous size estimation (based on observer size class categorisation) may have underestimated some Nile crocodile sizes. Surveys closer to hatching season could allow for this to be evaluated.

At least some of the discrepancies between the various estimations of the population size of this Nile crocodile population can be attributed to confounding factors. The anthropogenic border between South Africa and Mozambique limits the population survey to only one-half of the Olifants River Gorge, and a transboundary survey would be more representative of the actual Nile crocodile population in this region. The morphology of the Mozambique section of the Rio Dos Elephantes Gorge (more vegetation and shallower reaches) could provide more hiding spots for smaller individuals. Large Nile crocodiles (2.8 - 4.1 m in TL) tagged with GPS trackers have been recorded moving between the western section of the survey reach (trails camp) to the mouth of Lake Massingir in under 48 h (D. Pienaar, unpublished data). It is entirely plausible that this population exists dynamically between the mouth of Lake Massingir and the western boundary of the Kruger National Park, as there are no barriers that limit the free movement of Nile crocodiles between these two areas. The presence of subsistence fishermen in Lake Massingir may limit the movement of crocodiles within the Lake.

The distribution and stage structure of the Nile crocodile population in the Olifants River Gorge supports the notion that this region is an important breeding area for crocodiles in the Kruger National Park (Swanepoel 2000). Territorial behaviour, where smaller adult crocodiles are distributed throughout areas with only one or two larger crocodiles, suggests that males maintain breeding territories with females distributed throughout (Cott 1961; Combrink 2014). Stage structure models show relatively low juvenile survival rates for many crocodilian species (Briggs-Gonzalez et al. 2017).

We obtained lower biomass estimations in the Olifants River Gorge compared with Nile crocodile populations in the KwaZulu-Natal Province and elsewhere (see summary table in Warner et al. (2016)) when expressed per meter shoreline. The Olifants River Gorge has a relatively jagged shoreline on both the northern and southern banks, and expressing the biomass in kg/ha water area resulted in much larger biomass estimations than other studies (see summary table in Warner et al. 2016). Therefore, these parameters (as biomass per meter shoreline or biomass per area water) should be used with caution. For example, Wallace et al. (2013) found a significant deviation in shoreline estimation between different sampling efforts of the same region. Estimating shoreline length can be subject to observer bias, and the scale that defines shoreline length should be reported. For river systems, it may be more representative to express biomass in terms of the length of the river, as calculated as a single line following the river thalweg. In the Olifants River Gorge, this equated to a biomass of ± 3 tons per km. There is some debate over the diet of Nile crocodiles, but, in this area, it is evident that they are mostly reliant on the terrestrial ecosystem whilst fish provide seasonal resources (Woodborne et al. 2012). The cryptic nature of Nile crocodiles, coupled with high size dimorphism and changes in the diet throughout their lifespan (Radloff et al. 2012), requires a site-specific evaluation of resource use. Future research is required to define the resource base supporting Nile crocodiles in the Olifants River Gorge.

Reliance on various components of the terrestrial and aquatic ecosystems in this region makes the Nile crocodile population of the Olifants River Gorge an important indicator species for ecosystem state. Population censuses at greater frequencies, with increased accuracy, may provide indications of impending regime shifts, which can be prevented through pre-emptive management decisions. This UAV based survey lays the foundations for future census of the ecosystems of the Olifants River using Nile crocodiles as indicator species, but further research is required to link changes in ecosystem state to demographic shifts. Increased fishing pressure

from the communities surrounding Lake Massingir and rampant algal blooms are driven by pollution from upstream regions of the Olifants River (Woodborne et al. 2012; Woodborne 2021 unpublished data) will increase the likelihood of the Nile crocodile population demise in this region. Sufficient monitoring is required to detect and prevent this.

6.6 Acknowledgements

We thank the National Research Foundation (ZA, Grant 98404) and the University of KwaZulu-Natal (ZA) for providing funding that supported the fieldwork component of this research and Harvard University (through The DaviesLab (https://davieslab.oeb.harvard.edu/) for providing the equipment, funding and skills that allowed us to conduct the survey.

6.7 Literature cited

Aubert, C., Le Moguédec, G., Assio, C., Blatrix, R., Ahizi, M.N.D., Hedegbetan, G.C., Kpera, N.G., Lapeyre, V., Martin, D., Labbé, P. and Shirley, M.H., 2021. Evaluation of the use of drones to monitor a diverse crocodylian assemblage in West Africa. *Wildlife Research*. https://doi.org/10.1071/WR20170

Ashton, P.J. 2010. Demise of the Nile crocodile (*Crocodylus niloticus*) as a keystone species for aquatic ecosystem conservation in South Africa: the case of the Olifants River. Natural Resources and the Environment, CSIR, Pretoria, South Africa.

Biggs, R., Carpenter, S.R. and Brock, W.A. 2009. Turning back from the brink: detecting an impending regime shift in time to avert it. *Proceedings of the National Academy of Sciences, 106*, 826-831.

Bourquin, S.L., 2008. The population ecology of the Nile crocodile (*Crocodylus niloticus*) in the panhandle region of the Okavango Delta, Botswana. Doctoral dissertation, Stellenbosch University, Stellenbosch.

Briggs-Gonzalez, V., Bonenfant, C., Basille, M., Cherkiss, M., Beauchamp, J. and Mazzotti, F. 2017. Life histories and conservation of long-lived reptiles, an illustration with the American crocodile (*Crocodylus acutus*). *Journal of Animal Ecology, 86,* 1102-1113.

Caughley, G. 1974. Bias in aerial survey. *Journal of Wildlife Management, 38,* 921-933.

Cott, H. 1961. Scientific results of an inquiry into the ecology and economic status of the Nile crocodile (*Crocodylus niloticus*) in Uganda and Northern Rhodesia. *Transactions of the Zoological Society of London, 29,* 211-356.

Combrink, A.S. 2014. *Spatial and reproductive ecology and population status of the Nile crocodile (Crocodylus niloticus) in the Lake St Lucia estuarine system, South Africa.* PhD thesis, University of KwaZulu-Natal, Pietermaritzburg.

Craig, G.C., Gibson, D.S.C., Hutton, J.M. and Games, I., 1992. A population model from the Nile crocodile and simulation of different harvesting. *The CITES Nile Crocodile Project*, pp.1-52.

Da Silveira, R., Magnusson, W.E. and Thorbjarnarson, J.B. 2008. Factors affecting the number of caimans seen during spotlight surveys in the Mamirauá Reserve, Brazilian Amazonia. *Copeia, 2008*, 425-430.

Delany, M.F., Woodward, A.R., Kiltie, R.A. and Moore, C.T. 2011. Mortality of American alligators attributed to cannibalism. *Herpetologica, 67*, 174-185.

Downs CT, Greaver C, Taylor R (2008) Body temperature and basking behaviour of Nile crocodiles (*Crocodylus niloticus*) during winter. Journal of Thermal Biology 33:185-192.

Dobson, A., Lodge, D., Alder, J., Cumming, G.S., Keymer, J., McGlade, J., Mooney, H., Rusak, J.A., Sala, O., Wolters, V. and Wall, D. 2006. Habitat loss, trophic collapse, and the decline of ecosystem services. *Ecology, 87*, 1915-1924.

Erickson, G.M., Currie, P.J., Inouye, B.D. and Winn, A.A. 2006. Tyrannosaur life tables: an example of nonavian dinosaur population biology. *Science, 313*, 213-217.

Evans, L.J., Jones, T.H., Pang, K., Saimin, S. and Goossens, B. 2016. Spatial ecology of estuarine crocodile (*Crocodylus porosus*) nesting in a fragmented landscape. *Sensors, 16*, 1527.

Evans, L.J., Davies, A.B., Goossens, B. and Asner, G.P. 2017. Riparian vegetation structure and the hunting behavior of adult estuarine crocodiles. *PloS One, 12*, e0184804.

Ezat, M.A., Fritsch, C.J. and Downs, C.T., 2018. Use of an unmanned aerial vehicle (drone) to survey Nile crocodile populations: A case study at Lake Nyamithi, Ndumo game reserve, South Africa. *Biological Conservation, 223*, 76-81.

Fergusson, R., 2006. Populations of Nile crocodile (*Crocodylus niloticus*) and hippopotamus (Hippopotamus amphibius) in the Zambezi. *African Wildlife Foundation, Zambezi Heartland*.

Ferreira, S.M. and Pienaar, D. 2011. Degradation of the crocodile population in the Olifants River Gorge of Kruger National Park, South Africa. *Aquatic Conservation: Marine and Freshwater Ecosystems, 21*, 155-164.

Freckleton, R.P., Silva Matos, D.M., Bovi, M.L.A and Watkinson, A.R. 2003. Predicting the impacts of harvesting using structured population models: the importance of density-dependence and timing of harvest for a tropical palm tree. *Journal of Applied Ecology, 40*, 846-858.

Gangoso, L., Viana, D.S., Dokter, A.M., Shamoun-Baranes, J., Figuerola, J., Barbosa, S.A. and Bouten, W., 2020. Cascading effects of climate variability on the breeding success of an edge population of an apex predator. *Journal of Animal Ecology, 89*, 2631-2643.

Gotelli, N.J. 2007. A primer of Ecology. Chapter 3 - Crescimento Populacional Estruturado. 49-82. Planta. ISBN 85-99144-04-9

Hutton, J.M. (1984) Population Ecology of the Nile crocodile, *Crocodylus niloticus*, Laurenti 1768, at Ngezi, Zimbabwe. PhD thesis. University of Harare, Harare, Zimbabwe

Joubert, S.C.J., 1986. The Kruger National Park-an introduction. *Koedoe, 29*, pp.1-11.

Jordaan, P.R. 2021. The establishment of a multifaceted *Crocodylus niloticus* Laurenti 1768 monitoring programme on Maputo Special Reserve (Maputo Province, Mozambique) with preliminary notes on the population (Reptilia: Crocodylidae). *Herpetology Notes, 14*, 1155-1162.

Lane, E.P., Huchzermeyer, F.W., Govender, D., Bengis, R.G., Buss, P.E., Hofmeyr, M., Myburgh, J.G., Steyl, J.C., Pienaar, D.J. and Kotze, A. 2013. Pansteatitis of unknown etiology associated with large-scale Nile crocodile (*Crocodylus niloticus*) mortality in

Kruger National Park, South Africa: Pathologic findings. *Journal of Zoo and Wildlife Medicine*, *44*, 899-910.

Morris, T. and Letnic, M. 2017. Removal of an apex predator initiates a trophic cascade that extends from herbivores to vegetation and the soil nutrient pool. *Proceedings of the Royal Society B: Biological Sciences*, *284*, 20170111.

Nowak, M.M., Dziób, K. and Bogawski, P. 2018. Unmanned Aerial Vehicles (UAVs) in environmental biology: A review. *European Journal of Ecology*, *4*, 56-74.

Pacheco, L.F. 1996. Effects of environmental variables on black caiman counts in Bolivia. *Wildlife Society Bulletin*, *24*, 44-49.

Perretti, C.T. and Munch, S.B. 2012. Regime shift indicators fail under noise levels commonly observed in ecological systems. *Ecological Applications*, *22*, 1772-1779.

Pollock, K.H. and Kendall, W.L. 1987. Visibility bias in aerial surveys: a review of estimation procedures. *Journal of Wildlife Management*, *51*, 502-510.

Radloff, F.G., Hobson, K.A. and Leslie, A.J. 2012. Characterising ontogenetic niche shifts in Nile crocodiles using stable isotope (δ13C, δ15N) analyses of scute keratin. *Isotopes in Environmental and Health Studies*, *48*, 439-456.

Redfern, J.V., Viljoen, P.C., Kruger, J.M. and Getz, W.M. 2002. Biases in estimating population size from an aerial census: A case study in the Kruger National Park, South Africa: Starfield Festschrift. *South African Journal of Science*, *98*, 455-461.

RStudio Team (2021). RStudio: Integrated Development for R. RStudio, PBC, Boston, MA. http://www.rstudio.com/.

Sergio, F., Caro, T., Brown, D., Clucas, B., Hunter, J., Ketchum, J., McHugh, K. and Hiraldo, F. 2008. Top predators as conservation tools: ecological rationale, assumptions, and efficacy. *Annual Review of Ecology, Evolution, and Systematics*, *39*, 1-19.

Silva Matos, D.M., Freckleton, R.P. and Watkinson, A.R. 1999. The role of density dependence in the population dynamics of a tropical palm. *Ecology*, *80*, 2635-2650.

Somaweera, R., Brien, M. and Shine, R. 2013. The role of predation in shaping crocodilian natural history. *Herpetological Monographs*, *27*, 23-51.

Su, H., Wang, R., Feng, Y., Li, Y., Li, Y., Chen, J., Xu, C., Wang, S., Fang, J. and Xie, P. 2021. Long-term empirical evidence, early warning signals and multiple drivers of regime shifts in a lake ecosystem. *Journal of Ecology*, *109*, 3182-3194.

Swanepoel, D.G.J., Ferguson, N.S. and Perrin, M.R. 2000. Nesting ecology of Nile crocodiles (*Crocodylus niloticus*) in the Olifants River, Kruger National Park. *Koedoe*, *43*, 35-46.

Swanepoel, D.G.J. 1999. *Movements, nesting and the effects of pollution on the Nile crocodile (Crocodylus niloticus) in the Olifants River, Kruger National Park*. PhD thesis, University of Natal, Pietermaritzburg.

Thapa, G.J., Thapa, K., Thapa, R., Jnawali, S.R., Wich, S.A., Poudyal, L.P. and Karki, S. 2018. Counting crocodiles from the sky: monitoring the critically endangered gharial (*Gavialis gangeticus*) population with an unmanned aerial vehicle (UAV). *Journal of Unmanned Vehicle Systems*, *6*, 71-82.

Wallace, K.M., Leslie, A.J., Coulson, T. and Wallace, A.S., 2013. Population size and structure of the Nile crocodile *Crocodylus niloticus* in the lower Zambezi valley. *Oryx*, *47*, 457-465.

Warner, J.K., Combrink, X., Calverley, P., Champion, G. and Downs, C.T., 2016. Morphometrics, sex ratio, sexual size dimorphism, biomass, and population size of the Nile crocodile (*Crocodylus niloticus*) at its southern range limit in KwaZulu-Natal, South Africa. *Zoomorphology*, *135*, 511-521.

Woodborne, S., Botha, H., Huchzermeyer, D., Myburgh, J., Hall, G. and Myburgh, A., 2021. Ontogenetic dependence of Nile crocodile (*Crocodylus niloticus*) isotope diet-to-tissue discrimination factors. *Rapid Communications in Mass Spectrometry*, *35*, e9159.

Woodborne, S., Huchzermeyer, K.D.A., Govender, D., Pienaar, D.J., Hall, G., Myburgh, J.G., Deacon, A.R., Venter, J. and Lübcker, N., 2012. Ecosystem change and the Olifants River crocodile mass mortality events. *Ecosphere*, *3*, 1-17.

CHAPTER 7

Conclusions and Recommendations

7.1 Background and a brief discussion

Effective crocodile population management relies on informed management decisions, which require information on the temporal and spatial trends of the species population size, age structure, and an understanding of the species' trophic and behavioural ecology (Figure 7.1). Trophic and behavioural information relies on data from a collection of individuals, while demographic data are collected at the scale of entire populations or some form of an index that represents a population as a whole.

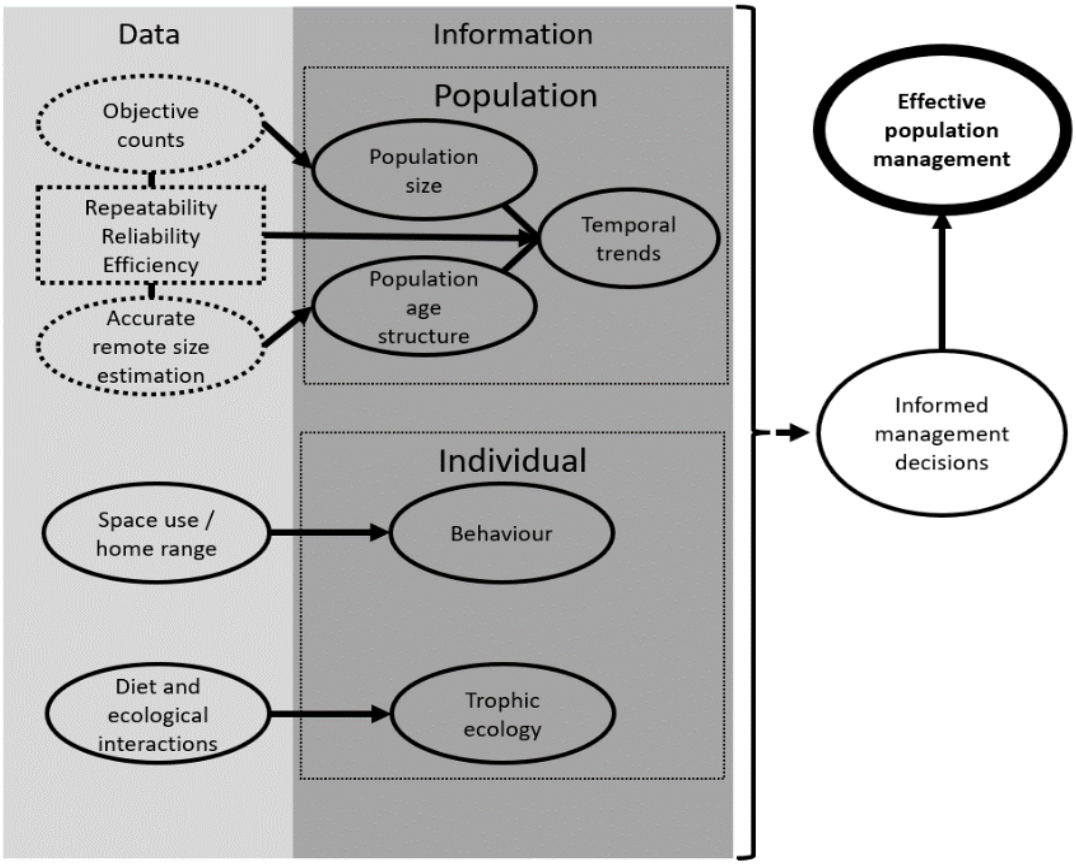

Figure 7.1: Framework that outlines the requirements for effective population management applicable to crocodiles, especially Nile crocodiles. (Source: A. Myburgh©).

The diet and behaviour of Nile crocodiles (*Crocodylus niloticus*) in southern Africa have been elucidated (Combrink et al. 2017; Myburgh et al. (in press)). The relative ease of capture of individual animals has allowed these data to be collected at relatively frequent intervals. Advances in global positioning systems (GPS) and battery technology have enabled the analysis of movement patterns and home ranges over large areas and temporal scales (Combrink 2014; Calverley and Downs 2015). Stable isotope analysis has rapidly advanced our understanding of the trophic ecology of Nile crocodiles in Southern Africa (Radloff et al. 2012; Woodborne et al. 2012; 2021; Myburgh et al. (in review)), but population-level information remains confounded by various factors.

This thesis aimed to address these limitations by evaluating the aspects and limitations related to emerging technologies that enable population monitoring of crocodiles. Although UAVs have previously been applied as a tool for crocodilian monitoring, these have generally been more expensive platforms that require additional post-flight investment in proprietary software packages. The methods presented here enable the same surveys to be conducted for a fraction of that cost and only require the purchase of a UAV and a once-off purchase of flight planning software. The added benefit of being able to process aerial imagery without an internet connection broadens the applicability of these methods to remote areas. Although many countries and institutions see this as arbitrary, the budget limitations in South Africa and more broadly throughout Africa limit the availability of UAV techniques and the methods presented here to broaden the availability of the method and could empower almost any nature conservation agency irrespective of their budget. The costs associated with the technique fall neatly within the limits of small grants, which are readily available through many NPO's (such as IDEAWild, https://www.ideawild.org/) and, in this respect, can be considered a no-cost alternative to alternative methods.

Crocodile population data (counts and size estimations) are traditionally obtained using helicopters, fixed-wing aircraft or boats (Ferreira and Pienaar 2011; Wallace et al. 2013; Warner et al. 2016). These approaches all rely on an observer to detect and judge the size of animals, in the moment, without any means of evaluating the accuracy of the census data after the surveys have been conducted. Post survey scrutineering is impossible, and size class categorisation is very broad. This hinders the development of accurate stage/age structure models for crocodilian populations, and most present models place crocodiles into very broad size classes (usually just four) (Wallace et al. 2013).

Some authors have applied unmanned aerial vehicles (UAVs) as a tool for crocodile population monitoring (Ezat et al. 2018; Thapa et al. 2018; Jordaan 2021; Aubert et al. 2021). UAVs are more affordable, allow surveys to be repeated more often, and provide photographs with sufficient overlap that can be processed with photogrammetry software to provide objective, accurate size estimations. There is a wide range of photogrammetry software packages available, but most of them are relatively costly subscription-based platforms that require a reliable funding source to support their long-term implementation. In South Africa, Nile crocodile populations outside of protected areas are either being surveyed intermittently using traditional approaches or not at all. This is directly related to available funds, as surveys can cost upward of ~R 10 000/ h (pers. comm., regional herpetologists at Mpumalanga Tourism and Parks Agency (MTPA) and Limpopo Economic Development, Environment and Tourism (LEDET)). UAVs offer a cost-effective platform that can reduce gaps and accuracy inefficiencies in the population data needed for the effective management of crocodile populations in South Africa and elsewhere, but several factors hinder their widespread implementation.

Post-flight processing software packages are costly, but open-source photogrammetry packages provide an alternative. Recent advances in the development of an open-source

photogrammetry package (Open Drone Map (ODM)) allow its broader application. In the last 3 years, ODM has developed from a package that relied on a Linux system and a command line, to one that could be run on a virtual machine through a basic graphical user interface on a windows platform, and recently into a standalone windows application that is installed locally within a few seconds. It is a no-cost alternative to proprietary drone mapping software. The ability to be run locally without an internet connection is a profound advantage over other packages that rely on server-based processing. It provides the ability to produce georeferenced orthophotograph maps of areas without an internet connection on a notebook. This is especially useful in developing countries, where large areas of unmonitored wildlife populations exist and where no/slow internet connectivity is available. Managers in these regions rely on transect surveying, either by vehicle or on foot and UAV based monitoring could greatly increase their efficiency (Jordaan 2021).

Chapter 2 of this thesis demonstrated that the low-cost combination of an entry-level consumer drone and open-source photogrammetry software is a viable alternative to more costly packages for ecological applications. It further explores areas in ecology where the technique could be applied and concludes that most ecological surveys would benefit from its methods. Although the focus of this thesis is on crocodiles, in particular, Chapter 2 is broadly applicable to any form of ecological survey where spatial data is required. The applied UAV platform is small, light and can be recharged multiple times from a portable power bank or solar panel, and it can be used in remote areas where other, larger UAV platforms would need dedicated teams and equipment (base stations, generators etc.). Furthermore, researchers and managers with small budgets can consider these methods as the total cost of the hardware and software are equal to 45 days of software subscription charges to proprietary packages, or to 1 hour of helicopter flight.

Chapter 3 applies the methods developed in Chapter 2 on Nile crocodiles, in particular, counting over 7000 crocodiles and measuring more than 2000 to provide novel data on commercial crocodile farms. For the first time, welfare parameters for commercially farmed Nile crocodiles could objectively be obtained and reported with a repeatable, low-cost, non-invasive method. Pen, pond and animal numbers on commercial crocodile farms are often estimates, evident in the vast discrepancies between the farmer estimates and the UAV derived counts. This chapter provides a tool that allows farmers and legislators to evaluate welfare parameters on commercial crocodile farms. The method is already being applied in other studies to develop body condition indices, evaluate the effects of runting and competition in pens, and monitor movement patterns during breeding seasons, providing novel data on crocodilian behaviour in captive environments. These methods have also been modified and used for thermal mapping with a UAV equipped with a thermal camera; here it allows spatial thermal data to be collected for use in thermal management on crocodile farms.

Chapter 4 used the availability of farmed crocodile data from winter surveys to produce allometric correction factors that can be used for larger-scale wild Nile crocodile monitoring. UAV based crocodilian monitoring is novel, and historical correction factors for the estimation of total lengths rely on parameters that are available from captured or deceased animals. The head length and snout-vent length, in particular, are difficult to estimate from UAV images with low resolution, and Chapter 4 addresses this issue. Total length is easily estimated from two novel morphometric parameters. Some insight is also gained into the realistic size classes that can be defined from UAV surveys of crocodile populations.

The ability to derive accurate size classes from a remote sensing platform opens the door to exploring possible age-size relationships. No methods have been developed to allow age estimations of living wild Nile crocodiles, and little information is available on the longevity of the size classes used in traditional survey methods. Chapter 5 of this thesis was an

attempt to assign individual ages based on the radiocarbon dating of crocodilian claws. The original hypothesis assumed that the retention of small amounts of cornified material on the unguis of crocodilian claws could be used to estimate the age of an animal, and from this, it would be possible to derive a size-age relationship that would add a time dimension to size-based population models, if they can be produced with some degree of accuracy, as in the case of UAV surveys. Although wear rates and replacement resulted in claws that were no older than a few years, they were shown to be useful in dietary reconstruction studies, and Chapter 5 was redesigned as a study with this as the main focus.

The methods developed in Chapters 2 to 4 could easily be applied to wild Nile crocodile populations in South Africa, but the South African Civil Aviation Authority (SACAA) regulations presently prohibit the use of unregistered UAVs in protected areas within the country (see Appendix 7.1). Consequently, during the survey conducted for Chapter 6, we flew a large multirotor UAV, registered under a remote operator's certificate (ROC), with a qualified pilot and associated operators and all the applicable permissions in place, during a survey of the crocodile population of the Olifants River Gorge in the Kruger National Park, in collaboration with Harvard University. Although a different platform and image processing package were used, the workflow and results are similar to that of the methods used throughout the thesis. This UAV approach detected approximately four times as many crocodiles as a traditional survey method, and we could derive size estimations for ¾ of the observed population, resulting in the most accurate population demographic data ever obtained for this crocodile population. This survey is scheduled to be repeated during a low flow season, and GPS-tagged Nile crocodiles in this region provide movement and space use information for this population. The crocodile population of the Olifants River Gorge is becoming one of the most well-studied crocodilian populations in South Africa. The combination and temporally overlapping availability of traditional and UAV based survey data will be used to estimate

correction factors for survey data from traditional methods. The UAV flown here is also equipped with a high precision LIDAR instrument, providing elevational data at the level of millimetres. In conjunction with movement and internal temperature data, this is a novel look at crocodile space-use and thermal management in natural environments.

These data chapters lay the foundation for accurate, repeatable and cost-effective monitoring of wild and captive Nile crocodile populations. Extended implementation of these methods will generate the population demographic data that are required to derive accurate age-structure models that can be used to inform management decisions within and outside of protected areas in South Africa and elsewhere.

Although this work was focused on Nile crocodiles, the methods are applicable to a wide range of species and environments. Their continued application will allow the development of databases for use in the training of neural networks and artificial intelligence, so that future census methodologies will require minimal human input. The development of these methods would produce real-time census data devoid of bias, covering larger areas more frequently and aiding in the effective management of wildlife populations.

7.2 Recommendations

Wild and captive crocodile management could be greatly improved through the implementation of UAV monitoring techniques outlined in these chapters. Farm managers on commercial crocodile farms could easily implement the methods of Chapter 3 as part of their monthly routines to monitor the welfare of the animals on their farms. Wild crocodile management agencies, especially those governing policies and decisions around rivers systems in the mid to upper catchment regions where crocodiles occur, could greatly improve their current crocodilian population models by implementing the methods outlined in Chapters 2, 4 and 6. For instance, the Mpumalanga Parks and Tourism Agency already has a collection of Phantom

4 UAVs that could be implemented for crocodilian monitoring without additional capital investment. For those departments that do not have UAV capabilities, there are now a plethora of low-cost platforms that could be attained through departmental funding or from small grants for conservation, such as the IDEAWild platform (https://www.ideawild.org/). Together, the implementation of these methods would produce a collection of data on crocodile populations with sufficient resolution, accuracy and objectivity to elucidate and preserve the demographics of these cryptic, aquatic predators.

7.3 References

Aubert, C., Le Moguédec, G., Assio, C., Blatrix, R., Ahizi, M.N.D., Hedegbetan, G.C., Kpera, N.G., Lapeyre, V., Martin, D., Labbé, P. and Shirley, M.H., 2021. Evaluation of the use of drones to monitor a diverse crocodylian assemblage in West Africa. *Wildlife Research* https://doi.org/10.1071/WR20170

Ezat, M.A., Fritsch, C.J. and Downs, C.T., 2018. Use of an unmanned aerial vehicle (drone) to survey Nile crocodile populations: A case study at Lake Nyamithi, Ndumo game reserve, South Africa. *Biological Conservation*, *223*, 76-81.

Ferreira, S.M. and Pienaar, D. 2011. Degradation of the crocodile population in the Olifants River Gorge of Kruger National Park, South Africa. *Aquatic Conservation: Marine and Freshwater Ecosystems*, *21*, 155-164.

Calverley, P.M. and Downs, C.T., 2015. Movement and home range of Nile crocodiles in Ndumo game reserve, South Africa. *Koedoe*, *57*, 1-13.

Combrink, A.S. 2014. Spatial and reproductive ecology and population status of the Nile crocodile (*Crocodylus niloticus*) in the Lake St Lucia estuarine system, South Africa. PhD thesis, University of KwaZulu-Natal, Pietermaritzburg.

Combrink, X., Warner, J.K. and Downs, C.T., 2017. Nest-site selection, nesting behaviour and spatial ecology of female Nile crocodiles (*Crocodylus niloticus*) in South Africa. *Behavioural Processes*, *135*,101-112.

Jordaan, P.R., 2021. The establishment of a multifaceted *Crocodylus niloticus* Laurenti 1768 monitoring programme on Maputo Special Reserve (Maputo Province, Mozambique) with preliminary notes on the population (Reptilia: Crocodylidae). *Herpetology Notes*, *14*, 1155-1162.

Myburgh, A., Botha, H., Combrink, X., Myburgh, J., Guillette, L.J., Hall, G., Chimimba, C., Woodborne, S., 2022. Terrestrial diet dependence in an unprotected Nile crocodile (*Crocodylus niloticus*) population. *Journal of Herpetology, provisionally accepted.*

Radloff, F.G., Hobson, K.A. and Leslie, A.J., 2012. Characterising ontogenetic niche shifts in Nile crocodile using stable isotope (δ13C, δ15N) analyses of scute keratin. *Isotopes in Environmental and Health Studies*, *48*, 439-456.

Thapa, G.J., Thapa, K., Thapa, R., Jnawali, S.R., Wich, S.A., Poudyal, L.P. and Karki, S., 2018. Counting crocodiles from the sky: monitoring the critically endangered gharial

(*Gavialis gangeticus*) population with an unmanned aerial vehicle (UAV). *Journal of Unmanned Vehicle Systems*, *6*, 71-82.

Wallace, K.M., Leslie, A.J., Coulson, T. and Wallace, A.S., 2013. Population size and structure of the Nile crocodile *Crocodylus niloticus* in the lower Zambezi valley. *Oryx*, *47*, 457-465.

Warner, J.K., Combrink, X., Calverley, P., Champion, G. and Downs, C.T., 2016. Morphometrics, sex ratio, sexual size dimorphism, biomass, and population size of the Nile crocodile (*Crocodylus niloticus*) at its southern range limit in KwaZulu-Natal, South Africa. *Zoomorphology*, *135*, 511-521.

Woodborne, S., Botha, H., Huchzermeyer, D., Myburgh, J., Hall, G. and Myburgh, A., 2021. Ontogenetic dependence of Nile crocodile (*Crocodylus niloticus*) isotope diet-to-tissue discrimination factors. *Rapid Communications in Mass Spectrometry*, *35*, e9159.

Woodborne, S., Huchzermeyer, K.D.A., Govender, D., Pienaar, D.J., Hall, G., Myburgh, J.G., Deacon, A.R., Venter, J. and Lübcker, N., 2012. Ecosystem change and the Olifants River crocodile mass mortality events. *Ecosphere*, *3*, 1-17.

7.4 Supplementary information

Appendix 7.1: Legal considerations for wildlife monitoring with UAVs in South Africa

In South Africa, UAV flights are governed by the SACAA through the CATS and CARS (Civil aviation technical standards and the Civil aviation regulations) documentation. In summary, any UAV (irrespective of the size and weight) that is not used for hobbyist purposes (a use where no form of monetary gains are made) or in restricted airspace falls under the regulations of the SACAA CATS and CARS and needs to adhere to the following; the UAV should be registered under a ROC (remote operators certificate) and flown by a qualified pilot (such a pilot should hold a SACAA issued RPL (remote pilots licence)) in an airspace where the SACAA commissioner has granted permission for the UAV to operate. These requirements are relatively costly and difficult to obtain owing to backlogs and regulatory level cost associations. For instance, the costs associated with obtaining an RPL in South Africa are ± R 20,000 during a process that takes between 1 and 3 months. A ROC is orders of magnitude more costly. Previous studies have neglected these requirements and have applied UAVs under the umbrella of the rules governing hobbyist flights. Unfortunately, this is not an option in areas such as the Kruger National Park, as its airspace is restricted (Figure S7.1), and any operations therein need to comply with the SACAA regulations. Consult the SACAA guidelines before flying a UAV in South Africa (see: http://www.caa.co.za/Pages/RPAS/Legislation.aspx). However, this is a progressive industry, and South African legislation is outdated, presently being revised to conform to international standards, which allow sub-250 g UAVs to be flown without licensing requirements. This development, coupled with the sub-250 g UAVs presently in development, makes this piece of research invaluable.

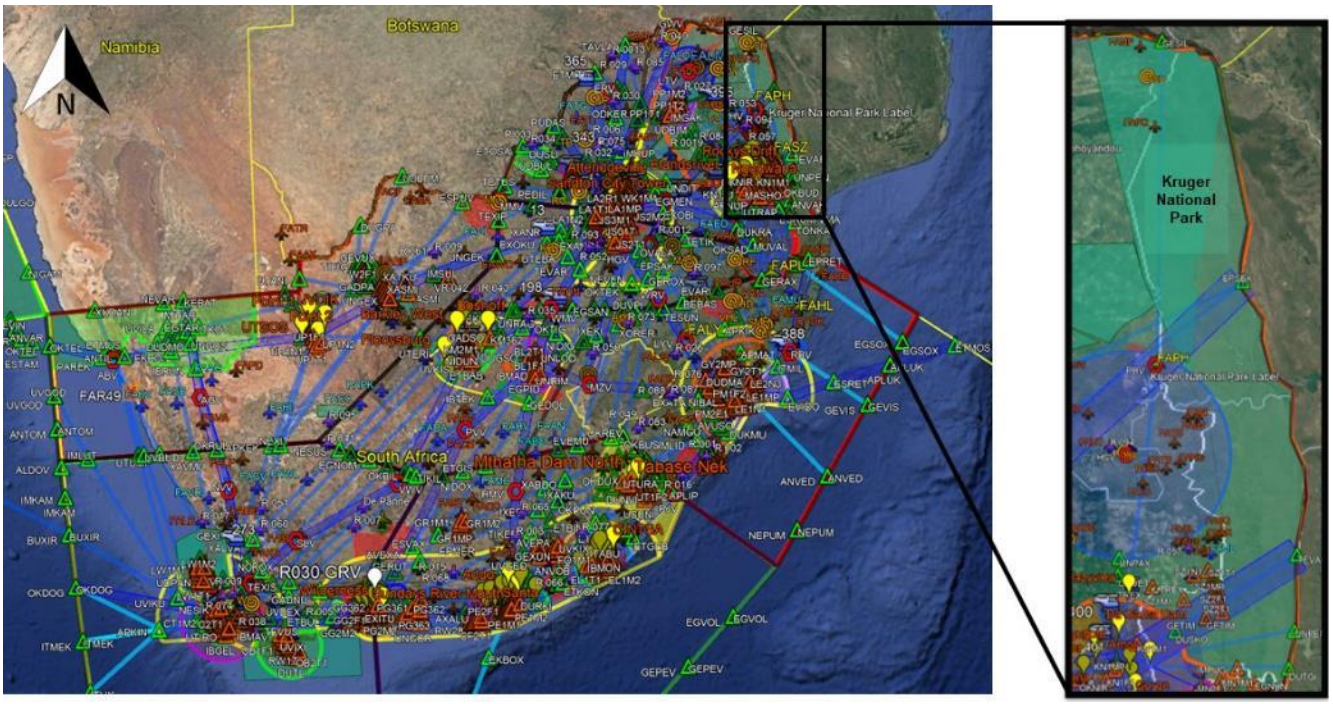

Figure S7.1: SACAA controlled airspaces in South Africa, with an excerpt depicting the restricted airspace (turquoise) of the Kruger National Park (FAR 78), which extends from GND (ground) to flight level FL105 (10500ft altitude). See https://www.atns.co.za/rsakmz.php for the downloadable 3D airspaces files. Satellite imagery: Maxxar technologies through Google Earth.